Glacial fluctuations and cryogenic environments in the Langtang Valley, Nepal Himalaya

by
Takayuki SHIRAIWA
白 岩 孝 行
The Institute of Low Temperature Science

Received October 1993

Abstract

This study aims at reconstructing the glacial distribution and climatic conditions since late Quaternary in the Himalaya. For this purpose, an inventory work of present glaciers, observations of present meteorological as well as glaciological phenomena, descriptions of present cryogenic features, and geomorphological studies of the late Quaternary glacial fluctuations, were carried out in the Langtang Valley, central Nepal Himalaya.

In the valley, glaciers cover an area of 137.5 km^2. Due to the northward decrease of summer monsoon precipitation, equilibrium line altitude of glaciers increases from 5120 m at the southern end to 5560 m at the northern end. Physical properties of deposited snow profiles on the Yala Glacier revealed that the monsoonal snow deposits are distinguished from the non-monsoonal ones by the snow types and the existence of a thin dirt layer. By observing deeper snow cores recovered on the Yala Glacier, contribution of the non-monsoonal precipitation to the annual mass balance was found to be amounted to approximately 30 % on average during the last nine years.

Measurements of the ground temperature indicate that the forefields of glaciers in the valley lack an alpine permafrost, regardless of sufficient coldness. This is also explained by the large amount of winter snow which covers the forefields enough to prevent the ground from deep-freezing in winter.

There exists six glacial steges in the valley, the *Lama* of the oldest (the penultimate or the early stage of the last glacial glaciation), the *Gora Tabela* of last glacial maximum (LGM), the *Langtang* dated between 3650 and 2850 yr. BP, the *Lirung* dated between 2980 and 550 yr. BP, and the *Yala* I and II *stages* of the Little Ice Age. The glacier extent decreases from the older to the younger.

Paleoclimate in the Langtang Valley was finally reconstructed by introducing a steady-state glacier mass balance model which considers both climatic parameters such as the summer mean air temperature (T_s), the summer total precipitation(P_s), the winter balance (B_w), and topographical parameters of the

* Contribution No. 3697 from the Institute of Low Temperature Science
北海道大学審査学位論文

ground surface area (S). With the aid of some geological paleoclimatic date, the model reconstructed reduced summer total precipitation (200 mm), increased winter balance (400 mm), and air temperature decrease of 6 °C during LGM (the *Gora Tabela Stage*), and for the Holocene maximum glaciation (the *Langtang Stage*), air temperature decrease of 4 °C, slight increase in the winter balance (300 mm), and the same amount of summer precipitation (200 mm) as that of today.

The simulated results suggest that the glacier extent of the *Gara Tabela Stage* is mainly supported by non-monsoonal precipitation. This can explain the dilemma how the Himalayan glaciers developed during the LGM when the summer monsoon, that maily supports the current Himarayan glaciers, was weakened.

Contents

I. Introduction

I.1. *Introduction*

Approximately 27,950 km^2 of glacier currently covers the Himalaya (Fujii, 1977) which forms the highest relief on the earth. As it is near to the boundary of the troposphere and stratosphere, it forms a remarkable obstacle against the course of jet streams, and, therefore, influences global atmospheric circulation. It also divides cold and warm air masses north and south of the mountain range (Mintz, 1968; Manabe and Terpstra, 1974): a cold air mass forms on the Tibetan Plateau in winter, while the plateau becomes a heat source in summer (Flohn, 1968). This characteristic thermal condition generates the monsoon circulation. As Hahn and Shukla (1976) demonstrated, an extensive snow cover on the Tibetan Plateau in spring reduces subsequent summer monsoon. This fact suggests that the areal changes of snow and glacier covers on the Tibetan Plateau and the Himalaya have controlled the monsoon circulation since geologic time. Fluctuations of glaciers in these areas, therefore, have significantly influenced the climate in Asia as well as the globe. Study of this problem is the most important task in order to reconstruct the paleoenvironments in Asia.

My study aims at reconstructing the glacial distribution and climatic conditions since the late Quaternary in the Himalaya. The long-term fluctuations of glaciers in the area have been studied since the 1950s; however, there still remain uncertainties with regard to the aerial distribution of glaciers, chronological basis, and climatic factors which induced past glaciations. Because glaciers change their volume in accordance with the change of climatic parameters, it should be possible to reconstruct the paleoclimate quantitatively by clarifying the past glacial distribution, and the relation between climatic parameters and glacier development. By attempting to complete this first, it becomes possible to estimate paleoclimatic conditions quantitatively in the Himalaya, which have so far been exclusively reconstructed qualitatively by such as a palynological method.

Exhaustive accessibility and political obstacles make it difficult to study the glacial fluctuations and their paleoclimatic significance in the Himalayan region. The Langtang Valley, central Nepal Himalaya, was selected for the present investigation, firstly because of its relatively easy accessibility. In addition, Japanese scientists had continued their glaciological and geomorphological studies in the Langtang Valley since 1981 under the name of GEN (Higuchi, 1984; Watanabe and Higuchi, 1987; Yamada, 1989; Yamada, 1991). I was a member of the expeditions of GEN 1987, 1989, 1991 and 1992, which largely supported my field work. My field surveys began in the summer of 1987, and were completed in the spring of 1992.

I.2. *Aims of the study*

The aim of this study is primarily to reconstruct the glacial fluctuations as well as the

climatic changes in the Langtang Valley since Last Glacial time. After this introduction (Chapter I), I briefly describe the physical setting of the Himalaya and the Langtang Valley (Chapter II). Chapter III is devoted to clarifying the present glaciological as well as meteorological conditions in the Langtang Valley: results of the glacial inventory, recent fluctuations of the glaciers, meteorological data, and glaciological features of several glaciers in the Langtang Valley are described to explain the glacier-climate relationships in the area.

Chapter IV describes the present cryogenic environment of the Langtang Valley. It involves results of field surveys of permafrost, distribution of periglacial landforms, and frost shattering rates measured in the area. Vertical zonation of the present cryogenic environment is also summarized.

Chapter V gives full account of glacial fluctuations in the Langtang Valley during the late Quaternary, on the basis of moraine staging, and relative and ^{14}C datings.

Chapter VI explains the last glacial and Holocene glacier advances in the Langtang Valley by a steady-state glacier mass balance model and the glacier-climate relationship clarified in Chapter III. Finally, I propose a model by which a quantitative paleoclimatic condition can be reconstructed, when the summer air temperature and precipitation condition are determined by other geological methods, such as pollen analysis.

The estimation of summer air temperature, summer precipitation, and the winter balance of the glaciers in the Langtang Valley during the Last Glacial and Holocene maximum glacier advance indicates the weakening of the summer monsoon during the Last Glacial time and the increase of winter balance during both the Last Glacial and Holocene maximum times. This is the main conclusion of this study and is summarized in Chapter VII.

II. Physical setting

II.1. *Landforms of the Nepal Himalaya*

The traditional definition of the Himalaya is the great mountain range that separates India from China (Tibet), along its north-central and northeastern frontier. It extends between latitudes 26°20' and 35°40' North, and between longitudes 74°50' and 95°40' East. In this sense, the Himalaya extends from the Indus Trench below Nanga Parbat (8125 m) in the west to the Yarlungtsangpo-Brahmaputra gorge below Namche Barwa (7756 m) in the east, with a total length of about 2500 km (Figure 1; Ives and Messerli, 1989).

The Nepal Himalaya is located at the central part of the Himalaya, extending between longitudes 80° and 88° East. The Himalaya culminates in this region, where nine peaks over-8000 m high exist (Figure 2). It is drained by three major river systems: the Karnali to the west, the Narayani in the center, and the Kosi to the east, all of which are the tributaries of the River Ganges. The Langtang Valley is one of the tributary valleys of Trisuli Gandaki of the Narayani River system, which divides the Langtang Himal to the east from the Ganesh

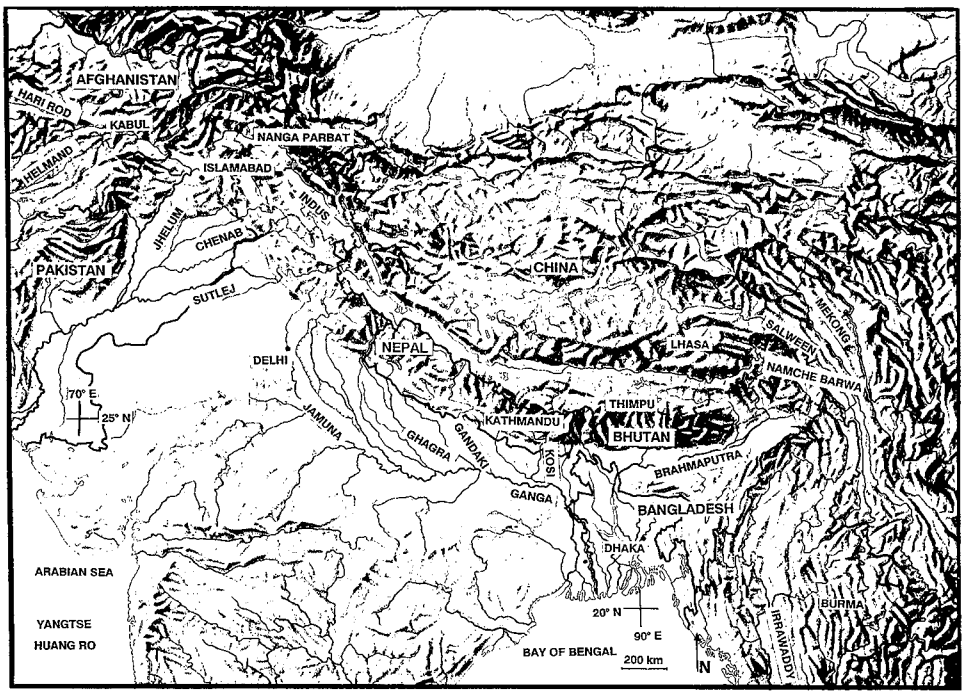

Figure 1 The Himalayan region, southern Tibet and northern India (after Ives and Messerli, 1989). The Himalaya extends from Nanga Parbat, above the Indus Gorge, to Namche Barwa, above the Brahmaputra.

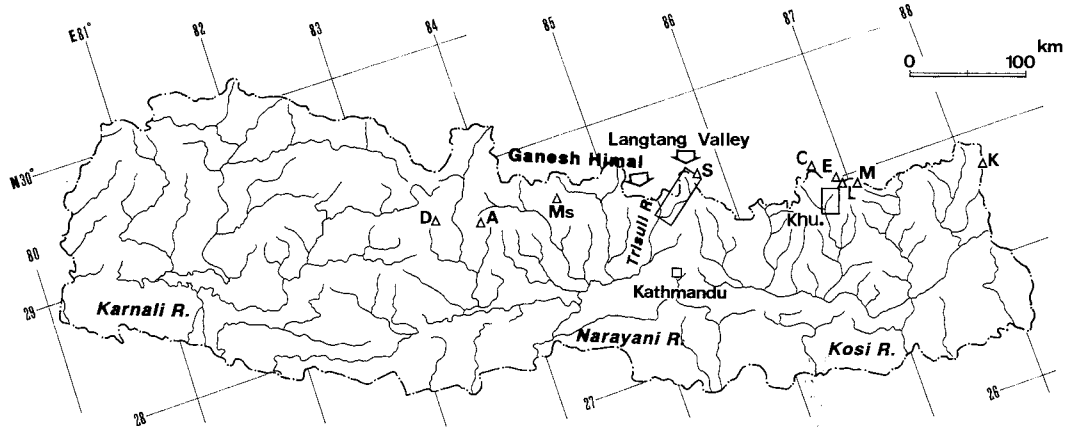

Figure 2 Location of the Langtang Valley. Abbreviations denote the names of over-8000 m high mountains. D: Daulagiri; A: Annapurna; Ms: Manasulu; S: Shishapangma; C: Cho Oyu; E: Everest; L: Lhotse; M: Makalu; K: Kangchengjunga. The area marked by Khu. is the Khumbu Region.

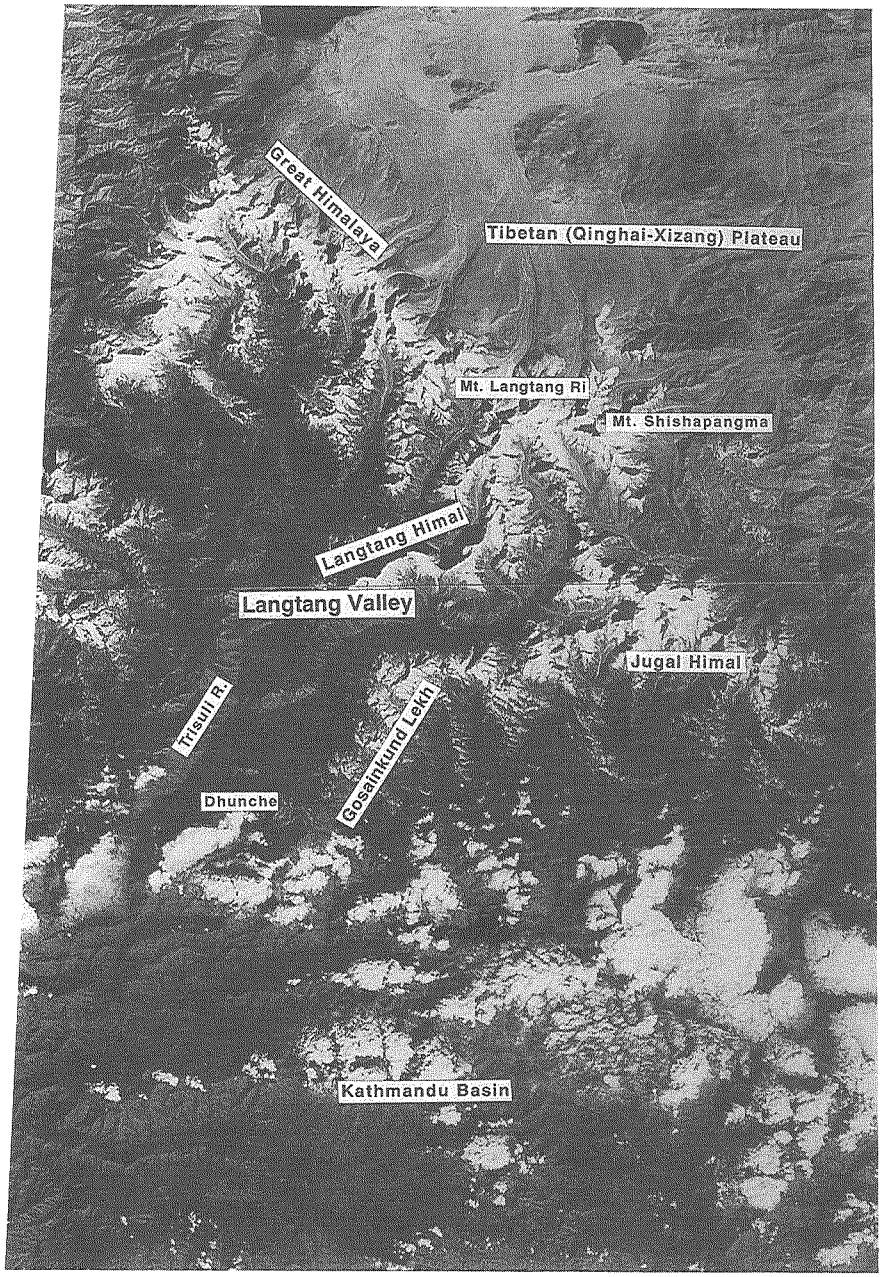

Figure 3 A MOS-1 MESSR image of the Langtang Valley (The data used was received by NRCT and produced by NASDA).

Himal to the west.

Figure 3 is a satellite image (MESSR of MOS-1) of the Langtang Valley and its surroundings. A deeply incised valley starts at Mt. Langtang Ri (7205 m), and drains southward and later westward to the confluent point (1400 m a.s.l.) with the Trisuli River. The valley is surrounded by high mountain ranges with altitudes of more than 5000 m; the Gosainkund Lekh to the south, the Jugal Himal to the east, and the Langtang Himal to the north. On the contrary, gentle slope extending on the northern side of the Great Himalaya, where moraine-fields and outwash plains are widespread. The image also clearly shows latitudinal as well as altitudinal changes of vegetation cover; from a dark-colored subtropical forest to the south or at a lower altitude, to a light-colored desert to the north or at a higher altitude.

II.2. *Climate of the Nepal Himalaya*

Climate of the Nepal Himalaya is basically determined by two seasonal atmospheric conditions: the summer monsoon and the winter westerlies. In summer, a thermal low develops over the heated Tibetan Plateau, while an anticyclone develops over the Indian Ocean. This results in the formation of the summer monsoon circulation which supplies a humid air flow from the Bay of Bengal to the Himalaya. In winter, in contrast, the Siberian anticyclone covers the Tibetan Plateau, and the westerly brings cyclones to the Nepal Himalaya along the southern limit of the anticyclone.

Monsoonal precipitation accounts for the large amount of annual precipitation in the Himalaya. The amount of precipitation decreases toward the west because it is supplied mainly from the southeast. It is also influenced by an orographic condition: the 'pockets' of very high precipitation are located at the southern slope of the Middle Mountains (Lesser Himalaya), where cumulus clouds develop by an orographically induced up-valley wind, and these clouds supply more than 3000 mm of precipitation during the monsoon season (Subramanian and Upadhyay, 1982; Dhar and Mandal, 1986).

Most of the winter precipitation, on the other hand, originates from cyclone disturbances associated with the trough embedded in the Subtropical Jet Stream flowing along the southern periphery of the Tibetan Plateau (Yasunari and Fujii, 1983). Disturbances form around the Mediterranean Sea, and are usually dissipated over the eastern Himalaya; therefore, the amount of precipitation in winter decreases towards the east.

Gulati (1972) shows the seasonal magnitude of precipitation in the Himalaya, by dividing a year into four traditional seasons. Table 1 summarizes the recalculated amount from Gulati's data when a year is divided into the monsoonal season (June to September) and the non-monsoonal one (October to May). The rate of non-monsoonal precipitation is higher in the western part of the Himalaya (46.4 % in the Kashimir Himalaya), and decreases to 12–15 % in the Nepal Himalaya. This suggests that the non-monsoonal precipitation contributes less to the glacier accumulation in the Nepal Himalaya than the monsoonal precipitation

Table 1 Monsoonal (June-September) and non-monsoonal precipitation magnitude in the Himalaya (compiled from data by Gulati, 1972).

Longitude	Name of mountain range	Seasonal rate of precipitation amount (%)	
		Monsoon (Jun.-Sept.)	Non-monsoon (Oct.-May)
W ↑	Kashmir Himalaya	53.6	46.4
	Panjub Himalaya	78.4	21.6
	Garwhal Himalaya	87.8	12.2
	Western Nepal Himalaya	88.0	12.0
	Eastern Nepal Himalaya	85.0	15.0
	Sikkim Himalaya	74.6	25.4
↓ E	Assam Himalaya	65.8	34.2

which, in fact, has been regarded as a major source of the mass input in the area (*e.g.*, Ageta, 1983a).

II.3. *Glaciers in the Nepal Himalaya*

Approximately 27,950 km^2 of glaciers currently cover the Himalaya. They form the most extensive glaciated area on the Eurasian continent. Of these areas, 2,620 km^2 (about 9 %) of glaciers are distributed in the Nepal Himalaya (Fujii, 1977), while the rest mainly develops at the western (6,200 km^2 in the Punjub Himalaya; 13,320 km^2 in the Kumaun Himalaya) and eastern (5,180 km^2 in the Assam Himalaya) ends. The large extent of the glaciers at both ends of the Himalaya is mainly explained by a larger amount of annual precipitation in these areas.

A snowline altitude of the glaciers increases towards the north in the Himalaya, probably reflecting the latitudinal gradient in the amount of precipitation. The highest snowline altitude is just north of the Great Himalaya, attaining at an altitude of 6000 to 6200 m. The longitudinal change of the snowline altitude is not clear in the central part of the Himalaya, but at the eastern (Nyainqentanglha Range) and western (Karakorum Range) ends, it is lower than 5000 m (Shi, 1980).

Termini of glaciers descend as low as 3000 m at the western and eastern ends of the Himalaya, while they are located at an altitude of, more or less, 5000 m in the central part of the Himalaya. Fujii (1977) explained this by the latitudinal effect and differences in the amount of precipitation.

III. Present glacial environments in the Langtang Valley

III.1. *Introduction*

The glacier distribution in the Nepal Himalaya has been unknown until the compilation of glacier inventories by Müller (1958/59, 1970) and Higuchi *et al.* (1978, 1980) in the Dudh Kosi region. Iida *et al.* (1984b) firstly listed glaciers in the Langtang Valley, mainly depend-

ing on oblique aerial photographs and official maps of Nepal. Although it was a great achievement, the lack of photographs around the Nepal-China national border did not allow them to document the glacier distribution in the upper reaches of the Langtang Valley. The first aim of my study was, therefore, to complete a detailed inventory of the glaciers in the valley. After a brief summary of the previous works on the glaciological and meteorological studies in the Langtang Valley (section 2), I will summarize the results of my inventory work (section 3).

A glacier fluctuates in relation to the climatic changes through processes of mass and energy exchanges and mechanical response (Meier, 1965). This means that short-term meteorological observations can only clarify a relation between the present glaciation and climate when the glacier is in a steady or quasi-steady state. Therefore, it must be examined whether the glacier is in equilibrium or not, before discussing the relationship between the present glaciation and climate. The observations of the terminal fluctuations of a specific glacier for seven years confirmed that the observed glacier was in a quasi-steady state. This is discussed in Section 4.

A mass balance study of the glacier reveals the relationship between glacier and climate. In the Dudh Kosi region, the mass exchange of the glaciers mainly occurs in the monsoon season (Ageta, 1983a), where the mass balance of the smaller glacier is strongly controlled by summer air temperature, while that of the larger valley glacier is influenced by the amount of summer precipitation (Ageta, 1983b). However, in the Langtang Valley, approximately 100 km west of the Dudh Kosi region, Iida *et al.* (1987) reported that the mass exchange of a glacier is controlled not only by monsoonal precipitation but also by winter precipitation. In addition, the upper part of the valley is reported to have a drier climate than the middle reaches (Ono, 1986). It is, therefore, necessary to know the spatial variation of climate and to quantify the contribution of seasonal mass input to the annual mass balance. In this context, Sections 5 and 6 are devoted to the description of the present meteorological condition and the mass balance of glaciers in the Langtang Valley. Section 6 deals with the spatial variation of the mass input on glaciers in the Langtang Valley, and discusses the seasonal variation of the glacier mass input.

Finally, in Section 7, I propose several climatic parameters which determine the glacier mass balance in the Langtang Valley.

III.2. *Previous work*

Studies of glaciers and climate of the Langtang Valley were initiated in 1981 by the Japanese Glaciological Expedition of Nepal (GEN-BP 1981-82; Higuchi, 1984), and were succeeded by GEN-LP 1985−86 (Watanabe and Higuchi, 1987), GEN-LP 1987−88 (Yamada, 1989) and several personal expeditions up to the present. These expeditions clarified many aspects regarding the glaciers and climate of the Langtang Valley. The aim of this section is to review briefly the important results which have been obtained so far as concerning the

present glaciation and the glacier-climate relationships.

Usselmann (1980) was the first to illustrate the distribution of glaciers as well as the geomorphological features in the Langtang Valley, although his data-base depended on a limited number of oblique aerial photographs and official maps. Iida *et al.* (1984b) made a more detailed map of the glacier distribution in the Langtang Valley. The map covers not only the Langtang Valley but also the Helambu and Jugal regions to the south. The official 1 : 50000 maps were also used as base maps. Their inventory work used many aerial photographs; however, the upper part of the valley was less accurately mapped due to the scarcity of photographs.

Japanese glaciological studies in the Langtang Valley were exclusively executed on the Yala Glacier, a plateau type small glacier spread over the gentle mountain slope on the right bank of the middle reaches of the valley. Drilling was done on the glacier both in the accumulation and ablation areas in 1981 and 1982, and the cores were analyzed both physically and chemically (Iida *et al.*, 1984a; Watanabe *et al.*, 1984). The core analyses clarified that the Yala Glacier has a temperate accumulation area and a cold ablation area. The temperate character of the glacier did not allow the reconstruction of the paleoclimate by using ice cores.

Drilling carried out in the accumulation area in 1987 revealed the superimposed ice formation on the Yala Glacier. Ozawa (1991) concluded that the superimposed ice formation contributes considerably to the glacier accumulation especially near the equilibrium line. He also found that the summer mass balance can be roughly estimated by Ageta's model (Ageta, 1983a) in the Langtang Valley.

The mass balance of the Yala Glacier was studied by stake measurements (Ageta *et al.*, 1984; Iida *et al.*, 1987; Motoyama and Yamada, 1989), by observations of crevasse cliffs (Ageta *et al.*, 1984), and by snow pits (Ageta *et al.*, 1984; Iida *et al.*, 1987; Kohshima, 1987; Shiraiwa *et al.*, 1992). These studies clarified that the major mass exchange occurs in the monsoon season. A significant contribution of non-monsoonal precipitation to glacier mass balance was, however, found first in 1985 (Iida *et al.*, 1987) and then in 1990 (Shiraiwa *et al.*, 1992). This was explained by a frequent passing of the western disturbances during the non-monsoonal periods (Seko, 1987; Seko and Takahashi, 1991; Ueno *et al.*, in press). The quantitative estimation of the contribution of non-monsoonal precipitation is one of the main themes of my study.

Formation processes of dirt layers were considered in relation to biological activity: a major dirt layer is initially formed at the beginning of the monsoon season, and develops throughout the monsoon season, while a minor dirt layer can occasionally be formed during the post-monsoon season by dry fall-out and subsequent snow fall (Iida *et al.*, 1987; Kohshima, 1984, 1987).

Takahara *et al.* (1984), Yamada *et al.* (1984) and Ageta *et al.* (1984) reported the results of meteorological observations in the valley, although the observational periods were limited

Table 2 List of glaciers in the Langtang Valley (Shiraiwa and Yamada, 1991). Further information is given in the text.

ID No.	Glacier Name	Aspect		Class.	Surface Area(km²)			Elevation(m)	
		Acc.	Abl.		Clean	Debris	Total	Max.	Min.
L010		SW	SW	750120	0.12	0	0.12	5220	5140
L020		SE	SE	750120	0.06	0	0.06	5960	5180
L030		S	S	750120	0.12	0	0.12	6581	5040
L040		S	S	750120	0.1	0	0.1	5520	5120
L050		S	SE	633520	2.25	0	2.25	6680	4760
L060		SW	S	630520	3.13	0.29	3.42	7234	4320
L070		S	S	630520	1	0.09	1.09	7120	4800
L080	Lirung	SE	S	530320	5	1.33	6.33	7234	4120
L090	Khymjung	SE	S	633410	3.2	0	3.2	6760	4380
L100		SW	SW	630310	3.12	0.49	3.61	6690	4680
L110	Yala	SW	SW	630112	2.49	0	2.49	5749	5090
L120	Shalbachum	S	S	530310	3.66	2	5.66	6578	4240
L130		SW	SW	633110	2.4	0	2.4	5980	4960
L140		SE	SE	640120	0.56	0	0.56	5920	5020
L150		E	E	633120	0.1	0	0.1	5840	5180
L160		NE	SE	520320	0.77	0.62	1.39	5980	4760
L170		SE	SE	640110	0.79	0	0.79	6220	5300
L180		S	S	630110	0.13	0	0.13	5560	5300
L190		SW	SW	630110	0.29	0	0.29	5691	5240
L200		S	S	750120	0.12	0	0.12	5780	5360
L210		S	S	633120	0.36	0	0.36	5780	5300
L220		E	E	630120	0.23	0	0.23	5639	5000
L230		N	N	630110	1.34	0	1.34	5690	5120
L240		E	NE	520120	2.45	1.05	3.5	6578	4880
L250		E	E	630120	0.4	0	0.4	6220	5220
L260		E	E	750120	0.14	0	0.14	5840	5180
L270		N	NE	630110	1.6	0	1.6	6220	5060
L280	Langtang	S	S	510120	18.4	11.95	30.35	7205	4520
L290		S	S	630110	3.43	0.55	3.98	6325	5060
L300		W	W	630420	1.05	0	1.05	6758	4840
L310		SW	W	633420	0.39	0	0.39	6900	5280
L320		SW	NW	520310	5.53	1.09	6.62	6560	4680
L330		NW	NW	630520	1.35	0	1.35	6460	4680
L340		NW	NW	633220	0.14	0	0.14	6460	5000
L350		S	S	633410	2.36	0	2.36	6460	4840
L360	Langshisa	W	NW	510120	13.76	5.49	19.25	7083	4360
L370		N	N	630210	0.78	0	0.78	6078	5380
L380		N	N	630110	3.33	2.46	5.79	6387	4700
L390		E	E	640120	0.44	0	0.44	6180	5040
L400		W	W	633120	0.33	0	0.33	6000	4980
L410		W	W	633320	1.06	0	1.06	6387	4780
L420		W	W	633120	0.5	0	0.5	6387	5360
L430		W	W	630110	1.2	0	1.2	6240	5020
L440		NE	N	520110	2.2	0.61	2.81	5702	4780
L450		SE	N	623110	1.48	0	1.48	5930	5080
L460		SE	SE	630120	0.22	0	0.22	5930	5260
L470		NE	NE	750120	0.08	0	0.08	5930	5520
L480		E	E	630120	0.33	0	0.33	5930	5220
L490		NE	NE	630120	0.33	0	0.33	5800	5180
L500		N	N	630120	0.25	0	0.25	5800	4820
L510		N	N	750120	0.07	0	0.07	5800	5040
L520		N	N	620110	3.54	0	3.54	5940	4720
L530		NE	NE	030100	0	0.27	0.27	5000	4880
L540		E	E	630110	0.56	0	0.56	5846	5080
L550		N	N	630110	0.67	0	0.67	5846	4860
L560		N	N	753220	0.15	0	0.15	5640	5040
L570		NE	N	633110	0.74	0	0.74	5846	4880
L580		N	N	633110	0.16	0	0.16	5560	5080
L590		N	N	630110	0.15	0	0.15	5560	5080
L600		NE	N	630110	2.63	0	2.63	5862	4880
L610		NE	NE	630110	1.67	0	1.67	5825	5100
L620		N	N	750110	0.13	0	0.13	5460	5160
L630		N	N	750110	0.2	0	0.2	5460	5080
L640		N	N	630110	0.48	0	0.48	5822	4960
L650		N	N	750110	0.09	0	0.09	5280	5060
L660		W	W	750120	0.49	0	0.49	5822	5240
L670		N	N	620110	1.77	0	1.77	5580	5060
L680		N	N	750110	0.18	0	0.18	5392	5020
L690		N	N	750110	0.08	0	0.08	5360	5090
L700		N	N	630110	0.23	0	0.23	5534	5040
L710		N	N	750110	0.09	0	0.09	5200	5040
L720		W	W	750120	0.26	0	0.26	5534	4920
						TOTAL	137.50		

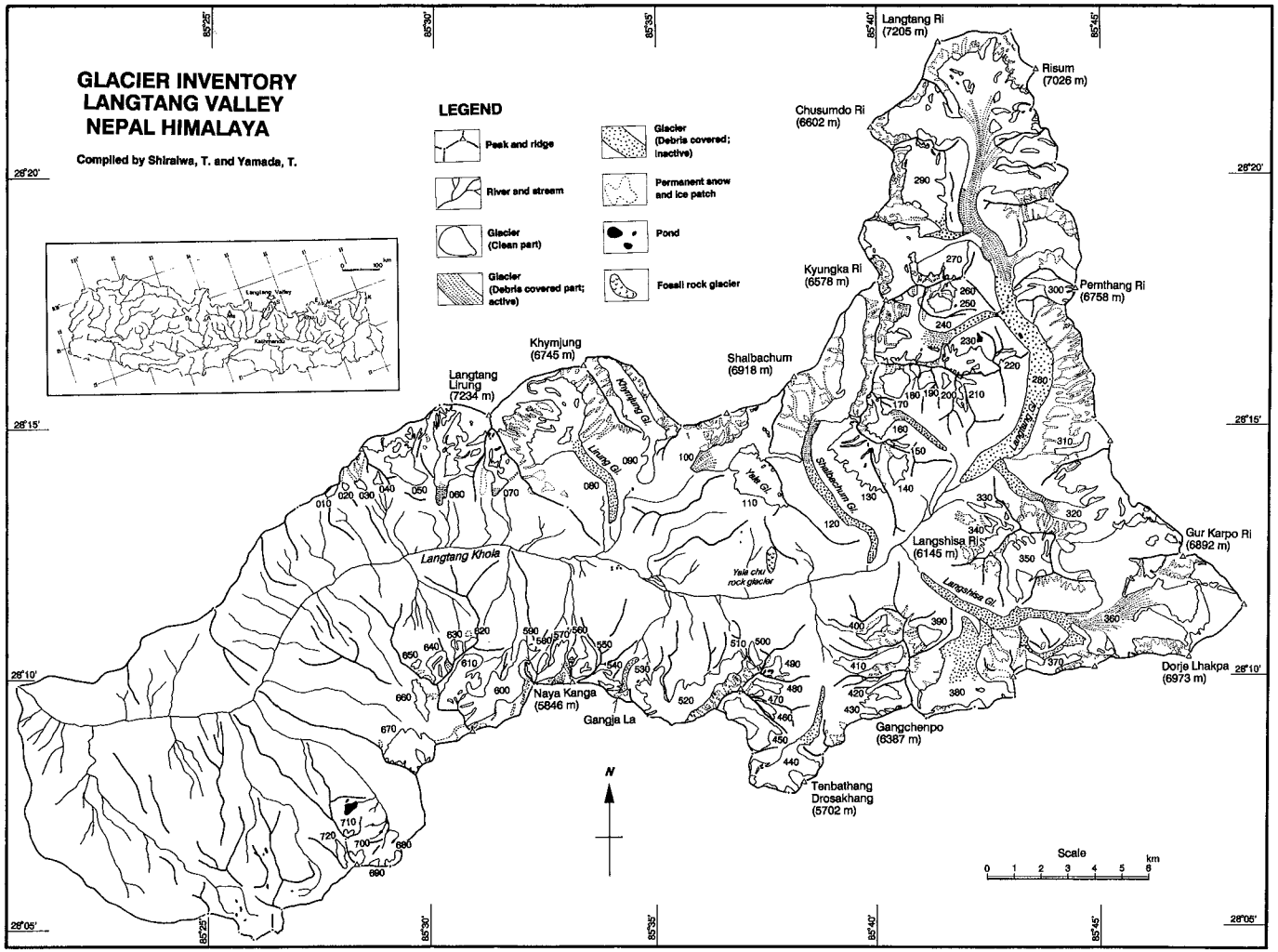

Figure 4 Glacier inventory of the Langtang Valley (Shiraiwa and Yamada, 1991).

from summer to autumn in 1982. They confirmed the climatic contrast in the rainy monsoon and dry post-monsoon.

Takahashi *et al.* (1987a) was the first to carry out and record meteorological observations for a full-year in Kyangchen at the middle reaches of the Langtang Valley, from July 1985 to June 1986. They observed variable meteorological features both in Kyangchen and at the terminus of the Yala Glacier. The results led Seko (1987) to find the altitudinal amplification of precipitation in each season, and to assign the mechanism of heavy non-monsoonal precipitation to the synoptic-scale winter disturbances. Seko and Takahashi (1991) extended the study to the whole Himalayan region, and emphasized the importance of the non-monsoonal precipitation to the glacier mass balance.

Distribution of monsoonal precipitation in the valley was later discussed by Ueno and Yamada (1990). They found three types of precipitation within a diurnal variation, each of which has a different spatial distribution. This suggests difficulty in estimation of the amount of precipitation around the Yala Glacier from the value measured at the valley bottom. Therefore, it is necessary to measure the precipitation near the glacier to discuss the relationship between glacier and climate.

III.3. *Distribution of the glaciers*

III.3.1. Inventory of the glaciers

Sources of data for the present inventory work are as follows: a) aerial oblique color photographs taken in 1991 (approximately 1000 prints); b) aerial oblique monochrome photographs taken in 1981 (approximately 500 prints); c) ground survey data and terrestrial photographs taken in 1987, 1988, 1989, 1990 and 1991; and d) 1/50,000 topographical maps published by the Austrian Alpine Club. The aerial oblique photographs were taken on 22 April 1991 by myself and my colleagues, and in 1981 by GEN－1981. Terrestrial photographs were taken by myself.

An identification system of the glaciers is based on the data format provided by the World Glacier Monitoring Service (WGMS, 1989), which was originally proposed by Müller *et al.* (1977). The inventory involves the following elements of glaciers: identification number, glacier name, aspect of accumulation and ablation areas, morphological classification, surface areas of accumulation and ablation areas, and the highest and lowest elevations of glaciers (Table 2; Shiraiwa and Yamada, 1991).

Three digits are adopted as a glacier identification number (ID No.). The third digit of an ID No. is '0' due to a need for a future numbering capacity for undiscovered glaciers.

In case of individualizing large valley glaciers such as the Langtang (L280), which consists of many sub-glaciers (or tributary glaciers), sub-glaciers flowing into the active part of the main glacier are regarded as parts of the latter. However, when the sub-glaciers flow into the stagnant part of the main glacier, or when they have no direct connection to the main glacier flow, they are regarded as independent from the main one (Figure 4).

III.3.2. Characteristics of the glaciers

The inventory identified 72 glaciers with a total area of 137.5 km^2 in the valley. They are variable both in area and elevation. They are, however, roughly divided into two types, *i.e.*, *clean-type* and *debris-covered-type* glaciers, according to the classification by Moribayashi and Higuchi (1977).

The *clean-type* glaciers are relatively small glaciers with clean surfaces, and develop on gently-inclined slopes or in cirques. The Yala (L110), Khymjung (L090) and Gangja La (L520) glaciers are examples.

The *debris-covered-type glaciers* are large valley glaciers occupying valley bottoms. The Langtang (L280), Lirung (L080) and Langshisa (L360) glaciers are included in this category. In addition to the above categories, permanent snow or ice patches and rock glaciers were identified as glacier-related landforms.

The glaciers spread in the altitudinal belt between 4120 and 7234 m. The lowest altitude is marked by the Lirung Glaciers, and the highest by the top of the same glaciers. *Debris-covered-type* glaciers characterize the low-altitude termini. Their excessively lower distribution is explained by the avalanche-nurishment and the insulation-effect of debris-cover against surface ablation (Inoue and Yoshida, 1980). The *clean-type* glaciers, on the contrary, almost all fall in the belt between 6500 and 4500 m. They are fed by natural precipitation only, and not protected from intensive ablation due to the lack of debris-cover on their surface. This explains their higher distribution.

The lowermost parts of the *debris-covered-type* glaciers are considered to be stagnant ice consisting of fossil glacial ice which has no direct relation to the present glacier flow. This was previously confirmed in the Khumbu region by a structural glaciological study (Fushimi, 1977a). Present active termini are probably situated in the middle part of the debris-covered tongues. Although it is difficult to point out their location without any measurement of glacier flow, they seem to be located at the boundary between organized surface structures, such as ogive and lineated longitudinal furrows and ridges, and disorganized or random surface structures.

The equilibrium line altitude (ELA) of the glaciers is reported to decline southward in the valley (Zheng *et al.*, 1984; Ono, 1986). However, the ELA was determined only in the Yala Glacier by measuring the mass balance (*e.g.*, Ozawa, 1991). It is located at an altitude of approximately 5230 m, although it varies annually.

The ELAs of some other glaciers in the valley are tentatively estimated by the median altitude of a glacier, surface mass balance, and literature (Figure 5-A). Glacier L710 is one of the glaciers located at the southernmost part of the valley (Figure 5-B). It covers the altitudinal belt between 5200 and 5040 m. The median altitude of this glacier is 5120 m. The surface mass balance study (Shiraiwa *et al.*, 1992) gives the Gangja La (L520) and Kyungka Ri NW (L270) glaciers ELAs of 5200 and 5350 m, respectively. The ELAs of the Langtang Glacier (L280) and glaciers immediately adjacent to the north of the valley are

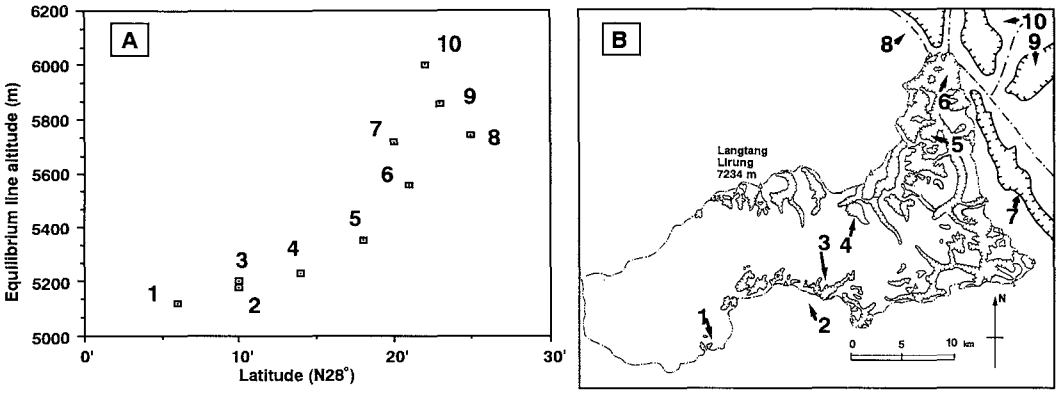

Figure 5 Present equilibrium line altitudes of the glaciers (A) and the ELA's sampling sites (B) in the Langtang Valley and its northern fringe of the Tibetan Plateau. The ELA data of the L280, Daqu, Fuqu, Unnamed, and Yebokangjial glaciers are cited from Academia Sinica (1986).

reported to be 5560 m and somewhat higher by Academia Sinica (1986). Plots of these values against latitude clearly illustrate the northward exponential rise of ELA (Figure 5-A).

III.4. *Recent fluctuations of the glaciers*

The Yala Glacier was selected for the monitoring of terminal fluctuation, since it is a *clean-type* glacier, which seems to be more sensitive to the climatic change than the *debris-covered-type* glaciers.

The terminal position of the Yala Glacier was determined both by photogrametry (Yokoyama, 1984) and ground survey (Ageta, *person. commu.*) in 1982. The location of the terminus was determined by measuring the distance between the terminus and nine fixed-base-points towards a given direction, using a plain compass and a tape with errors within 5 minute in angle and 5 cm in length. The terminus was surveyed again by myself and colleagues in October 1987 and December 1989, thereby obtaining the terminal fluctuations for seven years.

In addition to the measurement of the terminus of the Yala Glacier, a transverse profile of the Lirung Glacier was surveyed by myself. It was surveyed in the middle part of the glacier by triangulation from fixed points established at lateral moraines of the glacier, using a theodolite (WILD T-2) and Geodimeter (DISTMAT WILD DIOR-3002). The initial survey was conducted in October 1987, and the same part was re-surveyed in December 1989.

Table 3 shows the fluctuation of the Yala Glacier. The glacier terminus generally advanced between 1982 and 1987 by an amount of 0.4 to 10.2 m except the westernmost part of the glacier which retreated by 8.4 to 3.4 m. The general advancing trend in 1982–1987 changed to a retreating trend between 1987, 1989 and probably 1991 (Figure 6 A-C). The retreat of the terminus amounted to 0.2 to 6.9 m in those two years. Although the seven

Table 3 The fluctuation of the glacier in the Langtang region (Yamada *et al*, 1992). The negative values (in meters) of the fluctuations show a terminal retreat.

Area	Gl. No.	Gl. Name	Base No.	Fluctuation of glacier termini (m)
Langtang		Yala	1	(15 Oct.,'82) ····· (27 Sep.,'87) ····· (4 Dec.,'89) − 8.4 − 0.3
			2	(15 Oct.,'82) ····· (27 Sep.,'87) ····· (4 Dec.,'89) − 3.4 − 6.9
			3	(15 Oct.,'82) ····· (27 Sep.,'87) ····· (4 Dec.,'89) + 2.4 − 6.7
			4	(16 Oct.,'82) ····· (28 Sep.,'87) ····· (4 Dec.,'89) + 0.4 − 5.0
			5	(16 Oct.,'82) ····· (28 Sep.,'87) ····· (4 Dec.,'89) +10.1 − 3.6
			6	(16 Oct.,'82) ····· (28 Sep.,'87) ····· (5 Dec.,'89) + 2.6 + 0.2
			7	(16 Oct.,'82) ····· (28 Sep.,'87) ····· (5 Dec.,'89) +10.2 − 5.3
			8	(16 Oct.,'82) ····· (28 Sep.,'87) ····· (5 Dec.,'89) + 6.7 − 4.1
			9	(8 Oct.,'87) ····· (5 Dec.,'89) − 5.4

years fluctuation data are not sufficient to judge the state of the glacial regime, a small amount of advance and retreat both in different periods and in different portions of the glacier suggests that the Yala Glacier is in a quasi-steady state.

The transverse profiles of the Lirung Glacier both in 1987 and 1989 are shown in Figure 7. The result indicates that the glacier surface did not show a remarkable change; some parts were slightly lowered while others rose. This probably indicates that the stagnant part of the glacier is prevented from a rapid melting by the thick debris-cover.

III.5. *Meteorological condition of the glacial environment*

Among the various meteorological factors relating to the glacial system, both air temperature and precipitation are the most important and useful parameters in determining the glacial environment.

The air temperature was measured at three forefields of the glaciers; Glacier Camp (GC, 5090 m), Gangja La (GA, 5090 m) and Kyungka Ri NW (KY, 5140 m) (Figure 8; Shiraiwa *et al.*, 1992). Measurements at GC were carried out from May 1988 to February 1991, while measurements at the other two sites were done from June 1989 to March 1991. All measurement sites were located in wind-blown morainic fields, minimizing the possible influence of snow on the thermistor sensors which were installed 180 cm above the ground

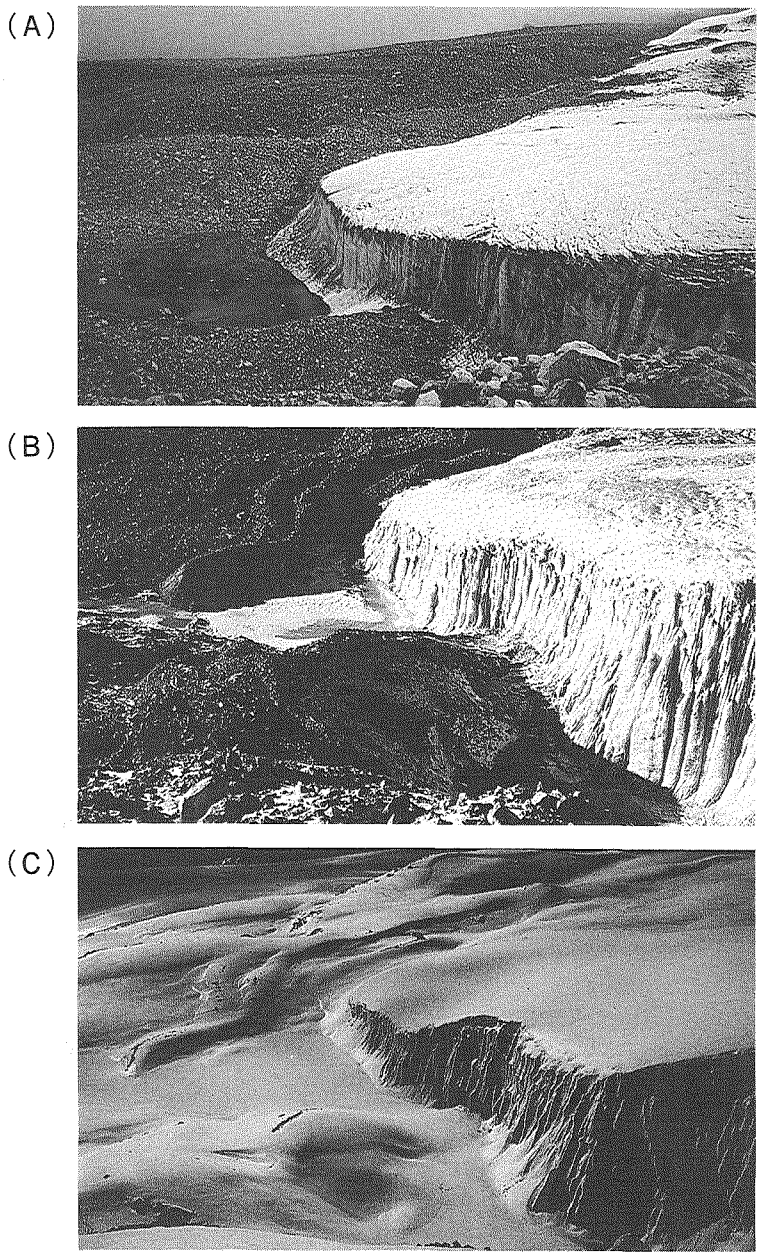

Figure 6 The terminal part of the Yala Glacier in the years of 1987 (A), 1989 (B) and 1991 (C). The terminus retreated slightly from 1987 to 1991, as shown by a distance between the minor moraine complex and the glacier terminus.

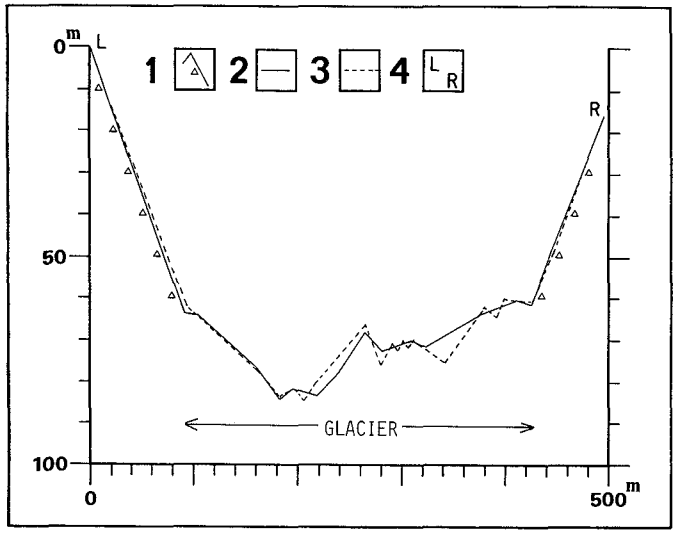

Figure 7 Transverse profile of the middle part of the Lirung Glacier in the Langtang Valley (Yamada *et al.*, 1992). Legend: 1. lateral moraine; 2. surface profile in 1987; 3. surface profile in 1989; 4; L and R indicate the left and right banks.

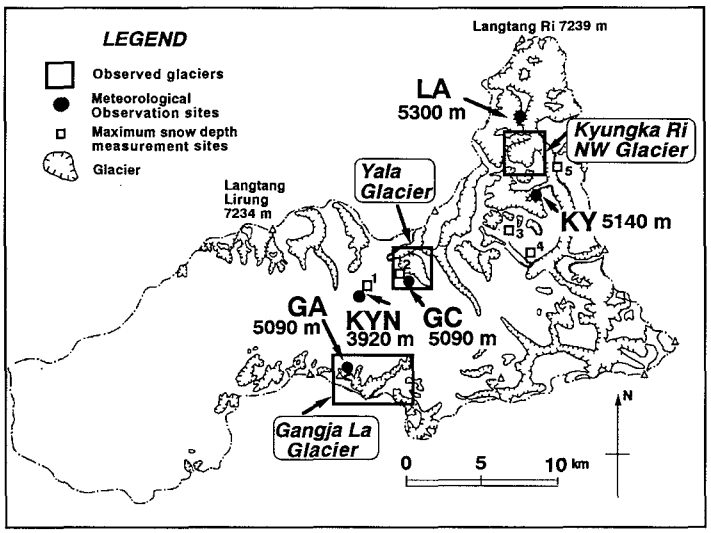

Figure 8 Glaciological and meteorological observation sites in the Langtang Valley (Shiraiwa *et al.*, 1992). Solid circles and squares indicate the meteorological observation sites and the sites where the maximum snow depth was measured, respectively. 1: Kyangchen (3920 m), 2: Glacier Camp (5090 m), 3: Pemdang Glacier (5013 m), 4: Pemdang Kalkha (4677 m), 5: Langtang Ri Base Camp (4942 m).

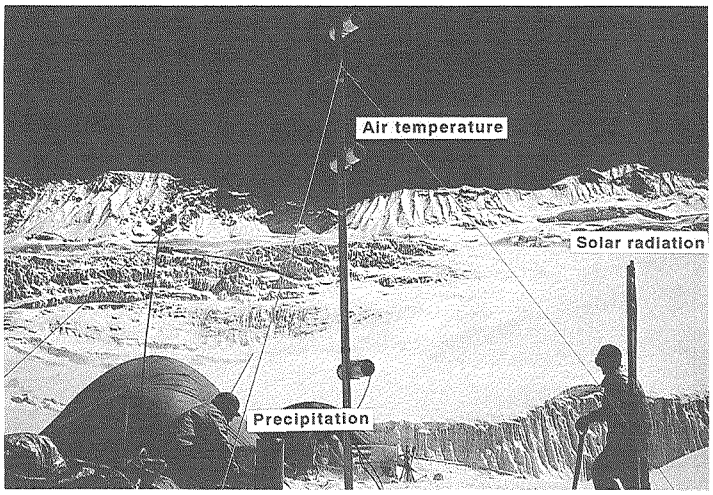

Figure 9 The typical meteorological equipments in the forefield of glaciers. This photograph shows the measurements of air temperature, precipitation and short wave radiation at Glacier Camp (GC; 5090 m).

surface and shaded with white pipes, and received natural ventilation (Figure 9). Data were recorded automatically every 30 minutes, and daily average values were used for analysis.

Precipitation was measured from June 1990 to April 1992 by a tipping-bucket gauge at Kyangchen (KYN, 3920 m), GC, GA and the Langtang Glacier (LA, 5300 m) (Figure 8). Hourly data were obtained from the automatic data-logger system. Daily accumulated data during the monsoon season, from June to September, were used for the analysis. Periods with probable snowfalls are excluded.

In addition, a maximum snow depth in winter was estimated at five locations in the valley using maximum snow depth meters. The meters were installed at KYN (Loc.1 in Figure 8), GC (Loc.2), the Pemdang Glacier (5013 m, Loc.3), the Pemdang Kalkha (4677 m, Loc. 4) and the Langtang Ri Base Camp (4942 m, Loc.5) in December 1989, and were withdrawn in June 1990.

Incoming solar radiation was measured at GA (5090 m), using a silicone photo diode which is sensitive to wave lengths from 0.4 to 1.1 μm. Measurements every hour were taken from June 1990 to February 1992, and the daily accumulated values were recorded.

III.5.1. Air temperature

Figure 10 shows the variation of daily mean air temperature in 1989 at GC. A gradual increase in air temperature characterizes the pre-monsoon season, from March to May. The monsoon season, from June to September, is dominated by positive air temperature

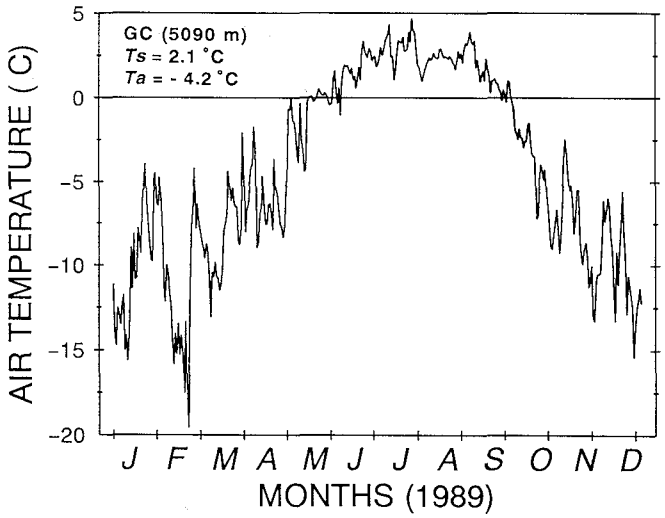

Figure 10 Daily mean air temperature in 1989, measured in the forefield of the Yala Glacier (GC) at an altitude of 5090 m.

values. In this season, diurnal variation of the air temperature is generally very small due to a thick cloud cover.

The monsoon season suddenly ends at the end of September and is followed by the post-monsoon season, from October to December. The air temperature decreases rapidly in this period, and the winter season begins in January. The winter is dominated by a daily mean air temperature of approximately −10 °C.

The daily air temperature during the four months of summer, from June to September, is always above freezing point. The average air temperature for the four summer months varies slightly from year to year with values of 2.4 °C in 1988, 2.1 °C in 1989, 2.6 °C in 1990 and 3.8 °C in 1991. A relatively higher average air temperature in the summer of 1991 is obvious.

The annual variation in the monthly air temperature at three stations indicates a similar pattern among the individual sites (Figure 11; Shiraiwa *et al.*, 1992); however, the variation of anomalies from the average values of three stations shows a seasonal difference (Figure 12; Shiraiwa *et al.*, 1992). In this figure, the 9-day running mean is plotted to eliminate day-to-day variations. From November to January, the three curves are similar to each other. On the contrary, during other periods, KY has relatively higher values and GC lower ones compared to the average of the three stations. Particularly in the period from the pre-monsoon to monsoon seasons, KY is almost +1 °C warmer than that of GC. GA has values very close to the average throughout the year except from February to April in 1990. The frequent cloud cover at GC, located at the southernmost part of the Langtang Valley, and the less cloud cover at KY, located at the northernmost part of the valley, explain well the

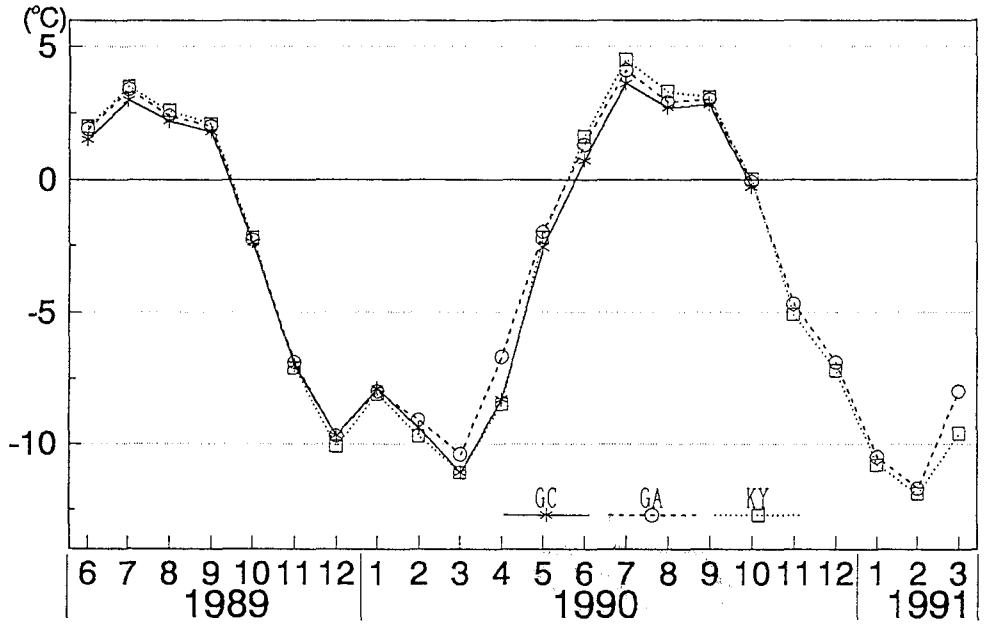

Figure 11 Monthly mean air temperature at three observation sites from June 1989 to March 1991 (Shiraiwa *et al.*, 1992). GC: Glacier Camp; GA: Gangja La; KY: Kyungka Ri.

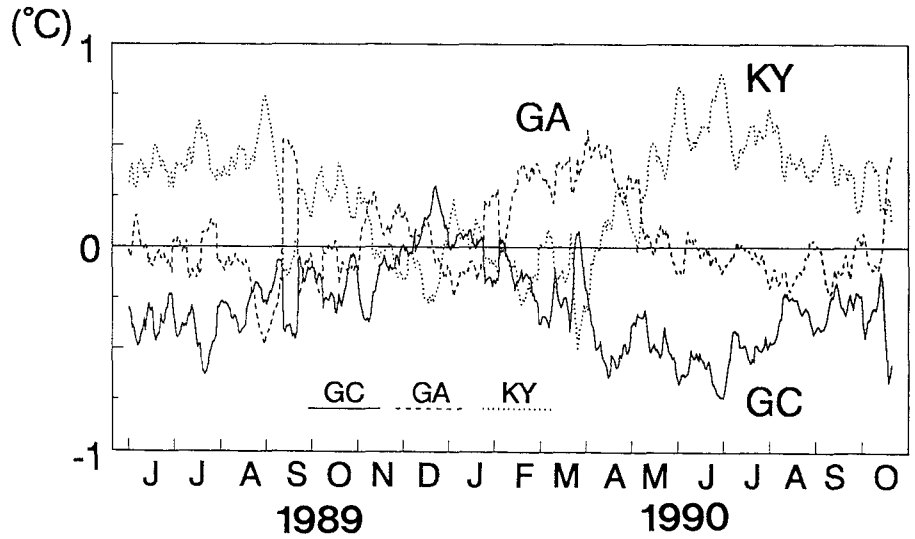

Figure 12 Time-series of the 9 days running mean values of the air temperature anomalies from the average values of three stations (Shiraiwa *et al.*, 1992). The air temperature at Station KY (5140 m) was calibrated to the air temperature at an altitude of 5090 m, using an air temperature lapse rate of 6 °C·km^{-1}. GC: Glacier Camp; GA: Gangja La; KY: Kyungka Ri.

temperature difference during the pre-monsoon and monsoon periods.

III.5.2. Precipitation

Precipitation is considered to be liquid during the monsoon season in Kyangchen, while it is supplied either as liquid or solid at other sites, judging from the empirical relationship between mean surface air temperature and the percentage of solid precipitation (Ageta, 1983a).

Figure 13 shows the daily precipitation changes during the monsoon seasons of 1990 and 1991. The monsoon season in 1990, defined as the time series of precipitation, unclearly started on the 15 June and suddenly ended on the 28 September, while in 1991 it continued from the 4 June to the 18 September.

The four time-series of both years change in the relatively same phase with cyclic fluctuations of 10 to 20 days, while the absolute amount of precipitation varies considerably from station to station. The total amount of monsoonal precipitation in both years was as follows: 530.5 and 427.0 mm at Kyangchen, 826.5 and 336.0 mm at the Glacier Camp, 967.0 and 942.0 mm at Gangja La and 556.0 and 512.5 mm at the Langtang Glacier. Large differences were not found in both years, except in the case of Glacier Camp. At this site, the rain gauge was installed at a calm site in 1990, then it was moved to a wind-blown field due to a shortage of sensor's cable. This re-installation probably reduced the collection efficiency of the gauge. The value of 336.0 mm, therefore, seems to underestimate the actual value.

The total amount of precipitation at KYN (3920 m) is almost two thirds of that at GC and GA. Station KYN is located at the bottom of the valley where less precipitation from the cumulus clouds is received, compared to the stations along the mountain slopes, as reported by Seko (1987) and Ueno and Yamada (1990). On the other hand, the precipitation at LA is nearly the same as KYN, although LA is located at almost the same altitude as GC and GA. This is because less moist air is conveyed to the upper part of the valley by monsoonal circulations which come from the south. The mountain barrier running from west to east at the southern side of the valley prevents the moisture at low levels from penetrating into the uppermost reaches of the valley.

Meanwhile, a small difference in the amount of precipitation between GC and GA indicates that nearly the same precipitation conditions exist between the south- and north-facing slopes at the middle reaches of the valley.

III.5.3. Maximum snow depth

Figure 14 (Shiraiwa *et al.*, 1992) indicates the maximum snow depth during the winter of 1989−1990 at five stations shown in Figure 8. It demonstrates the altitudinal dependence of the maximum snow depth; maximum snow depth increasing with increasing altitude. However, station 5, located in the upper part of the valley, received less snow compared to that of the middle reaches of the valley (Stations 2, 3 and 4), although these stations are

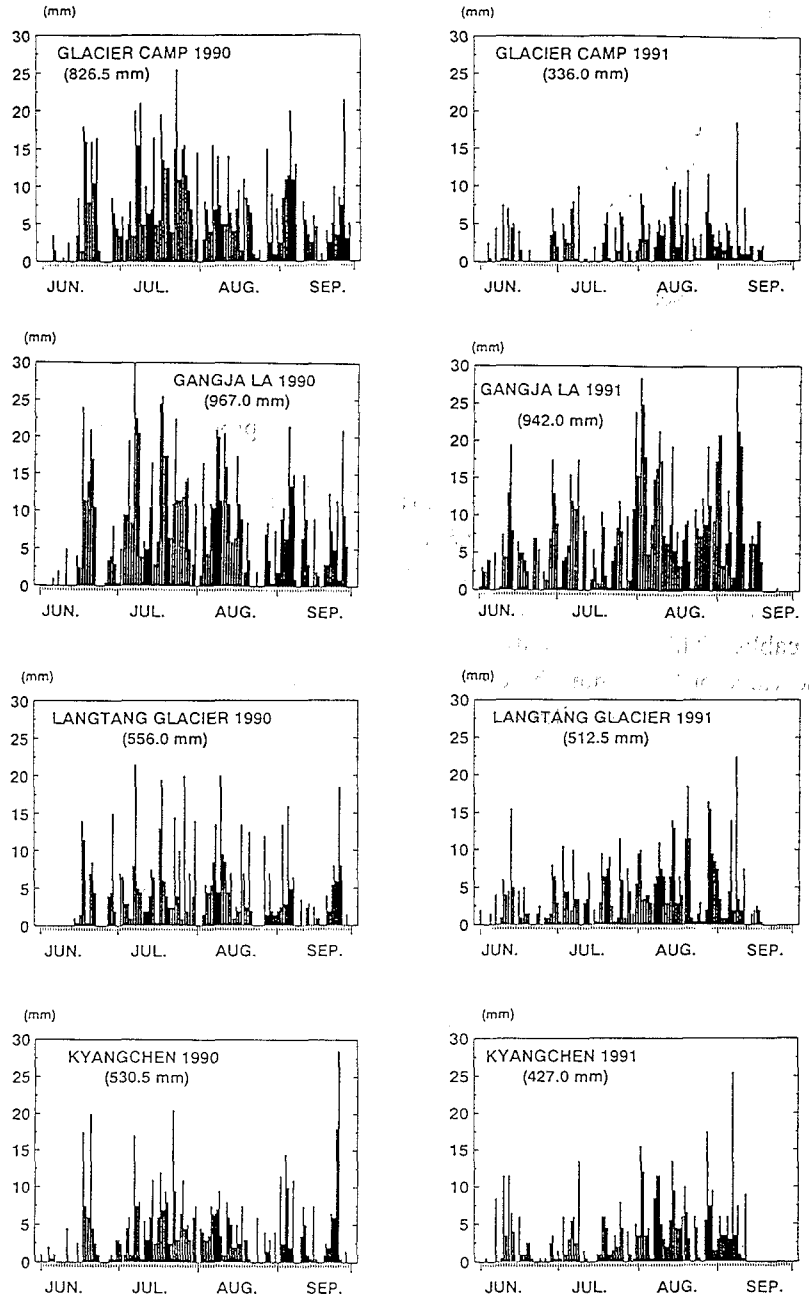

Figure 13 Daily precipitation changes at GC, GA, LA and KYN in the monsoon seasons of 1990 and 1991.

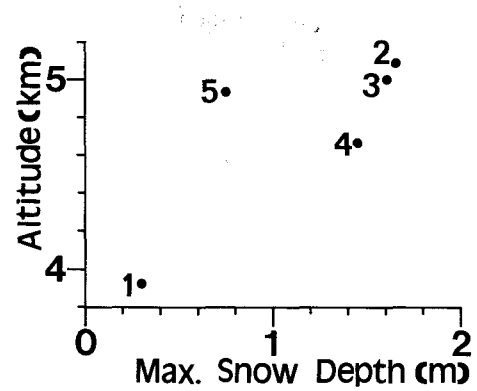

Figure 14 Relations between the maximum snow depth and the altitude in the winter 1989–1990 (Shiraiwa *et al.*, 1992). 1: Kyangchen (3920 m), 2: Glacier Camp (5090 m), 3: Pemdang Glacier (5013 m), 4: Pemdang Kalkha (4677 m), 5: Langtang Ri Base Camp (4942 m).

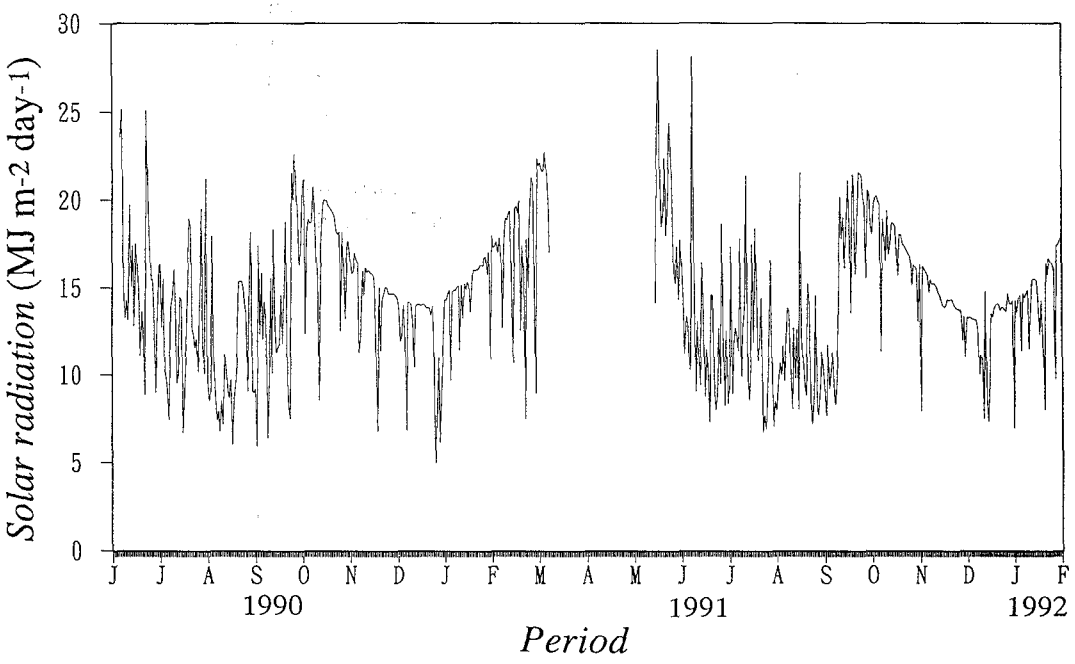

Figure 15 Annual variation of the incoming short wave radiation at the Gangja La (5090 m).

located at almost the same altitude. This result suggests that the precipitation during the winter of 1989/90 was also less in the upper part of the valley as in the summer of 1990 and 1991.

III.5.4. Short wave radiation

Figure 15 shows the daily incoming short wave radiation at Gangja La (5090 m). The

annual variation in the values represents the characteristics of the monsoon climate. The values are generally small and variable in the monsoon season due to the thick cloud cover. They are, in contrast, higher during both autumn and spring, and change in accordance with the solar altitude during the non-monsoonal period owing to the lack of cloud.

This fact strongly suggests that glacier ablation by incoming short wave radiation is not effective in summer but effective in autumn and spring. Since ablation by short wave radiation depends on the surface albedo of the glacier, it is necessary to know the condition of surface mass balance of the glacier during each season. This will be discussed later (section 6).

III.5.5. Regional characteristics of the climate in the Langtang Valley

The upper reaches of the valley are characterized by lower precipitation and higher air temperature during the monsoon season compared to the middle reaches of the valley. Less moisture-transport by monsoon circulation to the upper part of the valley, due to the barrier and inland effects, decreases convection and precipitation in the upper reaches. In this region, less cloud cover allows sufficient sensible heating from the ground which increases the air temperature higher than at the same altitude in the middle reaches.

On the contrary, the climate of the south- and the north-facing slopes in the middle reaches of the valley only displays a relatively small difference during the monsoon season. This suggests that monsoon winds initially supply moisture along the valley, and then, the moisture reaches the higher altitudes, over both slopes, by convection. The slightly higher air temperature recorded at GA than at GC during pre-monsoon and monsoon seasons (Figure 12) may reflect the less extensive cloud cover on the north-facing slopes.

III.6. *Seasonal variation of mass input on the glaciers and its significance*

Snow surveys were conducted on three small glaciers, the Yala, Gangja La and Kyungka Ri NW glaciers (Figure 16; Shiraiwa *et al.*, 1992). They are *clean-type* glaciers, having almost the same surface area (the Yala, 2.49 km^2; the Gangja La, 3.54 km^2; the Kyungka Ri NW, 1.60 km^2, respectively), and extending to almost the same altitudinal belt. They are mainly nourished by snowfalls rather than avalanches, since they are not surrounded by precipitous rock/ice walls. Furthermore, they represent three geographical conditions of the valley: south and north-facing slopes in the middle reaches, and the uppermost reaches of the valley.

Snow profiles were observed in May 1991 and April 1992, when the annual balance is likely to approach to the maximum in the Himalaya (Ageta, 1983b).

Snow pits were excavated down to the depth of the previous dirt layer at several altitudes on the glacier (Figure 16). Snow structure, thickness, density and temperature were measured at each profile.

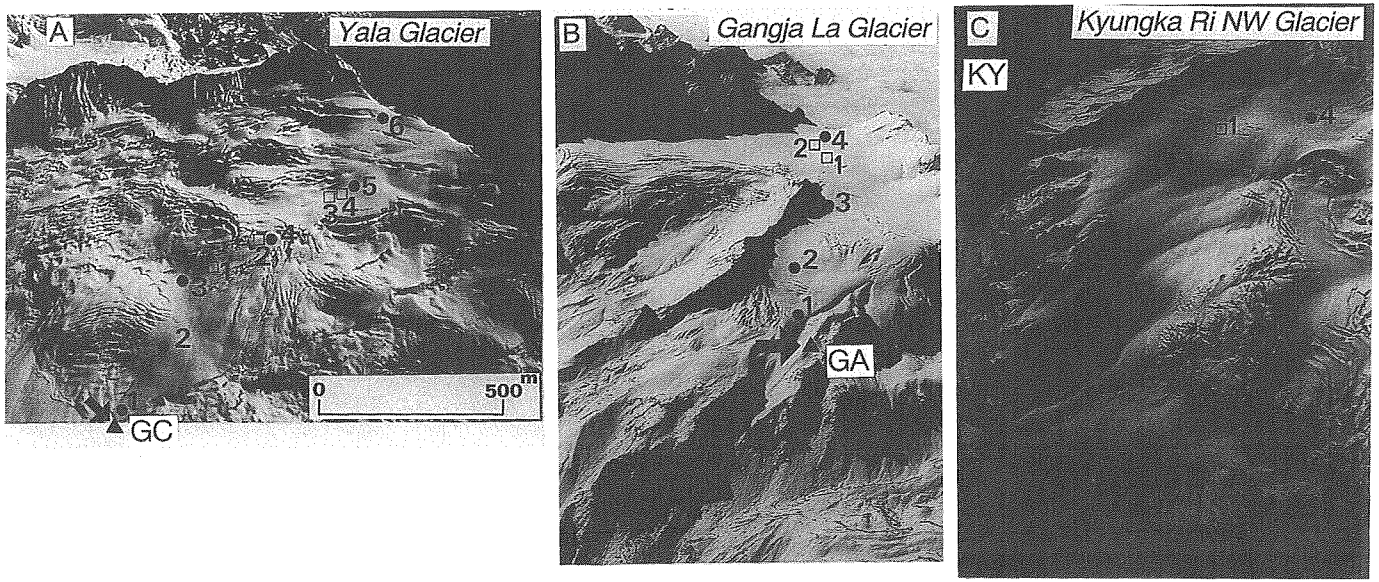

Figure 16 Snow survey sites on three glaciers. Solid circles indicate the sites where snow pits were excavated in 1991; while the open squares indicate those in 1992. Arrow indicates the location of meteorological observation site: GC, GA and KY. A: Yala, B: Gangja La, and C: Kyungka Ri NW Glaciers.

III.6.1. Spatial variation of mass input and characteristics of deposited snow on the glaciers

Figures 17 (Shiraiwa *et al.*, 1992) and 18 illustrate the snow profiles in the spring of 1991 and 1992, obtained at several altitudes on the three glaciers mentioned in the previous section.

A distinct dirt layer, often found at the bottom of the profile, marks the beginning of the monsoon season (Iida *et al.*, 1987; Kohshima, 1987). Therefore, the lowermost ice-layer and the major dirt layer at the bottom of the profiles are considered to represent the glacier surface at the beginning of the monsoon season of the preceding year. The profiles shown

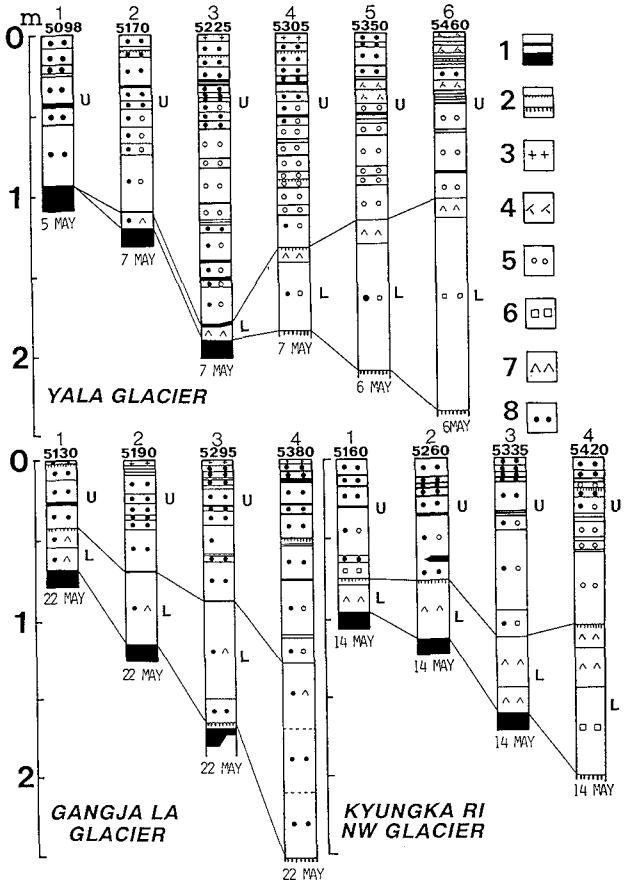

Figure 17 Snow profiles excavated at each glacier in May, 1991 (Shiraiwa *et al.*, 1992). 1: ice lens and ice layer, 2: thin and thick dirt layers, 3: new snow, 4: lightly compacted snow, 5: compacted snow, 6: solid-type depth hoar, 7: skeleton-type depth hoar, and 8: granular snow. The mixed symbols indicate the existence of several snow types.

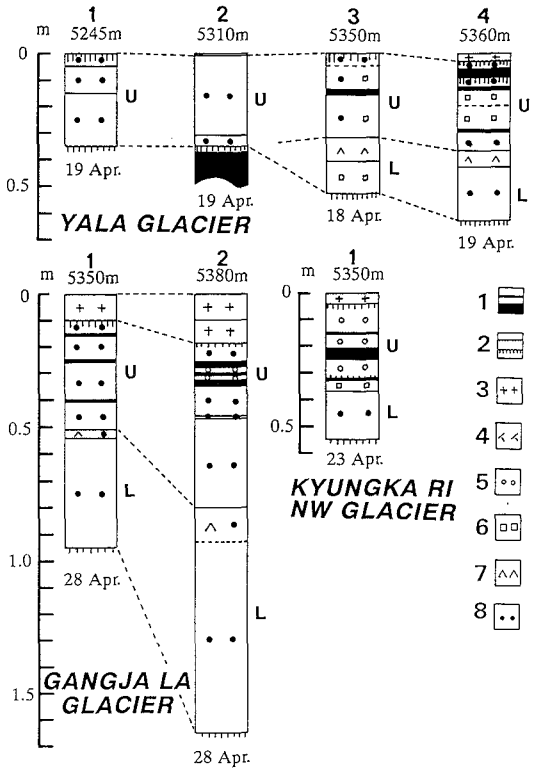

Figure 18 Snow profiles excavated at each glacier in April, 1992. Legends are the same as in Figure 17.

in Figures 17 and 18 represent the surface mass balance from the beginning of the monsoon in 1990 to May 1991, and from that in 1991 to April 1992.

Comparison of the amount of annually deposited snow in 1990–91 (Figure 17) on the three glaciers shows that most accumulation occurred on the Gangja Glacier, and the least on the Kyungka Ri NW Glacier, at an altitude of around 5350 m. This is also true in 1992 (Figure 18), although the amount of snow at Glacier Camp is considerably small in this year. The results in both years are consistent to those obtained by the meteorological observations which clarified that the upper reaches of the valley has a drier and warmer climate than the middle reaches during the monsoon season.

Snow profiles obtained on a higher part of the glaciers are divided roughly into two major snow layers (Figure 17): the Upper (U) composed of a series of thinly stratified compacted or granular snow layers intercalated with ambiguous dirt layers or ice lenses; and the Lower (L) recognized as a relatively homogeneously-grained snow layer mainly composed of solid-type or skeleton-type depth hoars. In the case of 1992, such characteristics

are less obvious; however, a depth hoar layer can be found at several profiles (Figure 18).

The Upper layer mainly consists of compacted and granular snow. During the study in 1991, it was observed that the compacted snow was metamorphosed into granular snow in the profiles excavated in the ablation area at the beginning of May and late May in the higher region. The grain size of the Upper layer is generally smaller than that of the Lower layer, while the temperature is higher.

The Lower layer is mainly composed of a depth hoar which is absent in the Upper layer. The grain size is large (up to 6 mm) especially in the skeleton-type depth hoar which is underlain by the solid-type depth hoar layer. The temperature of the Lower layer is slightly lower than the Upper layer. The boundary between the Upper and Lower layers is often marked by a thin dirt layer (Figure 17: profiles 5305 m of the Yala, 5130 m of the Gangja La, 5160 m, 5260 m, 5420 m of the Kyungka Ri Glaciers in the case of 1991).

A depth hoar layer can be formed by vapor transfer under a strong temperature gradient field at the snow surface (Akitaya, 1974; Fukuzawa and Akitaya, 1991). Figure 19 illustrates this process. In the monsoon season, wet snow continuously falls (dashed arrow) and accumulates a granular snow layer on the major dirt layer at the bottom of the profile (June-September). At the beginning of the post-monsoon season, continuation of clear days causes radiative cooling of the snow surface (thick arrow), and results in a strong temperature gradient near the surface which induces the formation of depth hoar (October). Sometimes,

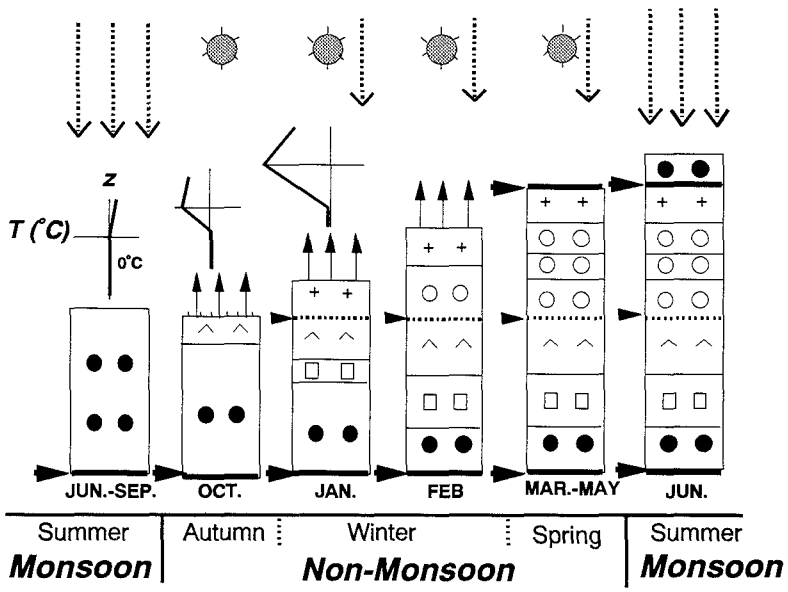

Figure 19 A scheme illustrating the snow accumulation in a year. Explanation is given in the text.

Sometimes, a dry fall-out makes a thin dirt layer on the surface (dashed line). Dry snow subsequently deposits intermittently (dashed arrow) above the hoar and dirt layers during the winter, and forms a stratified Upper layer (January-May). This process is repeated again in the next year (June).

The results of these observations and the interpretation of snow profiles described above lead to an important conclusion that the Upper and Lower layers represent the summer balance, and the balance between the beginning of the post-monsoon season and spring, respectively.

III.6.2. Seasonal and altitudinal variation in the mass balance of glaciers

The mass balance (b) at any time is the algebraic sum of the accumulation and ablation (Paterson, 1981). Since the snow profiles on the glaciers described before (Figure 17) represent the sum of the accumulation and ablation, they indicate also the mass balance for the period between the beginning of the monsoon season in 1990 and May 1991 at several points on the three glaciers.

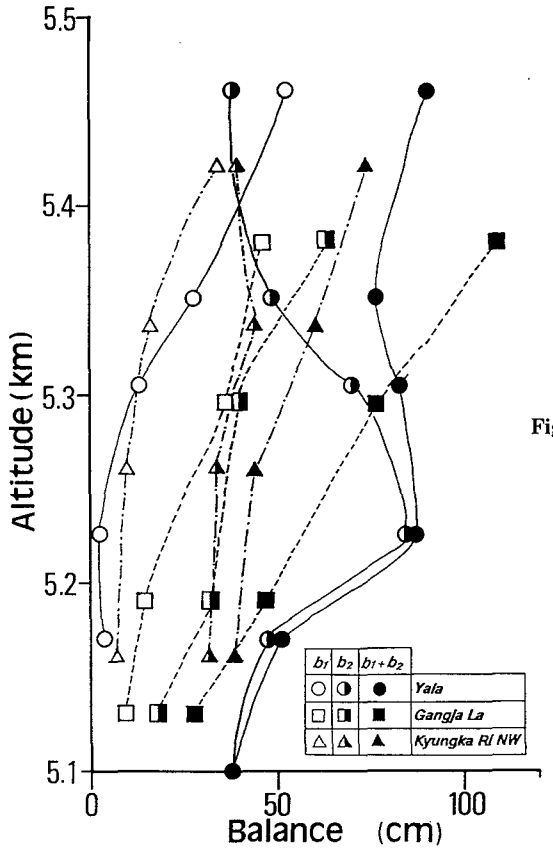

Figure 20 Altitudinal changes of the values of the surface mass balances (equivalent to water) obtained from the snow profiles (Shiraiwa *et al.*, 1992). The terms b_1 and b_2 indicate the surface mass balance during the monsoon season of 1990 and between the beginning of the post-monsoon seasons of 1990 and May 1991, respectively.

Figure 20 (Shiraiwa *et al.*, 1992) shows an altitudinal change in the water equivalent value of the surface mass balance which is divided into the balance of the monsoon season in 1990 (b_1: open symbols) and the balance from the beginning of the post-monsoon in 1990 to May 1991 (b_2: semi-open symbols). The term b_1 is the sum of the accumulation and ablation during the monsoon season, while the term b_2 only represents an accumulation during the rest of the observation period, because the ablation during this period is considered to be very small due to a cold air temperature and a negligible geothermal heat flux. Therefore, the summation of these two ($b_1 + b_2$: solid symbols) does not necessarily coincide with the annual net balance b_n, due to a lack of information for the month of June, 1991.

Seko (1987), Ohta *et al.* (1990) and Motoyama *et al.* (1990) pointed out the altitudinal dependence of the amount of solid precipitation in the Langtang Valley. In figure 20, an altitudinal dependence of b_1 seems to exist at these three glaciers, but that of term b_2 seems to be ambiguous. On the Yala Glacier, b_2 is exceptionally larger at altitudes of both 5225 m and 5305 m. This is because deposition of drift snow in winter disturbed the natural accumulation in these places. On the contrary, a slight decrease in b_2 at an altitude of 5420 m of the Kyungka Ri NW Glacier is probably caused by erosion of snow due to its windy location. Taking into account all the observational disadvantages mentioned above, it is difficult to find an altitudinal change in b_2. This probably reflects the narrowness of the altitudinal belt (only 400 m), defined by 3 glaciers studied here.

The spatial distribution of the surface mass balance was discussed in subsection III-6-1. Figure 20 also shows that the amount of b_1 is the largest on the Gangja La Glacier, and the least on the Kyungka Ri NW Glacier; while the amount of b_2 does not differ significantly among the three glaciers. This result leads to an interesting conclusion that the spatial variation of mass input on the glaciers is mainly determined by the summer monsoonal balance.

III.6.3. Reconstruction of the rate of seasonal mass input in a deeper profile

As described before, the result of snow profile observations reveals that the monsoonal snow accumulation can be distinguished from the non-monsoonal snow accumulation through detailed observation of snow profiles in spring. In this subsection, this interpretation is applied to a deeper snow profile in the accumulation area of the Yala Glacier, in order to reconstruct the rate of seasonal mass input into the glacier.

Figure 21 shows three deeper snow profiles obtained at an altitude of 5350 m on the Yala Glacier: the left column is a profile obtained by myself on 18 April 1992, the center and the right are those obtained at almost the same point in 1987 (Ozawa, 1991) and in 1985 (Iida *et al.*, 1987). Both in the 1992 and 1987 cores, most layers are metamorphosed to form firn and ice layers, except for the uppermost part. Six distinctive dirt layers are identified in the 1992 profile, each of which is easily found in the core. The 1987 profile, consisting of firn (granular snow), is intercalated with three dirt layers. In the case of the 1985 profile, depth

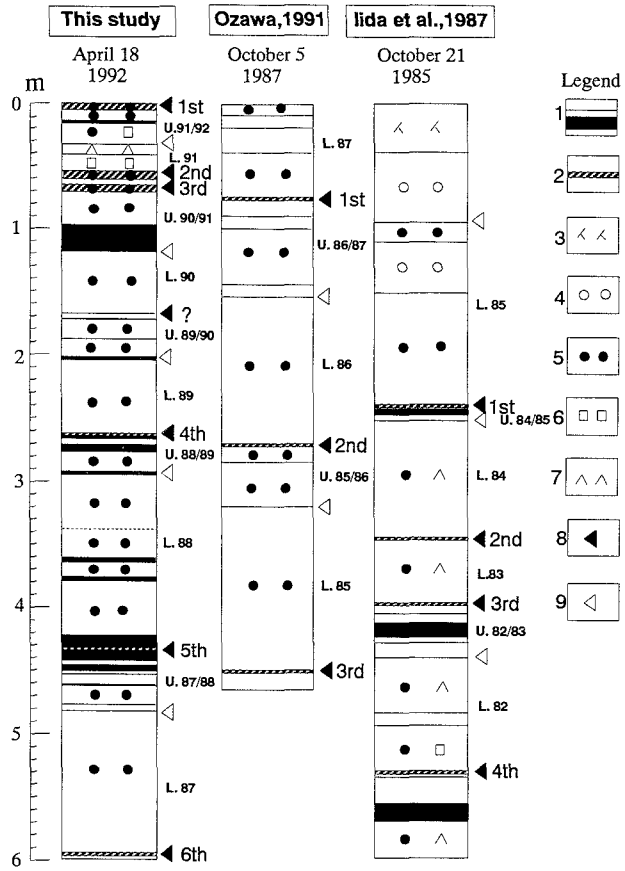

Figure 21 Surface snow cores excavated at an altitude of 5350 m from the Yala Glacier in 1992 (this study), and in 1987 (Ozawa, 1991) and 1985 (Iida *et al.*, 1987). Legend: 1; ice lense and ice layer, 2; dirt layers, 3; lightly compacted snow, 4; compacted snow, 5; granular snow, 6; solid-type depth hoar, 7; depth hoar, 8; boundary between the Lower and the Upper layers, and 9; boundary between the Upper and Lower layers.

hoar layers are found in a deeper section. There exist four dirt layers in this profile.

The formation process of dirt layers and different snow layers (Figure 19) allows the following interpretation regarding snow cores: in the 1992 core (Figure 21), the first dirt layer seems to be made by dry-fall out and biogenetic activity just before coring. The second and third ones indicate the surface in spring, 1991. The spring surface of 1990 can be located at a depth of 1.7 m, which makes the boundary between a large-grained granule layer (the

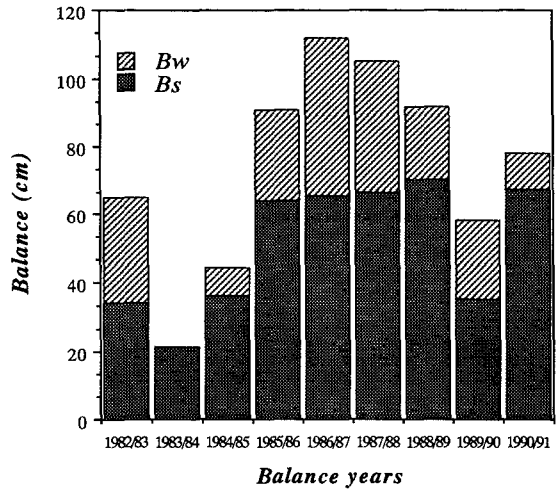

Figure 22 Inter-annual variation of the seasonal balance at an altitude of 5350 m of the Yala Glacier. B_w and B_s represent the non-monsoonal and monsoonal balance, respectively.

Lower layer) above and a thin stratified snow layer (the Upper layer) below. The fourth, fifth, and sixth dirt layers are considered to represent the spring surfaces of 1989, 1988, and 1987, respectively.

Open triangles in Figure 21 mark the boundary between the Upper and Lower layers, which represents the beginning of the post-monsoon season.

The 1987 and 1985 cores are also interpreted in this way in order to reconstruct the mass balance of the preceding years. Figure 22 illustrates the yearly variation of the annual and seasonal balance at an altitude of 5350 m from 1982 to 1990. The annual balance was at a minimum in the years 1983/84, and at a maximum in 1986/87. The summer monsoon balance has been surprisingly constant from 1985 to 1990, except for 1989. The non-monsoonal balance, on the contrary, varied considerably from year to year between the values of 0 mm (1983/84) and 465 mm (1986/87), in other words, 0% (1983/84) and 47% (1982/83) of the annual balance. These figures demonstrate that the non-monsoonal balance is not a negligible component in the annual value, since it often contributes to the annual balance at a rate of 30%.

III.7. *Glacier-climate relationship in the Langtang Valley*

III.7.1. Climatic features at the equilibrium line

In this section, the climatic features of the glacial environment in the Langtang Valley mentioned above are compared with those in the eastern Nepal Himalaya where intensive glaciological studies were conducted during the 1970s. Since the climatic features are variable in relation to altitudes, the comparison was done using values at equilibrium line altitudes (ELAs) for the glaciers.

Ageta (1983b) simulated both summer mean air temperature (T_s) and summer total

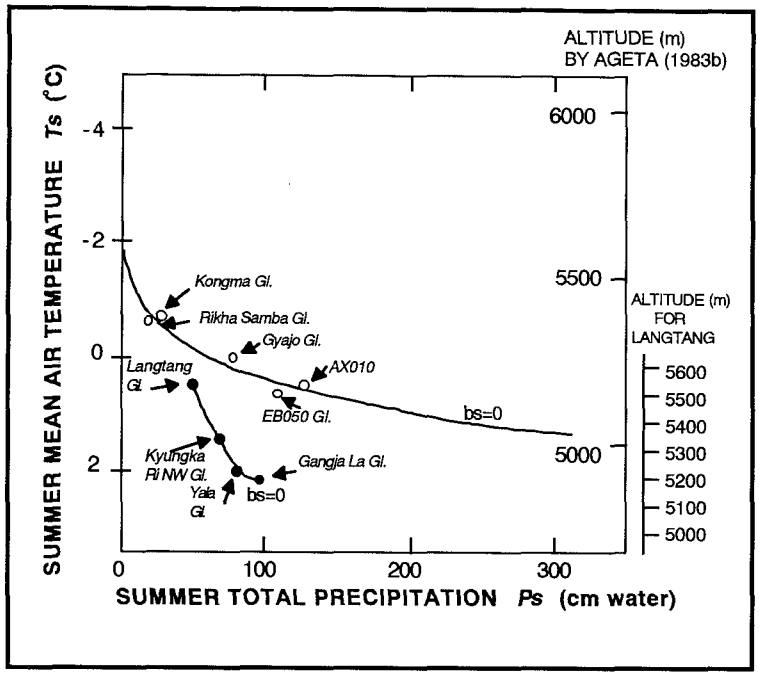

Figure 23 Simulated relationship between summer mean air temperature (T_s) and summer total precipitation (P_s) at ELA in the Nepal Himalaya (after Ageta, 1983b). The open circles are the values of several glaciers in the Nepal Himalaya, observed in the 1970s. The solid circles are plotted for the glaciers in the Langtang Valley, with the data collected for this study.

precipitation (P_s) at ELA in the Nepal Himalaya, on the basis of observations of the glacial environment in the Shorong region (Figure 23). Open circles were plotted, using the observational data for the individual glaciers. The simulated curve coincides well with the observed values of the glaciers. Glaciers were sampled from the Khumbu (Kongma, Gyajo, and EB050), the Shorong (AX010), and the Mukut Himal (Rikha Samba) regions. Ageta (1983b) considers this result to represent the glacier-climate relationship of the Nepal Himalaya (Ageta, 1983b, p.96, Figure 6).

The solid circles in the figure were plotted using my own observational data from the Langtang Valley. For the Langtang Glacier, T_s at LA (the name of observation site is shown in Figure 8) during 1991, and the mean value of P_s at LA during both 1990 and 1991, were adopted. For the Kyungka Ri NW Glacier, a mean value for T_s at KY both in 1989 and 1990 was used, while P_s was assumed to be between the values of GC and LA. For the Yala Glacier, a mean value of T_s at GC from 1988 to 1991, and the value of P_s at GC in 1990 were used. For the Gangja La Glacier, a mean value of T_s at GA from 1989 to 1991, and mean

value of P_s at GA both in 1990 and in 1991, were taken. The values of T_s at each glacier are subsequently converted to those at the equilibrium line altitude (ELA) for each glacier, using an air temperature lapse rate of 6 °C·km^{-1}.

In the Langtang Valley, T_s becomes lower and P_s becomes smaller at the ELA towards north. This northward change of climatic features is in accordance with the simulation by Ageta (1983b). The values are, however, significantly different from those presented by Ageta (1983b); the T_s values at ELA in the Langtang Valley are warmer than those of other regions of the Nepal Himalaya, as far as the same precipitation is considered. In other words, the ELA in the Langtang Valley is maintained in warmer climate than those of glaciers in other areas. On the other hand, if T_s is assumued to be the same, P_s at the ELA in the Langtang Valley is smaller than those of Ageta's diagram.

This can be explained by sufficient mass input during non-monsoonal periods in the Langtang Valley (Chapter III-6-2). The winter accumulation must lower the ELA, and this will increase air temperature at the ELA during summer. In other words, the winter accumulation compensates for the shortage during summer, therefore, the ELA can be maintained in a drier condition than those presented by Ageta (1983b). Since the glaciers presented by Ageta (1983b) are considered to have mainly accumulated during the summer monsoon season, differences can be explained by this seasonal difference of mass input.

III.7.2. Relationship between the glacier mass balance and climatic factors

Hahn and Shukla (1976) suggested that the intensity of the Indian monsoon represented by summer precipitation in India is related to the snow conditions of the preceding winter on the Eurasian continent. This relationship is now extended to a more complicated coupled cryosphere/atmosphere/ocean climate system (*e.g.* Yasunari, 1990). The non-monsoonal precipitation is, on the other hand, analyzed in relation to cyclonic activity over the Eurasian continent (Ueno *et al.*, in press). Since the sequential mass balance data of the Himalayan glacier record the seasonal variation in the amount of snow, they provide information on the past climatic condition.

In this section, the mass balance data of the Yala Glacier and selected climatic data in Kathmandu are compared to discuss a possible relationship between the glacier mass balance and climatic conditions in the Himalaya.

Figure 24 shows inter-annual variations in the monsoonal (B_s) and non-monsoonal (B_w) balance at an altitude of 5350 m at the Yala Glacier in conjunction with the mean summer air temperature (T_{sk}), total monsoonal (P_{sk}) and non-monsoonal precipitation (P_{wk}) in Kathmandu during the last decade (DIHM, 1984, 1986 and 1988). B_s is discussed in relation to T_{sk} and P_{sk} since all of these factors are determined by the summer monsoon climatic system, while B_w is related to P_{wk} as they are controlled by the non-monsoonal climatic system.

The inter-annual variation of B_s has a negative correlation with T_{sk} and has a weak

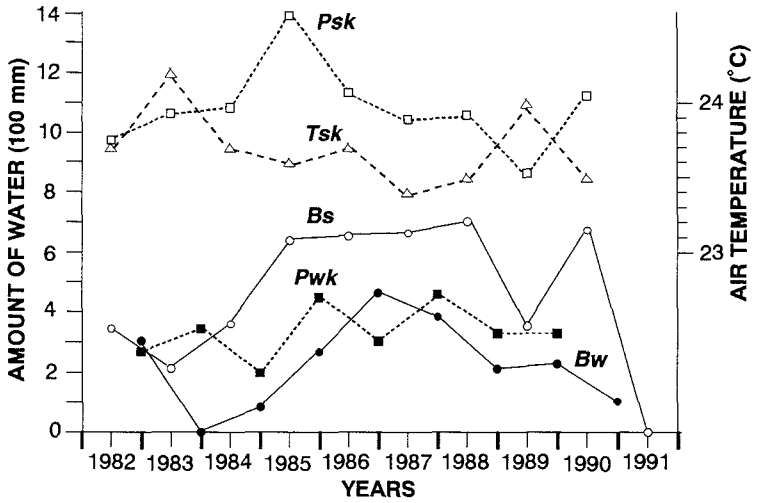

Figure 24 Inter-annual variation of the mean summer air temperature at Kathmandu (T_{sk}), total summer precipitation at Kathmandu (P_{sk}), total winter precipitation at Kathmandu (P_{wk}), the mosoonal (B_s) and non-monsoonal balance (B_w) of the Yala Glacier at an altitude of 5350 m.

positive correlation with P_{sk}. A closer relationship between B_s and T_{sk} can be ascribed to a strong dependence of the glacier mass balance on the summer air temperature as first noted by Ageta (1983a). Considering a consistent amount of B_s in the period between 1985 and 1988, when the value of P_{sk} changes greatly, the amount of summer precipitation does not seem to play an important role in determining the summer balance of the small glaciers.

Although it is not very clear, a weak positive correlation can be found between B_w and P_{wk}. This fact suggests that the amount of precipitation becomes more important in determining the non-monsoonal balance of the glacier, for it is mostly supplied as snow, and the ablation by positive air temperature is strictly limited during this period.

It is concluded from the discussion above that the intensive monsoon climate increases the monsoon balance both by supplying sufficient precipitation and probably by reducing air temperature by shading, indirectly reducing the incoming solar radiation. Meanwhile, the amount of non-monsoonal precipitation determined by cyclonic activity directly influences the non-monsoonal balance of the glaciers. The annual balance of the glacier is, therefore, controlled by two different climatic systems.

IV. Present cryogenic environments

IV.1. *Introduction*

Present cryogenic environments are composed not only of glacial features but also of periglacial phenomena, and these two are closely related to each other. In considering the extent of the present and past glaciations, periglacial features provide a valuable information on the problem.

Distribution of permafrost is, for example, strongly influenced by glacial activity. Permafrost, defined as ground remaining frozen for more than a year, is inhibited from developing under glaciers, because glaciers prevent ground from intensive freezing during winter. Thus, the altitudinal distribution of an alpine permafrost zone is demarcated by the ELA and air temperature, and it varies in relation to the amount of precipitation (Haeberli, 1983).

Distribution of periglacial features is also related to the present glacier extention: several kinds of patterned ground preferentially develop at the forefields of glaciers, since meltwater is sufficient there; and in the mountains in Norway, development of patterned ground is discussed in relation to a time span after deglaciation (Ballantyne and Matthews, 1982).

Rock debris on ablation areas of glaciers, on the other hand, significantly influences ablation processes of glaciers in the Himalaya (Inoue and Yoshida, 1980). This debris originates from both frost-shattered rockfall (Matsuoka, 1984) and subglacial erosional processes. It is, therefore, an important task to clarify both the mechanism and the volume of fractured rocks as a controlling factor of the glaciation in the Himalaya. Fushimi (1980) suggested that the amount of debris supplied onto the glaciers increases with increasing area of free-face since the deglaciation time, based on his experience on the Khumbu Glacier in East Nepal (Fushimi *et al.*, 1980). This implies that the present cryogenic processes are closely related to the glacier fluctuations in the Himalaya.

Interactions between glacial and periglacial phenomena are, thus, very important in understanding the present alpine environments.

In this chapter, at first, the occurrence of the permafrost is estimated by freezing and thawing indices, and by direct measurement of ground temperatures. Then, the periglacial landforms are described. Next, the present cryogenic processes in the Langtang Valley are discussed by emphasizing the rock breakdown caused by frost shattering. The rock surface temperature data provide an important key to explaining this process. Finally, the vertical zonation of the cryogenic environment is discussed in conjunction with the glacial environment.

IV.2. *Previous work*

Cryogenic environments in the Himalaya have been mainly discussed with regard to the

following three topics; permafrost, periglacial features, and frost-shattering. Although the number of previous studies is limited, some of the results are reviewed here.

Permafrost in the Nepal Himalaya was first noted by Müller (1958/59) who observed a seasonal freeze-thaw process of ground at Gorakshep (ca. 5150 m) in the Khumbu region. He reported patterned ground as well as two ice-wedge casts, but he denied the existence of permafrost.

Studies on the permafrost in the Nepal Himalaya were subsequently conducted by Fujii and Higuchi (1976) and Fujii (1980). The occurrence of alpine permafrost was estimated by measuring the change in altitudinal lapse rate at 50 cm-depth ground temperatures. The work clarified that the lower boundary of alpine permafrost in the Khumbu region is situated at an altitude of about 5000 m, and the mean annual air temperature at the boundary corresponds to −2.4 to −3.0 °C. Fujii (1980) also noted that the existence of well developed patterned ground is closely related to the occurrence of alpine permafrost in the Mukut Himal in western Nepal.

Periglacial landforms and their vertical zonation were described in the Khumbu (Iwata, 1976b, 1978), Mukut Himal (Fujii, 1976) and Langtang Valley (Watanabe *et al.*, 1989). They described various types of periglacial phenomena such as talus, rock glacier, block stream, block slope, and several types of patterned ground. By considering both climatic and geomorphic factors in the Khumbu and Mukut Himal, Iwata *et al.* (1976) clarified the characteristics of vertical zonation of the periglacial belt in the Himalaya. They concluded that the Tibetan slopes of the Himalaya are characterized by a vertically wide range of sorted patterned ground, while the Nepalese slopes are characterized by vegetated patterned ground. They explained this contrast by a basic difference in the topography in the Himalaya between the Tibetan and Nepalese sides: a wide gentle debris-covered slope at a high altitude in the former, and the occupation of the same slopes by precipitous rocky walls or glaciers in the latter.

Matsuoka (1984) estimated that the altitudinal belt between approximately 5000 and 5500 m currently suffers the most active frost-shattering in the Great Himalaya, on the basis of both air temperature and precipitation. On the other hand, Whalley *et al.* (1984) suggested chemical weathering is significant in the Karakoram Range by observing both rock surface temperature and weathering conditions. However, no quantitative measurements of rock breakdown by frost-shattering have been done in the Himalaya, although the rock surface temperature has been occasionally recorded in the Himalaya as a controlling factor for rock breakdown (Hewitt, 1968; Dronia, 1978; Kuhle, 1986a, 1988b; Francou, 1989).

IV.3. *Permafrost*

Occurrence of alpine permafrost was investigated in the Langtang Valley by means of two different methods: an estimation by climatic indicators, and a direct measurement of ground temperature profiles.

The relationship between the climatic parameters and the occurrence of permafrost has long been one of the main topics in the study of periglacial environments. The occurrence of permafrost has been discussed in relation to mean annual air temperature (*e.g.*, Brown and Péwé, 1973), the mean air temperature of the coldest and warmest months (Fujii, 1980), and freezing and thawing indices (Harris, 1981). Among these relationships, the freezing and thawing indices, given in degree days of freezing and thawing over an unbroken freezing or thawing period (Sanger, 1966), are of particular value in demarcating permafrost environments in areas with snow cover less than 50 cm thick in winter (Harris, 1981; Sone, 1990). These indices have been obtained for several locations in the forefields of the glaciers in the Langtang Valley.

IV.3.1. Estimation by freezing and thawing indices

The freezing and thawing indices were calculated by measuring air temperature in the forefield of glaciers over 1 year. Air temperature at 180 cm above the ground surface was monitored at Glacier Camp (GC: 5090 m), Gangja La (GA: 5090 m), Gangja La South (GAS: 4920 m), Semsethang (SEM: 5000 m), Kyungka Ri (KY: 5140 m) and Kyangchen (KYN: 3920 m) from 1 June, 1989 to 31 May, 1990 (Figure 25). It was subsequently measured at Pemdang (PEM: 5160 m) from 16 June, 1990 to 15 May, 1991, and at Langtang Glacier (LA: 5300 m) from

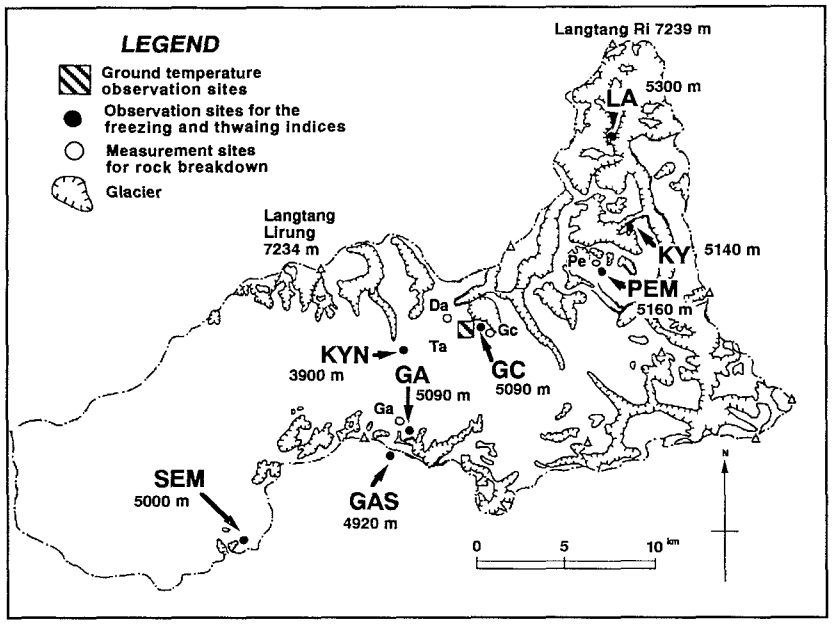

Figure 25 Location map of several observations on cryogenic phenomena in the Langtang Valley.

14 May, 1991 to 23 April, 1992. Air temperatures were measured every 30 minutes, and they were converted to a daily mean value to calculate the freezing and thawing indices. The period of data obtained at Pemdang and Langtang Glacier was slightly less than a year; however, these data were tentatively used for analysis because the missing period was less than a month.

The measurement sites are located in the morainic fields just in front of the glaciers, except for Kyangchen (KYN). Therefore, they represent the highest point in the periglacial environment of the valley. They are arranged latitudinally, from 28°5′N to 28°19′N. Their altitude rises northward. It means that the periglacial belt ascends altitudinally toward the north, reflecting the northward rise of the ELAs. Only site KYN is located at the bottom of the main valley at an altitude of 3920 m.

Table 4 Mean annual air temperature, freezing and thawing indices of the glacier forefields of the Langtang Valley.

LOCATION NAME	ALTITUDE (m)	LATITUDE	LONGITUDE	MEAN TEMP. (℃)	F. INDEX (℃·days/yr.)	T. INDEX (℃·days/yr.)	DURATION OF OBSERVATION
GC	5090	N 28°14′	85°37′ E	-4.0	1735.0	269.1	Jun.1,89-May 31, 90
GA	5090	N 28°10′	85°35′ E	-3.6	1610.2	312.0	Jun.1,89-May 31, 90
GAS	4920	N 28°09′	85°34′ E	-2.9	1405.7	356.9	Jun.1,89-May 31, 90
SEM	5000	N 28°07′	85°30′ E	-4.0	1749.7	276.6	Jun.1,89-May 31, 90
PEM	5160	N 28°16′	85°41′ E	-3.8	1561.8	284.7	Jun.16,90-May 15,91
KY	5140	N 28°17′	85°42′ E	-3.9	1743.8	329.0	Jun.1,89-May 31, 90
KYN	3920	N 28°13′	85°34′ E	3.3	381.6	1571.3	Jun.1,89-May 31, 90
LA	5300	N 28°19′	85°42′ E	-4.6	1883.0	276.0	May 14,91-Apr.23,92

Table 4 indicates the freezing and thawing indices at each site. Even excluding site KYN, the freezing index varies considerably from the largest value recorded at LA (1883 °C·days/yr.) to the smallest one at GAS (1406 °C·days/yr.). This is mainly because LA is the highest (5300 m) and GAS is the lowest (4920 m) site in the valley. The thawing index, however, does not vary significantly among the sites. Although the reason is not clear at present, it may be explained by a relatively short thawing period at the sites.

The plot of freezing and thawing indices obtained in the valley to Harris's diagrams (Harris, 1981) shows a possible occurrence of continuous permafrost (Figure 26). According to Harris (1981), the upper right of the diagram represents a continental climate, while the lower left represents a maritime climate. The plot of index values in the Langtang Valley falls in the continuous permafrost zone in a maritime climate.

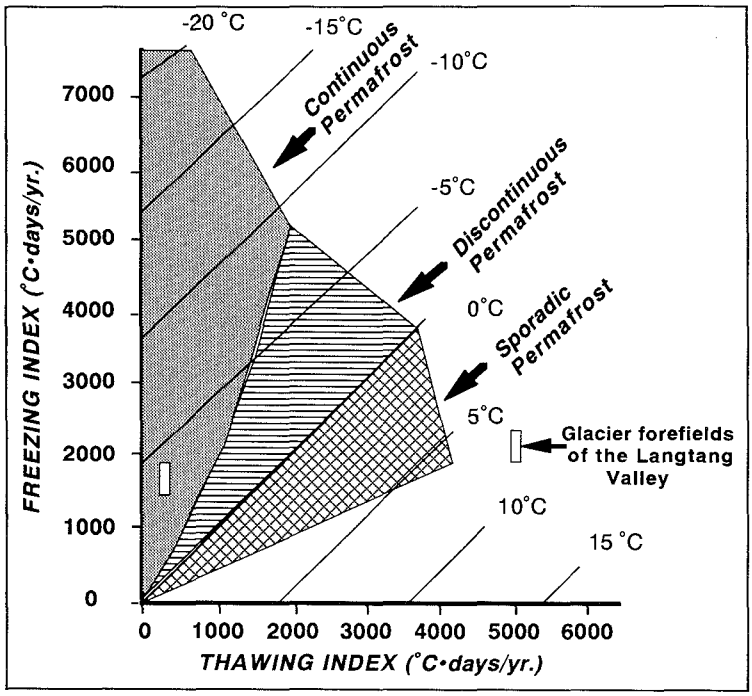

Figure 26 Diagram illustrating the relation between permafrost zones and freezing and thawing indices (Harris, 1981). The values of the glacier forefields of the Langtang Valley are plotted in the figure.

IV.3.2. Measurements of ground temperature

Ground temperature was measured temporarily and annually at GC (5090 m), just in front of the Yala Glacier. Temporal measurements of the ground temperature profiles were conducted at four sites: sites 1 to 3 at GC, and site 4 in KYN (Figure 25) in September 1987, when the thickness of the active layer attained its maximum. The ground temperature in this season is, therefore, considered to represent the highest value during the year.

Figure 27 shows the temporal ground temperature profiles. At KYN (site 4), the profile is far above the freezing point, and the gradient of the profile is almost neutral in the deeper part, thus, it is concluded that Kyangchen is not underlain by permafrost. Takahashi *et al.* (1987b) also gives a value of 6.8 °C as a mean annual ground temperature at 100 cm depth in Kyangchen.

At three stations in GC, the profiles are much closer to the freezing point. Near-surface temperatures are considerably different in each profile, because profile 1 was measured in snowy condition, while 2 and 3 were measured in clear weather. The difference between 2 and 3 is ascribed to the measuring time; profile 2 was measured at 16:00 when a daily

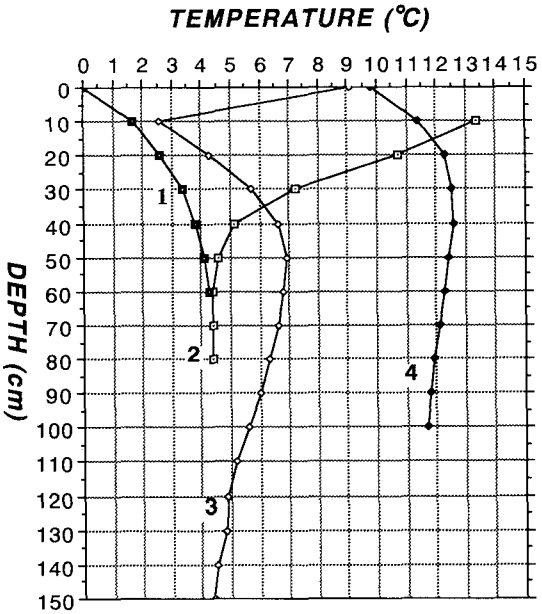

Figure 27 The ground temperature profiles around the margin of the Yala Glacier. The altitude, weather, time and date of the measurements are as follows; 1: 5090 m, snow, 16: 40, 11 September, 1987, 2: 5070 m, clear, 16:14, 16 September, 1987, 3: 5090 m, clear, 11:30, 29 September, 1987, and 4: 3920 m, cloudy, 07:45, 23 September, 1987.

warming of the ground proceeded into the deeper horizon, while profile 3 was measured in the morning at 8:30 when only the surface was heated. With all the differences near the surface, the deeper part below 60 cm has almost the same temperature at 4.5 °C. Because the gradients of the profiles are almost neutral at this depth, the occurrence of permafrost is difficult to confirm at GC.

In order to confirm this judgement, a full-year observation of the ground temperature profile was conducted from June 1990 to February 1992 in the moraine field of the Yala Glacier at an altitude of approximately 5090 m (Figure 25). The site is located on the Little Ice Age moraine of the Yala Glacier. The ground is composed of till of variable components from silt-sand to gravel. From June 1990 to May 1991, the ground temperatures were measured at depths of 30, 60, 90, 120, and 150 cm below the surface, and from May 1991 to February 1992, at depths of 2, 10, and 30 cm. The sensors were platinum resistance thermometers of 100 ohm, and the data were recorded on an automatic data logger (DATAMARK of Hakusan Kogyo Co.). The data were recorded every 3 hours from June 1990 to May 1991, and every 1 hour from May 1991 to February 1992.

Figure 28 shows the time series of the ground temperatures every 3 hours at depths of 30, 60, 90, 120, and 150 cm. The temperatures at each depth remained positive from mid-June to mid-October, and negative during the rest of the period. The data imply that there is no permafrost at least down to 150 cm below the surface at this site. Daily fluctuation of temperature is remarkable at a depth of 30 cm, while, below that depth, it becomes small. Only one freeze-thaw cycle of ground temperature at each depth could be counted. There-

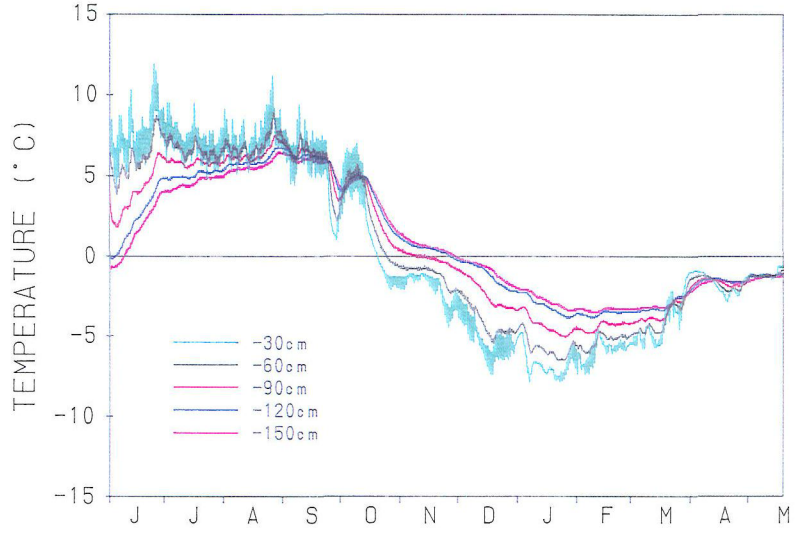

Figure 28 Changes in the 3-hour ground temperatures in the forefields of the Yala Glacier (5090 m; GC in Figure 25) from June 1990 to May 1991.

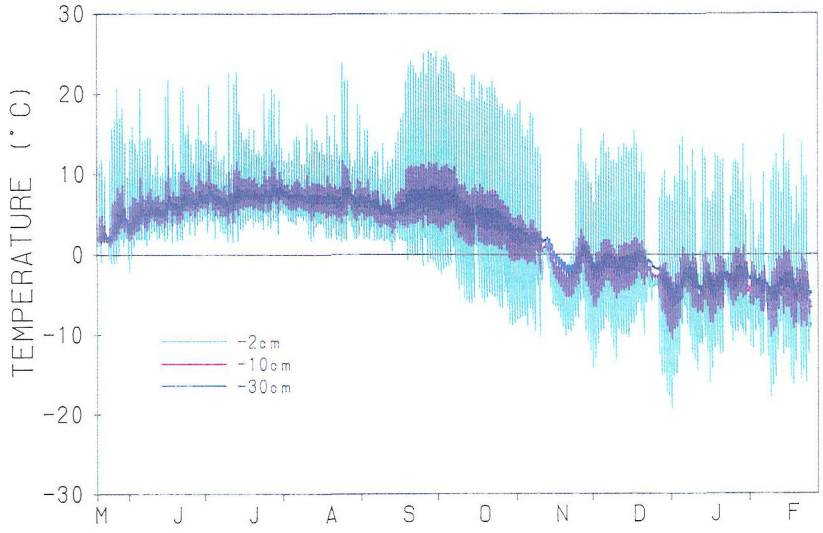

Figure 29 Changes in the hourly ground temperatures at Glacier Camp (5090m) from May 1991 to February 1992.

fore the freeze-thaw cycle is an annual one.

However, the daily fluctuations of ground temperatures are considerably large near to the surface (2 cm depth), and often oscillated around 0 °C during winter (Figure 29). This is, however, partly due to the snow condition during the year; the winter of 1991−92 was characterized by an exceptionally thin snow cover. The freeze-thaw cycle of the ground surface must be smaller in ordinary years due to a thick snow cover. Meanwhile, the figure shows that the daily freeze-thaw cycle occurs only near the surface, and that the freeze-thaw cycle of the ground is probably a yearly one at depths below 10 cm from the surface.

For the deeper section, the occurrence of permafrost is estimated by extrapolating the minimum and average profiles toward the deeper part of the section (Figure 30). The seasonal fluctuation of ground temperature is estimated to penetrate 500 cm. Seasonal frost on the ground may penetrate down to a depth of 425 cm. The profile of the average ground temperature suggests that there exists no permafrost at this site. However, since the temperature at 500 cm depth is estimated to be about 1 °C, the site must be very close to the lower boundary of a discontinuous permafrost zone.

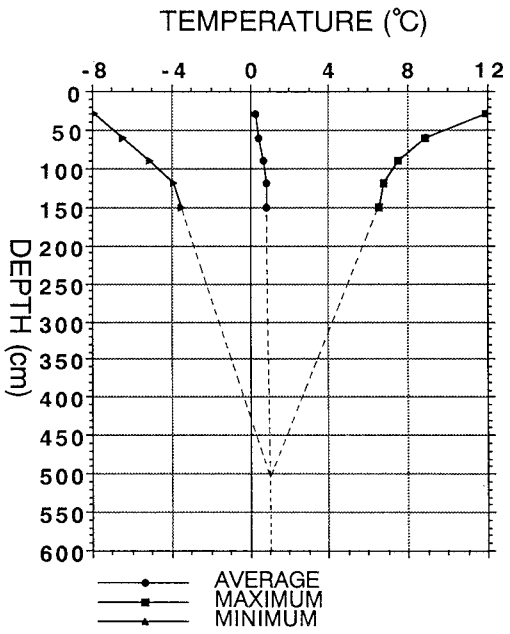

Figure 30 Thermal regime in the forefields of the Yala Glacier (5090 m).

IV.3.3. Reason for the lack of permafrost

The forefields of glaciers in the Langtang Valley were examined in relation to the occurrence of alpine permafrost, by means of the freezing and thawing indices, and by direct measurement of ground temperatures. The former method suggests the possibility of occurrence of permafrost, while the latter denies it, although the measurement was limited to one place. The reason for this contradiction is discussed here.

According to Fujii and Higuchi (1976), the altitude and the annual air temperature at the lower boundary of permafrost in the Khumbu region are about 4900−5000 m and from −2.4 to −3.0 °C. Since the altitude and the mean annual air temperature of the observation sites in the Langtang Valley are from 4920 m (GAS) to 5300 m (LA), and from −2.9 °C (GAS) to −4.6 °C (LA) (Table 4), all the sites should have been located in the permafrost zone.

One of the significant differences in the climatic environments between the Khumbu and Langtang regions is the amount of non-monsoonal precipitation. The Langtang Valley has received a considerable amount of non-monsoonal precipitation for the last 9 years (Figure 22), and the forefield of the glacier has been covered with thick snow during the winter. On the other hand, the Khumbu region is characterized by a dry winter, and the ground surface is scarcely covered with thick snow.

According to Higashi (1954), long-term persistence of snow of at least 15 cm thickness on the ground can disturb the freezing of the ground. Therefore, the thick snow cover in the Langtang Valley in winter is likely to have a negative effect on the development of permafrost. This seems to be the primary reason to explain the lack of permafrost in the Langtang Valley.

Although the lack of permafrost was confirmed only at GC among the 7 glacier-forefields, a spatially uniform distribution of winter precipitation in the valley likely causes a negative effect on the rest of the forefields, and results in a lack of permafrost due to the thick snow cover. Therefore, the distribution of permafrost in the Langtang Valley seems to be considerably elevated by a local climatic condition rather than global climatic factors.

IV.4. *Periglacial landforms*

This section describes several periglacial landforms which are considered to be important in the zonation of cryogenic environments in the valley. These landforms include sorted and vegetated polygons, and other periglacial features. Features such as earth hummocks, solifluction lobes, turf-banked terraces, and talus slopes were described in this valley by myself and my colleagues (Watanabe *et al.*, 1989); therefore, they are only briefly reviewed in this section.

IV.4.1. Polygons

Sorted and vegetated polygons develop at several locations in the valley. Although both active and inactive features exist in the valley, only active features are described here.

Sorted polygons occur on the bottom of moraine-dammed seasonal ponds (4908 m) to the northeast of Mt. Tserko (Figure 31 A). They are 100−400 cm in diameter. The margin of the polygons is surrounded by sub-angular large boulders of 15−100 cm in diameter, while the central part consists of sand and small gravel on the surface, and fine silt with a small amount of gravel below. The central part is occasionally subdivided into smaller polygons.

The polygons are usually covered with snow from January to early May. The lakes are filled with snow melt-water during the early monsoon season (Figure 31-B); therefore, the period available for frost action is limited.

Sorted polygons also occur in ponds around the Laurebina Pass (4609 m) of the Gosainkund Range. They develop at the northern margin of Surja Kund (about 4600 m), and the western part of the northern-most pond (about 4600m). The diameter of the polygons varies

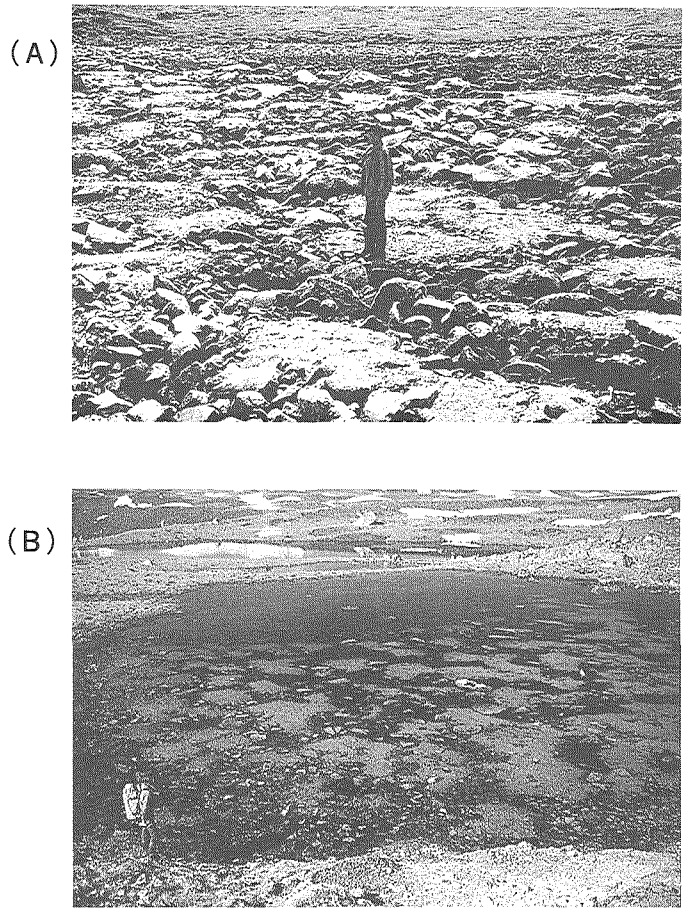

Figure 31 Sorted polygons at the bottom of a seasonal lake (4908 m) near Mt. Tserko. The lake is dried up in autumn (A: 19 September 1987). The polygons are covered with snowmelt water during spring (B: 27 May 1988).

from 50 to 330 cm. The materials forming the polygons are the same as those north-east of Mt. Tserko. The polygons around the ponds at the Laurebina Pass are the lowest features in the Langtang Valley.

At these sites, the sorted polygons develop nearer to the ponds, and they become gradually vegetated away from the ponds. This spatial distribution implies that sorted-unvegetated features exist only at the bottom of seasonal lakes.

Sorted polygons also occur, in some cases with stone stripes, on the convex slope in front of the Yala Glacier, above about 5000 m elevation. Their diameter ranges from 1 to 5 m, and

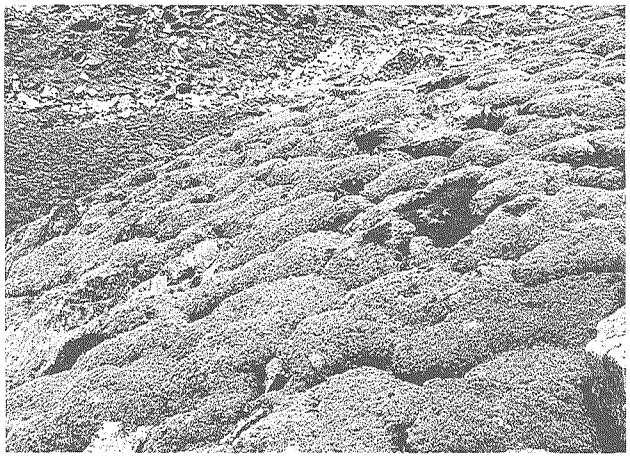

Figure 32 Well developed vegetated polygons at an altitude of 5300 m in the uppermost reaches of the valley. A camera in the center is for scale.

the margin of the polygons is made up of sub-angular blocks 10 to 40 cm in size. The polygonal pattern, however, is not as clear as that at the lake bottom near Mt. Tserko, mentioned above. The sorted polygons are located on the annual moraines, which are thought to have been formed between 1887 and 1903 (Ono, 1984, 1985). If this idea is supported, the sorted polygons were made within the past 100 years.

Vegetated polygons develop very well on degraded moraine-ridges in the upper part of the Langtang Valley. Most impressive features are encountered on a moraine hill at the right bank of the Langtang Glacier, where a meteorological observation site (LA) was established (5300 m; Figures 8 and 32). The polygons are 60 to 80 cm in diameter, and covered with herbaceous plants. Minor-scale vegetated polygons are also found on the right bank-moraine near the meteorological observation site KY (5140 m).

Well-developed vegetated polygons have scarcely been found in the middle reaches of the valley. This is probably due to a disturbance of surface vegetation by transhumance (Ono and Sadakane, 1986). Instead, yak-related patterned ground develops well in the middle reaches (Watanabe *et al.*, 1989).

IV.4.2. Other periglacial landforms

Earth hummocks are spread widely across the moist surface above the level of the Langtang Village (3410 m). They develop mainly at Tsona (3780 m), Tarna (4165 m), Tsongdu (3800 m), Thangdemo (4620 m), and Numothang (4050 m). The general dimensions of the earth hummocks in the Langtang Valley are 20−70 cm in diameter and 10−35 cm in height.

The turf-banked or the vegetated solifluction lobes occur above 3425 m elevation, while stone-banked or unvegetated solifluction lobes occur above 4900 m, on the southwest-facing debris-covered slope near the Yala Chu. They are also observed on the steep side slopes of the Little Ice Age moraines in front of the Yala Glacier.

Active talus slopes, with frost-shattered fresh fragments on their surface, fringe the basal part of the steep rocky valley walls above the level of Kyangchen (3920 m). Along the left bank of the Tajar Chu, many angular granite blocks without lichen cover lie on the large talus slopes (3985 m). They are currently supplied from the upper bedrock exposures above an altitude of 4200 m. Other large talus slopes, whose relative height reaches 400−500 m, stretch along the right bank of the Chubi Chu. In the main valley, the talus slopes are more or less related to avalanches, spreading downslope from the glaciers hanging above the steep valley wall.

IV.5. *Frost shattering*

Rock breakdown and rock surface temperature were both measured to estimate the current frost shattering rate in the Langtang Valley (Shiraiwa, 1992). The results were then extended tentatively to a different altitudinal belt.

IV.5.1. Measurement of rock breakdown

Procedures for the field measurement of rock breakdown followed Matsuoka (1990a). A quadrangle of 50×50 cm was initially painted in red on a free face (Figure 33-A), and the percentage of the shattered area within the painted part was quantified by photographs taken at several time intervals (Figure 33-B). Joint spacings, which are determined by an average distance between the joints, were also measured for each quadrangle in the field. The measurement sites were at Gangja La (Ga-1 to 3, 5090 m), Dakpatsen (Da-1 to 6, 4692 m to 4714 m), Tarchipesa (Ta-1 to 8, 4070 m to 4318 m), Glacier Camp (GC-1 to 3, 5090 m) and Pemdang (Pe-1, 2, 5160 m)(Figure 25). Most of them were established in May 1988, and photographs were taken in May 1989, December 1989 and June 1990.

Table 5 shows the cumulative shattered area (%) during each interval, and a monthly shattering rate during the whole observation period. Rock breakdown was most obvious at the Dakpatsen site where all quadrangles experienced breakage from 0.4 to 6.5 %·month^{-1}. The breakdown at Da-4 was the highest among the quadrangles, and amounted to 155 % in total over 2 years. The Tarchipesa site also suffered rock breakdown, but the rates were generally low, with exception of Ta-1 which recorded a value of 86.5 % over 2 years. The quadrangles in the Gangja La, Glacier Camp and Pemdang sites have not changed at all, although a slight change was found at GC-1 (7.6 %·2 yrs.$^{-1}$). This indicates that frost shattering is more active at lower rather than higher altitudes within the study area.

A major rock breakdown is generally followed by a smaller one as shown at sites Da-2, 4, 5, 6, and Ta-1, although the intervals of the measurement were not uniform. This suggests

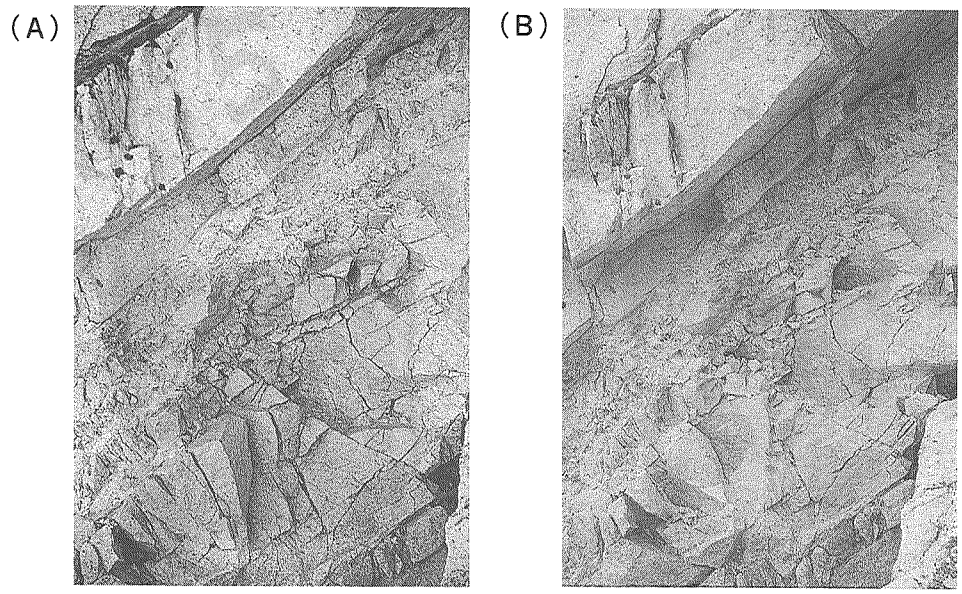

Figure 33 A painted rock surface for the measurement of rock breakdown (A: 23 May 1988) and the surface with some fracture one year after the paint (B: 23 May 1989).

Table 5 Characteristics of the painted rockwalls and shattering rates. Ga: Gangja La, Da: Dakpatsen, Ta: Tarchipesa, GC: Glacier Camp, and Pe: Pemdang. Gr: Granite, Gn: Gneiss, nd: data not available, s: spring, and f: fall or autumn.

Location number	Rock type	Aspect	Altitude (m)	Joint Spacing (cm)	Cumulative shattered area (%) '88s - '89s	'89s - '89f	'89f - '90s	Monthly shattering rate (% / month) [duration]
Ga-1	Gr	S34°W	5,090	> 100.0	0.0	nd	0.0	0.0 [24 months]
Ga-2	Gr	S26°W	5,078	50.0	0.0	nd	0.0	0.0 [24 months]
Ga-3	Gn	S26°W	5,070	8.7	0.0	nd	0.0	0.0 [24 months]
Da-1	Gr	N10°E	4,700	4.4	4.9	8.3	1.2	0.6 [24 months]
Da-2	Gr	E	4,692	4.2	44.5	31.8	1.4	3.2 [24 months]
Da-3	Gr	N80°W	4,692	6.7	6.1	16.2	0.0	0.9 [24 months]
Da-4	Gr	S40°E	4,712	< 4.0	87.5	41.0	26.5	6.5 [24 months]
Da-5	Gr	S30°W	4,712	6.1	nd	8.0	1.1	0.8 [12 months]
Da-6	Gr	S15°E	4,714	9.5	nd	4.2	0.5	0.4 [12 months]
Ta-1	Gr	N12°W	4,162	10.5	86.1	0.0	0.4	3.6 [24 months]
Ta-2	Gr	N39°W	4,152	8.7	0.0	0.0	0.0	0.0 [24 months]
Ta-3	Gr	S47°W	4,070	12.5	nd	nd	0.0	0.0 [6 months]
Ta-4	Gr	N25°E	4,080	6.9	nd	nd	0.0	0.0 [6 months]
Ta-5	Gr	N40°E	4,100	12.5	nd	nd	0.0	0.0 [6 months]
Ta-6	Gr	S63°W	4,310	< 3.4	nd	nd	0.0	0.0 [6 months]
Ta-7	Gr	S22°E	4,317	6.1	nd	nd	11.5	1.9 [6 months]
Ta-8	Gr	N82°E	4,318	6.9	nd	nd	0.0	0.0 [6 months]
GC-1	Gr	S77°W	5,095	6.3	0.0	1.2	6.1	0.3 [24 months]
GC-2	Gr	W	5,095	6.1	nd	0.0	0.0	0.0 [12 months]
GC-3	Gr	S80°W	5,093	8.0	nd	nd	0.0	0.0 [6 months]
Pe-1	Gr	N70°W	5,162	10.5	nd	0.0	0.0	0.0 [13 months]
Pe-2	Gr	E	5,162	10.5	nd	0.0	0.0	0.0 [13 months]

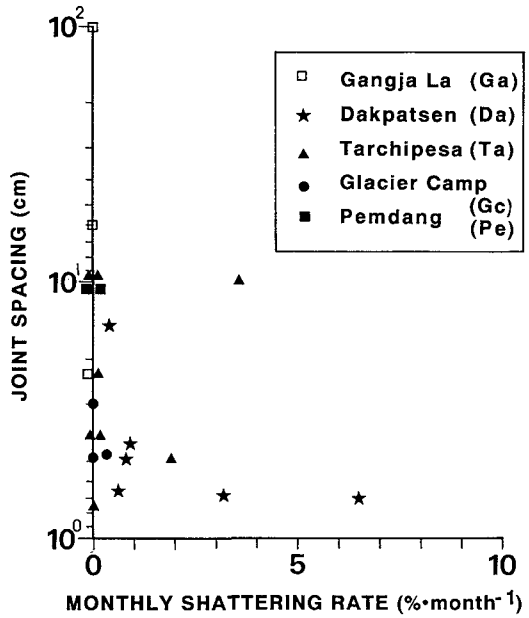

Figure 34 Monthly shattering rate (%·month^{-1}) as a function of joint spacings (cm).

that the mechanical weathering of rock requires a certain threshold time period for re-fracturing after a major breakage.

The joint spacings are generally smaller in the quadrangles which suffered greater rock breakdown than those of the unchanged ones (Figure 34). This indicates that the joint spacing is closely related to rock breakdown.

IV.5.2. Measurement of air and rock surface temperatures

Air and rock surface temperatures were observed to estimate the frequency of freeze-thaw activities in the valley. The observation sites are shown in Figure 25. The Glacier Camp site represents the south-facing slope, while the Gangja La represents the north-facing one. Both sites are located in flat morainic fields in front of the glaciers. The sites are located in a windward place, although the surroundings are generally covered with deep snow from January to mid-April.

The air temperature at 180 cm above the ground was measured using a thermistor shaded with a white pipe surrounding it. Artificial ventilation was not used. The thermistor was connected to an automatic data-logger (KADEC-U of KONA System Co.) in which the data were stored every hour.

The rock surface temperature was recorded on outcropping rocky cliffs near the sites of the air temperature observations. A thermistor was installed in a drilled pit 1.5 cm in depth

below the rock surface, and the pit was filled with silicone rubber mixed with granules. The data were recorded hourly in the automatic data logger mentioned above.

The measurement continued from June 1988 to May 1990. The data for the Gangja La site, however, were limited from June 1989 to May 1990 because of unexpected damage to the instruments. Hereafter, the data from June 1988 to May 1989 are referred to as 1988's data,

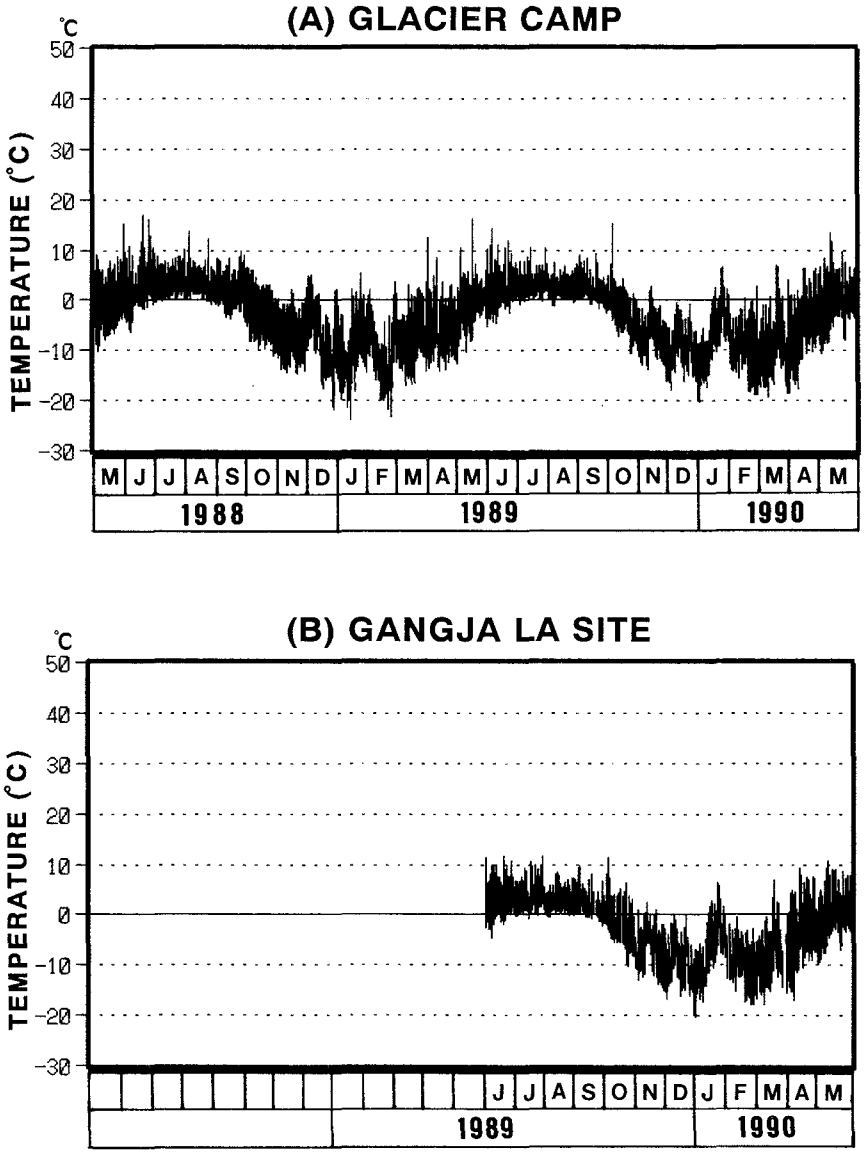

Figure 35 Diurnal ranges in air temperature. (A): Glacier Camp (5090 m), and (B): Gangja La (5090 m).

and those from June 1989 to May 1990 as 1989's data.

Figure 35 shows the diurnal ranges in air temperature at Glacier Camp (A) and Gangja La (B) sites through the observation period. The measurement of air temperature at these sites revealed no significant difference between north- and south-facing slopes. The average air temperature is above 0 °C during three summer months (July through September).

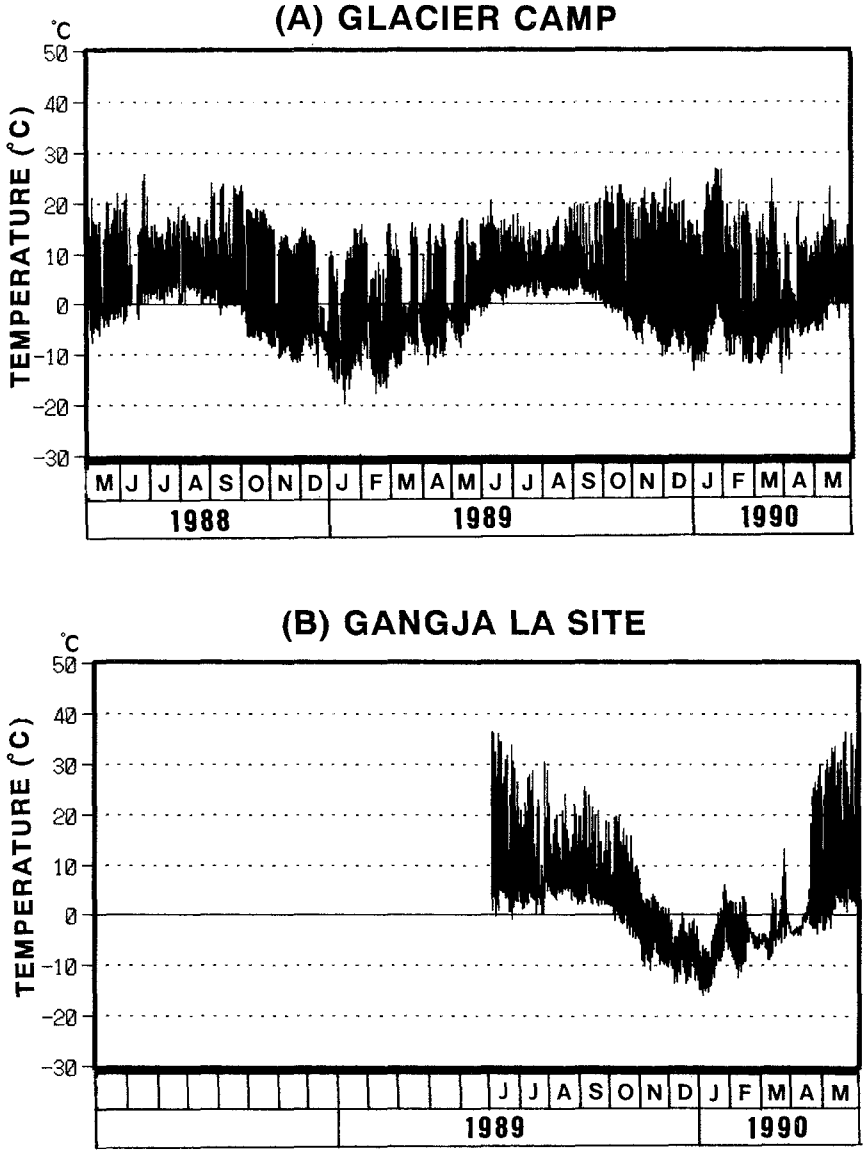

Figure 36 Diurnal ranges in rock surface temperature. (A): Glacier Camp (5110 m), and (B): Gangja La (5090 m).

Conversely, it is below 0 °C during the five winter months (November through March), although the air temperature fluctuates around 0 °C in the intermittent warm periods at both sites. The freeze-thaw cycles of air temperature, therefore, occurred mainly in spring and autumn at an altitude of 5090 m. Matsuoka (1984) thought that freeze-thaw activity occurs during the monsoon season between 5000 and 5500 m in the Khumbu region, approximately 100 km east of the Langtang Valley, using freeze-thaw cycle data derived from air temperature. The results obtained in my study are, therefore, inconsistent with his idea.

The diurnal range is generally small during the monsoon season from July to September, because the thick monsoon clouds shade the whole area in the afternoon, when the daily air temperature usually attains its maximum. In the non-monsoon season, however, the diurnal range is large.

The diurnal range in rock surface temperature is shown in Figure 36. The annual fluctuations of rock surface temperature are generally similar to those of air temperature. The rock surface temperature, however, has a larger diurnal range than that of air temperature. This can be attributed to a short wave radiation absorbed by the rocks with a low albedo. As a result, the rock surface temperature often oscillated around 0 °C in the winter season. In this context, a significant contrast exists in the magnitude of the diurnal range of the rock surface temperature during the winter season between the south- and north-facing slopes. The temperature frequently fluctuated around 0 °C at the Glacier Camp site, while at the Gangja La site it was constantly below 0 °C. This is explained by a seasonal difference in the solar angle, which is high enough to provide an effective short wave radiation on both slopes only during the summer, *i.e.*, a lower solar angle during winter is less effective for heating the north-facing slope. As a result, a frequent freeze-thaw cycle occurs only on the south-facing slope during the winter.

Here, the freeze-thaw cycle is defined as the effective freeze-thaw cycle (EFTC) which is a temperature-fall below −2 °C followed by a rise above +2 °C (Matsuoka, 1990a), because several experiments have clarified that a rock temperature fluctuation slightly below and above 0 °C is not sufficient to cause frost shattering (*e.g.*, McGreevy and Whalley, 1982; Matsuoka, 1990b). The annual number of EFTC totalled 188 events in 1988, and 190 in 1989 at the Glacier Camp site, and 62 in 1989 at the Gangja La site (Table 6).

Table 6 Number of EFTC at the Glacier Camp and Gangja La sites during the observational periods. nd: data not available.

Location	'88								'89												'90			
	M	*J*	*J*	*A*	*S*	*O*	*N*	*D*	*J*	*F*	*M*	*A*	*M*	*J*	*J*	*A*	*S*	*O*	*N*	*D*	*J*	*F*	*M*	*A*
Glacier Camp	22	6	0	0	1	27	27	19	27	20	17	22	15	0	0	0	0	12	30	31	27	22	27	26
Gangja La Site	nd	nd	nd	nd	nd	nd	nd	nd	nd	nd	nd	nd	nd	0	0	0	0	18	11	0	12	5	8	7

IV.5.3. Altitudinal distribution of the number of freeze-thaw cycles

The rate of frost shattering is controlled, in broad terms, by three factors: temperature, moisture, and rock properties (Matsuoka, 1990a). Only the altitudinal distribution of the number of EFTCs is discussed here, because only the thermal factors were measured in this study. The EFTC number is however, considered to be an important factor influencing frost shattering in a moist environment.

A linear regression analysis was performed in order to define the relationship between the rock surface temperature and the air temperature (Figure 37). The regression equations were calculated for a daily maximum rock surface temperature [$T_{r(max)}$] against a daily maximum air temperature [$T_{a(max)}$](a and d); a daily minimum rock surface temperature [$T_{r(min)}$] against a daily minimum air temperature [$T_{a(min)}$](b and e); and $T_{r(min)}$ against a daily average air temperature [$T_{a(avg)}$](c and f), for the two sites: Glacier Camp and Gangja La. The most significant result was found between $T_{r(min)}$ and $T_{a(min)}$ at the Glacier Camp site (b; $r=0.92$), while the least significant was between $T_{r(max)}$ and $T_{a(max)}$ at the Glacier Camp (a; $r=0.37$). The $T_{r(max)}$ was much closer to the $T_{a(max)}$ on the north-facing slope (e; $r=0.80$).

The rock surface temperature at different altitudes was estimated by the following procedures. At first, the air temperature at each altitude was calculated for every 100 m in elevation using the temperature lapse rate of -6 °C·km^{-1} through the year; the value is based on earlier observations in this valley (Takahashi *et al.*, 1987a). The calculated air temperature was then converted to the rock surface temperature using the regression equations mentioned above, assuming that the regression equations are constant at different altitudes. The maximum rock surface temperature on the south-facing slope was, however, extrapolated from the rock surface temperature at the Glacier Camp site using a lapse rate of -15.1 °C·km^{-1} (Kuhle, 1986a, 1988b), because a correlation coefficient of the equation obtained here was very low ($r=0.37$). The lapse rate of -15.1 °C·km^{-1}, obtained by a direct measurement of the rock surface temperature using a passive infra-red detector, seems to be too high, considering the fact that the short wave radiation increases with increasing altitude. However, no reliable data on the lapse rate of rock surface temperature, except the results of Kuhle (1986a, 1988b), lead to the application of this value.

Figure 38 shows the result of the computation in the form of altitudinal distribution of the EFTC number on the south- (A) and north-facing (B) slopes. The highest annual EFTC number appears at altitudes of 5600 m (216 times) and 6200 m (125 times), for south- and north-facing slopes, respectively. The EFTC disappears above altitudes of 6600 m (south) and 7400 m (north), and below 2600 m (south) and 2800 m (north). The results obtained here seem to be somewhat unrealistic, because the south-facing slope receives more incoming solar radiation than the north-facing one; hence, at a higher altitude, the EFTCs should occur more frequently on the south-facing slope than the north. The reason is attributed to the application of Kuhle's (1986a, 1988b) lapse rate of -15.1 °C·km^{-1}. If we apply a lower value for the lapse rate, the south-facing slope will receive more frequent EFTCs at higher altitudes; the

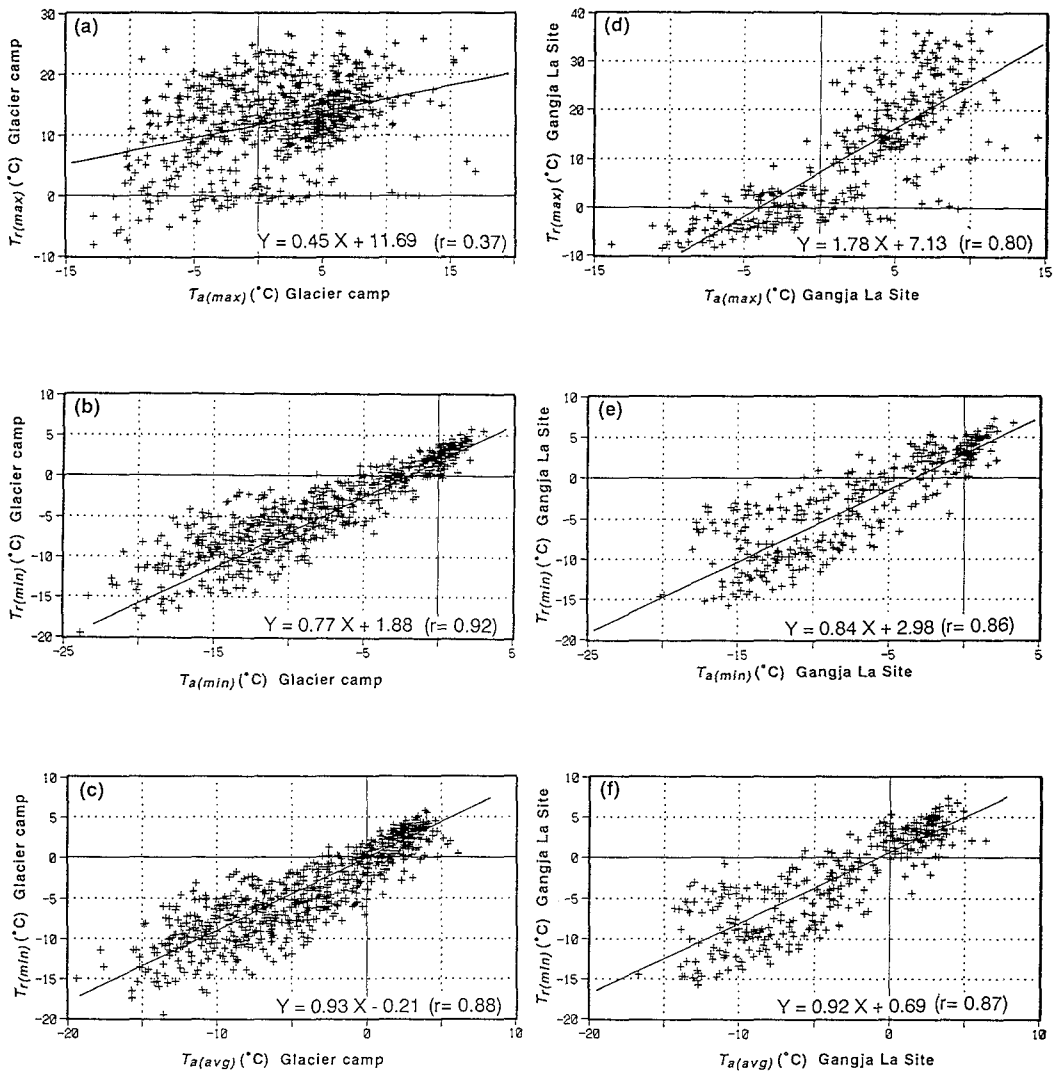

Figure 37 Results of a linear regression analysis between the air temperature and the rock surface temperature. T_a: air temperature, T_r: rock surface temperature, (max): daily maximum, and (min): daily minimum. (a) and (d): $T_{r(\max)} - T_{a(max)}$, (b) and (e): $T_{r(\min)} - T_{a(\min)}$, and (c) and (f): $T_{r(\min)} - T_{a(\mathrm{avg})}$. (a), (b) and (c) are the relations at the Glacier Camp site, while (d), (e) and (f) are the relations at the Gangja La site.

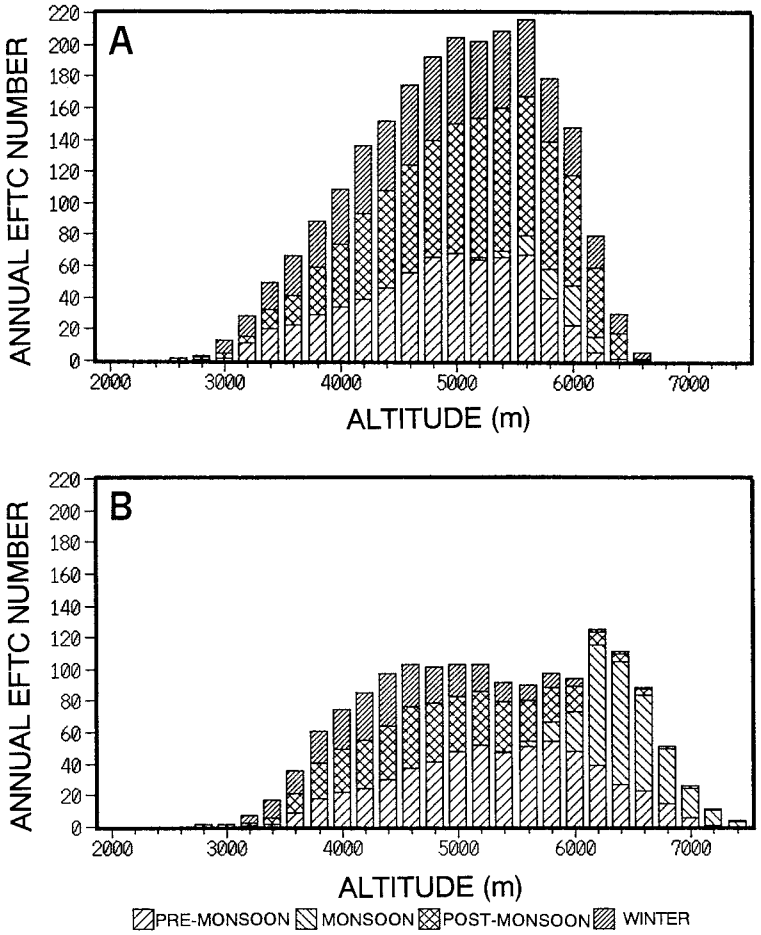

Figure 38 Computed altitudinal distribution of the annual number of effective freeze-thaw cycles (EFTCs) on the south-(A) and north-facing (B) slopes. Note that the seasonal distribution of EFTC at each altitude is considerably different.

lack of data, however, prevents us from estimating the actual condition of the EFTCs at higher altitudes on the south-facing slope.

The EFTC during the humid season will contribute more to frost shattering by suppling water into a joint of rock as Matsuoka (1984) noted. The seasonal moisture condition in the Langtang Valley is discussed here in relation to the magnitude of frost shattering.

The climate of the Langtang Valley can generally be divided into four seasons: the monsoon, post-monsoon, winter, and pre-monsoon. The monsoon season, from June to September, is characterized by a continuous but weak precipitation, while the post-monsoon

season, from October to December, is the driest season throughout the year. Winter, January and February, is rather dry, although intermittent snowfall covers the ground, and the joints of the rock masses are generally filled with snow. In the pre-monsoon season, *i. e.*, March to May, both the ground and the cliffs are wet, because both melt-water and intermittent precipitation occur.

As a result, EFTCs occurring in the monsoon and the pre-monsoon seasons are most likely to contribute to the frost shattering in the area. The number of EFTCs during these seasons varies from 1 (2800 m) to 79 (5600 m) on the south-facing slope, and from 1 (3200 m) to 115 (6200 m) on the north-facing slope, as shown in Figure 38. The frost-shattering may thus be most active around altitudes of approximately 5600 and 6200 m, for the south- and north-facing slopes respectively.

The number of EFTCs during a wetter season is, however, less variable between 4000 m and 5200 m, where all measurement sites of the rock breakdown are located. Therefore, the field measurement which showed that the rock breakdown culminated at the lower sites (Dakpatsen and Tarchipesa) rather than at the higher sites (Glacier Camp, Gangja La, and Pemdang) suggests that the number of EFTC cannot be regarded as a dominant factor that affected the magnitude of the frost shattering in this study. The difference in the rate of rock breakdown can be attributed to the difference in the rock properties at the sites as shown by the joint spacing listed in Table 5.

IV.6. *Vertical zonation of cryogenic environments*

A vertical zonation of periglacial features in the Langtang Valley was previously proposed by Watanabe *et al.* (1989), in which four periglacial belts were recognized. In this section, I will add a latitudinal change and climatic data to the zonation, and propose a new zonation (Figure 39). The climatic data are given as mean annual air temperature and summer precipitation: the former is plotted in relation to altitude, and the latter to latitudes. Since the observed climatic data are limited both in time and space, the values given in the figure are tentative ones.

The basic boundary to demarcate the upper limit of the periglacial belt is ELA. Above ELA, the cryogenic activity is basically constrained by snow cover, except for places such as rocky walls and glacier-free summits where intensive frost action can be expected to occur. The ELA rises northward in the valley from 5120 m at the southern most part to 5560 m at the northern most one (Chapter III-3-2), mainly due to the decrease of precipitation (Chapter III-5-2). Thus, the upper limit of the periglacial belt rises northward, and it is characterized by an annual air temperature of -4 °C in the south and -6.5 °C in the north.

The lower limit of the periglacial belt corresponds to the occurrence of effective freeze-thaw cycles; thus it is located at 2600 m on the south-facing slope and at 2800 m on the north-facing one (Figure 38). However, the limit is actually delineated by the timberline below which frost action is strictly reduced due to a dense vegetation cover. In the valley, *Betula-*

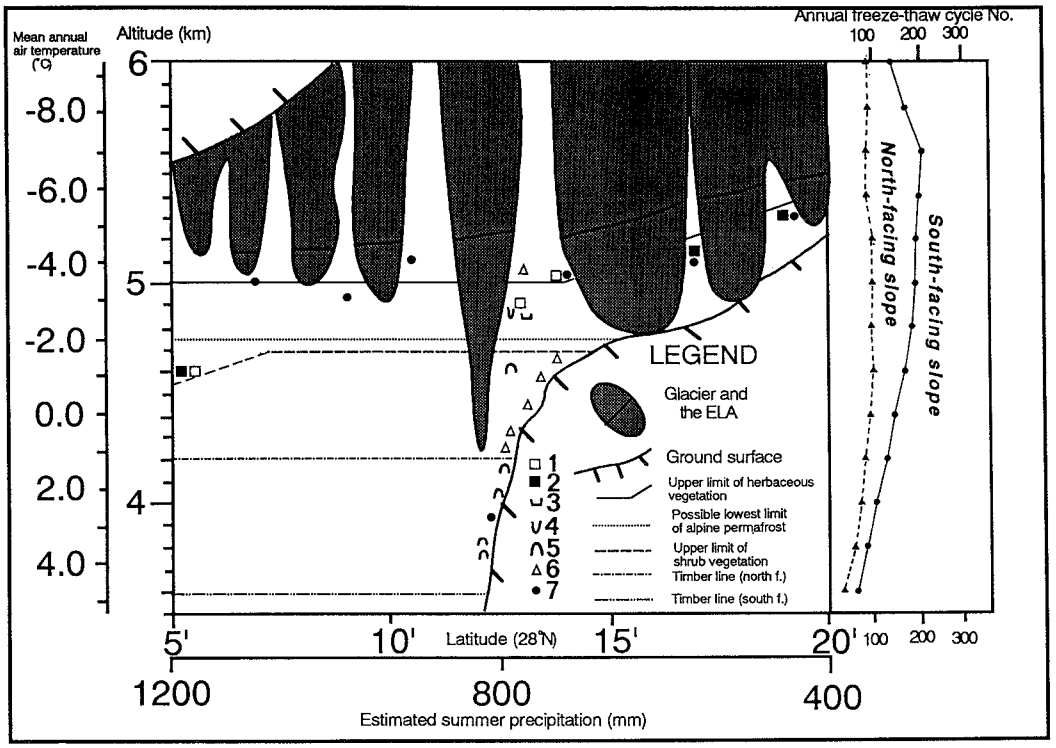

Figure 39 Vertical distribution and tentative zonation of vegetation and periglacial landforms in the Langtang Valley. 1: sorted polygons, 2: vegetated polygons, 3: turf–banked terraces, 4: vegetated solifluction lobes, 5: earth hummocks, 6: talus slopes, and 7: meteorological observation sites. The possible lowest limit of alpine permafrost is drawn where the mean annual air temperature is −2 °C.

Rhododendron forest extends up to a maximum elevation of 4200 m on the north-facing slope, while coniferous forest forms the timberline on the south-facing slope at an altitude of 3600 m. As a latitudinal gradient in the timberline is not found in the valley, potentially, the periglacial belt in the Langtang Valley becomes wider northward. The annual air temperature at the lower limit of the periglacial belt is about 5 °C on the south-facing and 1 °C on the north-facing slopes.

The periglacial belt can be subdivided into *vegetated* and *non-vegetated periglacial belts.* The limit is defined by herbaceous vegetation which rises northward from 5000 m to 5300 m. Although the reason for this rise is not clear, it seems to reflect a sunny and temperate climate in the upper part of the Langtang Valley (Chapter III-5-1).

The *non-vegetated periglacial belt* occupies a very narrow altitudinal range as much as 100 to 200 m. In other high mountains of the world, sorted polygons usually characterize this belt (Höllerman, 1967). However, in the Langtang Valley, a sufficient snow cover in winter

(Chapter III-6-2) which prevents the alpine permafrost from developing, also seems to disturb the development of sorted polygons. Freeze-thaw cycles occur most frequently in this belt, although the number does not change significantly between 5600 and 4800 m.

The *vegetated periglacial belt* is divided into the upper and lower belts by the upper limit of shrub vegetation. The *upper vegetated periglacial belt* is characterized by well-developed vegetated polygons, solifluction lobes and turf-banked terraces. The belt rises northward up an altitude of 5300 m, while in the southernmost part, the lower altitude of shrub limit enables vegetated polygons to develop as low as 4600 m. In this belt, sorted polygons develop exclusively on the bottom of seasonal ponds. If the ponds dry up, the sorted polygons will gradually become vegetated as shown in some examples mentioned in section IV-4-1.

The *lower vegetated periglacial belt* forms the lowest periglacial belt. Periglacial landforms are poor in this belt, except for frost-shattered talus slopes and earth hummocks, due to a vegetation cover such as shrubs of juniper. The habitants in the valley use this belt intensively for transhumance (Ono and Sadakane, 1986), and the development of earth hummocks seem to be accelerated by cattle trampling.

V. Glacial fluctuations in the Langtang Valley during the late Quaternary

V.1. *Introduction*

Climatic changes from the late Quaternary to the Holocene caused a drastic shrinkage of glaciers all over the world. Although geological evidence has gradually accumulated in many parts of the world, studies are still not sufficient in the Himalaya. Heuberger (1956) and Müller (1958/59) first described a series of moraine sequences in the Khumbu region. Studies which followed in the Nepal Himalaya (Figure 40) opened a controversial discussion on the maximum extent of glaciers since the late Quaternary. Fushimi (1977b, 1978), for instance, reconstructed an extensive glaciation of the *Lukhla Stage* in the Dudh Kosi region, while others (*e.g.*, Williams, 1983) questioned Fushimi's idea. Kuhle (1982) also proposed a vast glaciation in the Kari Gandaki region, although Iwata (1984) reconstructed a smaller one in the same area.

Another problem in the Nepal Himalaya arises from a lack of absolute dating for moraine deposits. For example, the age of the famous *Periche moraine* in the Dudh Kosi region has been tentatively assigned to the 16th century (Müller, 1958/59) or to the Last Glacial Maximum (Iwata, 1976a; Röthlisberger, 1986). The lack of numerical datings closely related to moraine landforms makes it difficult to fix the proposed stages chronologically.

In this chapter, glacial fluctuations in the Langtang Valley are reconstructed by geomorphological methods, and a glacial chronology is proposed using both ^{14}C and relative dating methods.

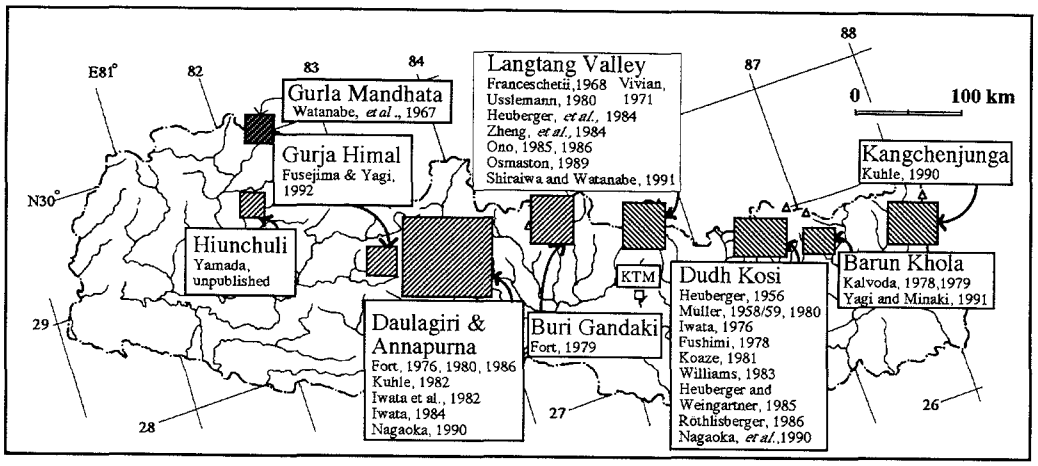

Figure 40 The locations of previous study areas on the Quaternary glaciations in the Nepal Himalaya. KTM: Kathmandu, the capital of Nepal.

V.2. *Previous work*

Fluctuations of glaciers in the Langtang Valley were first described by Franceschetti (1968) and Vivian (1971). They recognized several moraines and associated terraces in the main valley. Usslemann (1980) made a geomorphological map of the valley, and found six stages of the former glacial fronts. He believed the lowest limit of the past glaciation was located at an altitude of 2400 m.

Heuberger *et al.* (1984) studied the middle reaches of the valley, and presented four major glacial stages; (1) *Present* and *Post-glacial*, (2) *younger Late-glacial*, (3) *older Late-glacial*, and (4) *earliest Late-glacial* and *the maximum of the Last Main Glaciation*. They correlated the *Lirung Stage* of the *younger Late-glacial* with the *Nubmatang Stage* of Franceschetti (1968). The lowest limit was estimated further below at an altitude of 2400 m, depending on the estimated ELA during *the maximum of the Last Main Glaciation*.

Ono (1986) subsequently studied the valley, and recognized five main stages; (1) *Little Ice Age*, (2) *Neoglacial*, (3) *Late-glacial younger*, (4) *Late-glacial older*, and (5) older than *Late-glacial* advances. The *Little Ice Age* advance was subdivided into two stages by counting annual moraine ridges in the forefield of the Yala Glacier (Ono, 1985).

Zheng *et al.* (1984) briefly mentioned the fluctuation of glaciers in the valley, and correlated moraines, immediately adjacent to an innermost huge moraine, with the neoglacial moraines in the Qinghai-Xizang Plateau.

Although many authors discussed the Quaternary glacial fluctuations in the Langtang Valley as briefly described above, a great deal of uncertainty remains concerning the glacial chronology. This is largely due to lack of both ^{14}C and systematic relative dating data.

Consequently, there remains many unanswered questions concerning the spatial and chronological fluctuations of past glaciers.

V.3. *Study methods*

Figure 41 (Shiraiwa and Watanabe, 1991) illustrates the study area and the moraine stagings. The moraines in the valley were first classified into four moraine complexes according to their geographical positions. Relative dating (RD) data were gathered on the moraine complexes. With a few exceptions, data sampling sites were set on or near the crest of the terminal moraines to minimize the errors related to site variances.

The following RD methods were used: Schmidt hammer rebound value (RV) of the boulder surface; thickness of the weathering rind (WR); percentage of the clasts with oxidation stain (OS); height of the mineral projection (MP) on the clast surface; pit depth (PD)

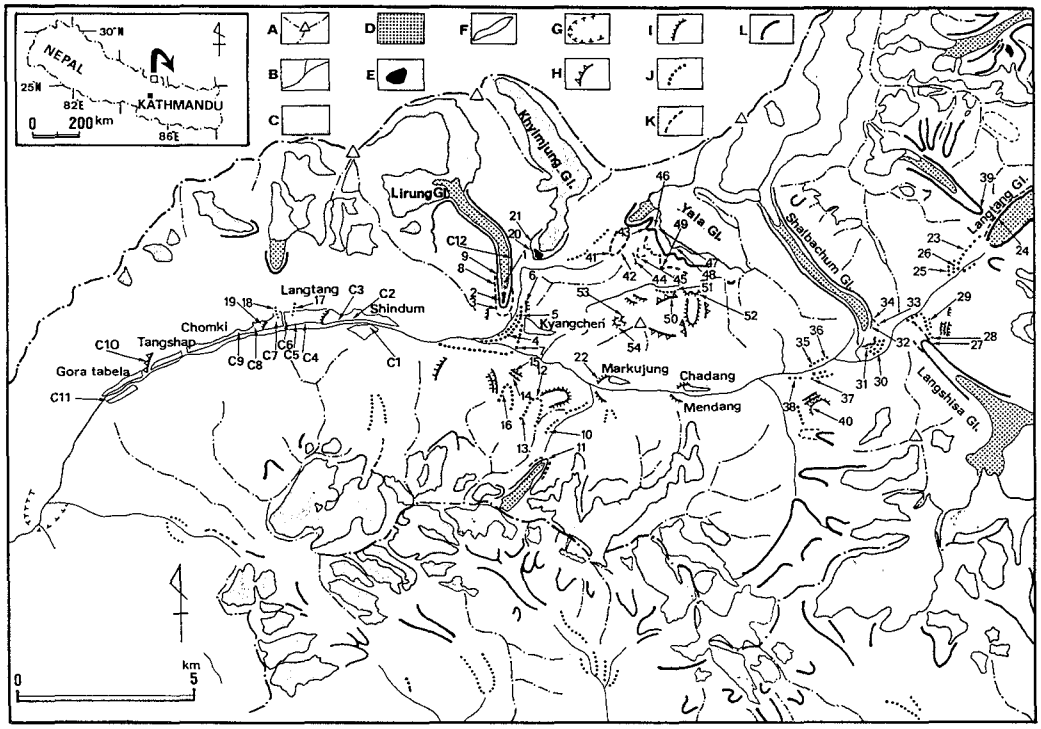

Figure 41 Distribution of glaciers and related moraines in the Langtang Valley (Shiraiwa and Watanabe, 1991). A: ridge and peak, B: river and stream, C: active part of glaciers, D: inactive part of glaciers, E: lake or pond, F: flat surface, G: lower limit of U-shaped valley, H: lowest limit of the *Lower till*, I: outermost moraine complex or the *Upper till* surface, J: outer moraine complex, K: inner moraine complex, L: innermost moraine complex. Locs. 1 to 54 denote the sampling site of the RD data, while the Locs. C1 to C12 are the outcrops for the columnar sections shown in Figure 43.

on the clast surface; soil development; and soil color index.

The dating method using Schmidt-hammer rebound values (RV) is based on the assumption that weathering of boulder surfaces begin after their stabilization (Day and Goudie, 1977; Matthews and Shakesby, 1984). This study used the mean value of three measurements for each of 30 boulders. All sampling sites were classified into two groups according to the proportion of granitic or gneissic clasts within the boulders being tested: those with more than 50 % of granitic boulders or gneissic boulders were termed granitic and gneissic sites, respectively.

The thickness of the weathering rind (WR; Birkeland, 1973) and the percentage of rock fragments with oxidation stain (OS) were measured for 25 clasts after breaking them with a hammer, and the average values of these two parameters were used in the analysis. The degree of superficial weathering of the rock clasts was quantified by the following two parameters: the height of mineral projection (MP), and the pit depth (PD) on the clast surface (Birkeland, 1973). The maximum values of these two parameters were also recorded.

Soil profiles developed on the moraines were described to classify the maturity of the soil according to the nomenclature of Birkeland (1984a). In addition, the Hurst Color Index (HCI; Hurst, 1977) was calculated for further classification. Moist color was used in all cases (Birkeland, 1984b).

As the surfaces of the older moraines were already covered with thick colluvial deposits, particularly in the middle reaches of the valley, it was difficult to apply the above methods to them. Therefore, a weathering test was carried out on rock-clast samples collected from a 3 m×3 m quadrangle on the outcropping cliffs. The weathering condition of 50 clast samples was determined and then classified into three categories as follows: unweathered clasts with fresh appearance, jointed clasts, or completely disintegrated clasts. A depth of burial of sediments can affect their weathering rates as known in the weathering-rind studies (*e.g.*, Porter, 1975; Colman and Pierce, 1981). Therefore, all data were taken on the exposed cliffs to eliminate the depth factor.

The RD data obtained were subjected to a Student's t-test in order to check the initial classification by the geographical positions of the moraine ridges, and in a few instances, the classification was later modified.

V.4. *Glacial landforms*

The moraines and related landforms in the valley were investigated during field surveys in 1987, 1988, 1989, and 1990 with the aid of oblique photographs taken by the Japanese Glaciological Expedition of Nepal (GEN) in 1981. The distribution of moraines in the Langtang Valley is shown in Figure 41.

The stagnant ice fronts of the valley glaciers forms a huge unvegetated moraine complex. Such a moraine complex immediately adjacent to the glacier has at least two crests in the case of the Lirung and Khymjung Glaciers, four along the Langtang Glacier, and one

along the Langshisa and Shalbachum Glaciers. It also fringes the margin of high-altitude, plateau-like glaciers such as the Yala Glacier. These are referred to as the "innermost moraine complex (IM)".

A slightly degraded, older moraine complex is situated beyond the innermost moraine complex in front of the Yala, Lirung and Langtang Glaciers. It is referred to as the "inner moraine complex (I)".

Beyond the innermost and inner moraine complexes, three or possibly four minor terminal moraine ridges are well defined. Tracing these ridges to their lateral position, they gradually coalesce to form a single ridge, referred to as the "outer moraine complex (O)". This complex is most clearly defined in front of the Lirung Glacier, and represents the *Lirung Stage* of Heuberger *et al.* (1984).

Ono (1986) recognized a glaciofluvial terrace, the Kyangchen Surface, in the middle reaches of the Langtang Valley, and correlated it with our outer moraine complex of the Lirung Glacier. However, it is older than the outer moraine complex, as the former is cut by the latter at the west end of the Kyangchen Surface (Figure 42; Shiraiwa and Watanabe, 1991).

Downvalley of the outer moraine complex of the Lirung Glacier, moraine landforms are scarcely preserved, and a thick valley train, which was named the Shindum Surface by Ono (1986), spreads out in this valley (Figure 42). The deposits (column C3 in Figures 42) are composed of the following layers (from the lower to the upper): the "*Lower till*" of semi-

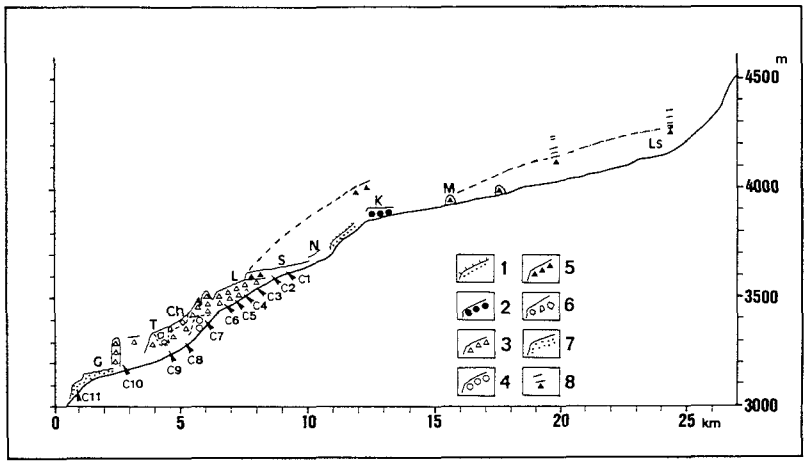

Figure 42 Longitudinal profile of the Langtang Valley and the deposits (Shiraiwa and Watanabe, 1991). 1: outer moraine complex, 2: Kyangchen Surface, 3: *Lower till*, 4: glaciofluvial deposits, 5: *Upper till*, 6: landslide deposits, 7: Gora Tabela Surface, and 8: outermost moraine complex. Ls: Langshisa, M: Markujung, K: Kyangchen, N: Nesapari, S: Shindum, L: Langtang, Ch: Chomki, T: Tangshap, G: Gora Tabela. Locs. C1 to C12 correspond to the columnar sections shown in Figure 43.

consolidated lodgement facies with a maximum thickness of approximately 5 m (No.5 of C3 in Figure 43-A; Shiraiwa and Watanabe, 1991); the *Lower till* of unconsolidated ablation or meltout facies with a thickness of 22 m (No.4); stratified gravel, sand and silt layers with a thickness of 1.6 to 2.5 m, interbedded with a humic horizon (No.3); oxidized gravel layer, 0.3 m thick; the "*Upper till*" of semi-consolidated lodgement facies with a maximum thickness of 3.5 m (No.2); the *Upper till* of unconsolidated ablation facies (No.2), quite variable in thickness; and overlying stratified sand and gravel layers. The fact that the distribution of the *Upper till* is confined between the lowest points of both the outer moraine complex of the Lirung Glacier and the Shindum Surface suggests that it forms an "outermost moraine complex (OM)", although the terminal and lateral moraine ridges are not clear.

A series of dissected lateral moraines are perched along the main stream of the Langtang

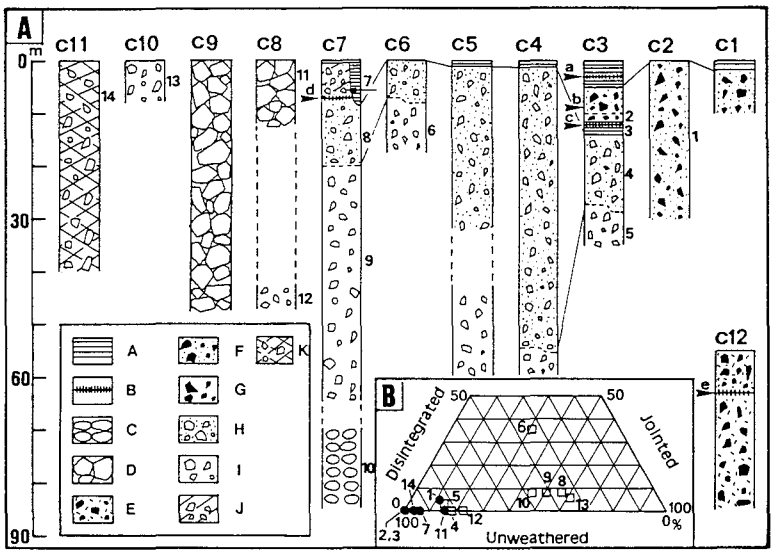

Figure 43 (A) Columnar sections of the deposits (Shiraiwa and Watanabe, 1991). A: fluvial deposit, B: buried humic layer, C: fluvial gravel, D: landslide deposit, E: till of the innermost moraine complex, F: *Upper* (ablation) *till*, G: *Upper* (lodgement) *till*, H: *Lower* (ablation) *till*, I: *Lower* (lodgement) *till*, J: till of the outer moraine complex, and K: unidentified diamicton. Locations of each column are shown in Figures 41 and 42. The dates of the humic layers denoted by the arrows (a-e) are shown in Table 10. The figures at the right side of the columns (1−14) show the sampling points for the weathering test shown in Figure 43-B. (B) A ternary plot showing the degree of the weathering of the clasts from the till. Black circles: clasts from the *Upper till*, open squares: clasts from the *Lower till*.

Khola beyond the lowest limit of the outer moraine complex. They are located tens of meters above the present river bed along the Lirung Glacier (loc. 6 in Figure 41) and 150–250 m above the right bank of the Langshisa Glacier. The longitudinal profile of the valley (Figure 42) suggests that these higher lateral moraines are related to a glacial advance which formed the Shindum Surface and to the morainic hills between the Markujung (3880 m) and Chadang (3950 m) Kalkhas. This means that both the morainic hills and the lateral moraines above are correlated with the outermost moraine complex.

The Chomki Surface (Ono, 1986) stretches downvalley to the Langtang village (Figure 42). The surface is composed of five different layers from the lower to the upper (column C7 in Figure 43-A): glaciofluvial deposits with a minimum thickness of 15 m (No.10); the *Lower till* of semi-consolidated facies, 43 m thick {including both ablation (No.8) and lodgement (No.9) facies}; a buried A horizon; the till of the outer moraine complex (No. 7) of tributary origin, and glaciofluvial deposits. A landslide deposit covers the surface at the lower points (columns C8 and C9 in Figure 43-A). The morainic terrace, therefore, is predated by the glaciofluvial activity and is postdated by the landslide and glacial activities.

A well-developed stepped surface is evident in the Langtang Valley. The upper surface corresponds to the Chomki Surface, while farther downvalley the flat lower one corresponds to the Gora Tabela Surface, regarded as the lowest existing moraine in the Langtang Valley (Usslemann, 1980; Heuberger *et al.*, 1984; Ono, 1986). The deposits of the Gora Tabela Surface, however, seem to have been derived from the collapsed morainic material from the southern side of the main river. A dominance of gneissic clasts and their freshness support this idea. On the other hand, as Ono (1986) noted, a large dissected ridge at the confluence of the Tara Chu (column C10 in Figures 41, 42 and 43), composed of consolidated *Lower till*, appears to be a remnant of the terminal moraine.

There seem to be no glacial depositional forms below a clear knick point at Gora Tabela (ca. 3100 m a.s.l.). No evidence sufficient enough to define the lowest limit of past glaciation maxima was obtained. Nevertheless, the change of valley morphology and direction from an ambiguous U-shape to a V-shape along the Langtang Khola at an altitude of approximately 2600 m may indicate the former maximum glacier extent.

V.5. *Results of relative dating methods*

V.5.1. Schmidt hammer RV test

The site-mean rebound values (RV) with standard errors are shown in Table 7 (Shiraiwa and Watanabe, 1991). The mean values with a 95 % confidence interval range from 29.7±1.7 (loc. 15) to 53.1±1.6 (loc.48). The rebound values are generally lower at the gneissic sites than at the granitic sites when compared within the same moraine complex. This is due to the difference in texture of rock surfaces: fine-grained granite generally shows a relatively higher rebound value compared to the coarse-grained gneiss.

The complex-mean values with a 90 % confidence interval are 51.1±2.9 (R; taken from

Table 7 The RD data obtained from the Langtang Valley (Shiraiwa and Watanabe, 1991).

Loc. no.	Glacier	Altitude (m)	Moraine complex	R value	WR (mm)	OS (%)	MP (mm)	PD (mm)
1	Li*	4057	R	48.9±1.8	0.0	–	–	–
2	Li*	4063	IM	43.8±2.5	0.0	16	0	0
3	Li*	3963	I	38.9±2.3	1.3	52	0	0
4	Li*	3913	O	36.0±2.2	1.0	64	7	31
5	Li*	3925	O	38.6±2.5	1.0	68	8	19
6	Li*	4025	OM	37.7±2.4	–	–	–	–
7	Li*	3875	O	37.7±2.5	4.0	80	6	20
8	Li*	4098	I	36.8±2.3	1.0	40	0	0
9	Li*	4100	IM	42.7±2.5	0.0	20	0	0
10	Ka*	4440	O	35.9±1.6	3.7	80	6	14
11	Ka*	4863	IM	48.3±1.4	1.0	14	0	0
12	Na*	4130	O	36.0±2.1	–	–	14	27
13	Na*	4228	O	32.6±1.5	3.0	70	14	33
14	Na*	4202	OM	30.8±1.6	4.0	76	14	24
15	Na*	4203	OM	29.7±1.7	–	–	–	82
16	Na*	4192	O	33.5±1.7	4.7	72	14	48
17	SL	3522	O	38.7±2.0	–	–	–	–
18	SL	3530	O	39.0±2.0	–	–	–	–
19	SL	3498	OM	35.9±2.4	–	–	–	–
20	KJ	4276	IM	49.3±1.6	0.0	2	0	0
21	KJ	4322	IM	49.3±1.9	0.0	30	0	0
22	La	3935	OM	37.6±2.7	6.0	–	13	19
23	La	4448	O	42.6±2.5	–	–	6	15
24	La	4646	IM	50.0±1.9	0.0	44	2	6
25	La	4320	O	41.4±2.3	6.0	66	11	14
26	La	4365	O	41.0±2.1	0.0	56	12	9
27	Ls	4312	IM	49.1±2.1	0.0	22	1	0
28	Ls	4328	O	42.9±2.2	0.0	56	3	0
29	Ls	4283	O	42.4±2.9	2.3	50	6	24
30	Sh	4199	O	41.3±2.8	–	–	6	22
31	Sh	4235	I	46.3±1.6	0.0	34	5	11
32	Sh	4226	IM	50.1±1.7	0.0	12	2	0
33	Sh	4250	I	48.6±2.5	0.0	22	1	0
34	Sh	4315	I	48.7±2.2	3.3	34	0	0
35	Sh	4037	O	38.7±2.2	5.1	68	9	13
36	Sh	4050	?	43.7±2.1	–	–	10	14
37	Sh	4107	?	42.6±1.7	3.5	68	10	16
38	Sh	4030	?	42.8±1.9	3.6	64	10	15
39	Pe	4741	IM	48.3±2.2	3.0	40	2	0
40	Ga	4207	OM	36.1±2.0	3.1	68	15	24
41	Un	4530	I	47.6±1.9	–	–	–	–
42	Un	4533	I	49.2±1.9	–	–	–	–
43	Un	4962	IM	50.8±2.4	0.0	28	0	0
44	Ya	4872	I	46.3±2.1	1.5	44	4	14
45	Ya	4915	I	48.7±1.9	1.8	40	4	10
46	Ya	4970	R	50.6±1.7	0.0	22	0	0
47	Ya	4975	R	51.2±1.5	0.0	12	0	0
48	Ya	5090	R	53.1±1.6	–	–	–	–
49	Ya	4850	I	45.7±2.3	2.5	70	5	18
50	Ya	4918	OM	34.7±1.4	3.5	84	19	65
51	Ya	4820	O	42.2±2.1	3.0	–	11	25
52	Ya	4872	O	36.9±2.7	–	–	11	21
53	Ts	4558	?	33.9±1.8	5.0	82	21	36
54	Ts	4562	?	36.3±2.3	2.5	68	18	34

[a]The locations with asterisks show the gneissic site. The names of the glaciers are: Li: Lirung; Ka: Kangja La; Na: Naya Kanga; SL: Southern Langtang Lirung; KJ: Khymjung; La: Langtang; Ls: Langshisa; Sh: Shalbachum; Pe: Pemdang; Ga: Gangchenpo; Un: unnamed; Ya: Yala; and Ts: Tserko. Moraine complex: R: debris covering the stagnant ice; IM: innermost moraine complex; I: inner moraine complex; O: outer moraine complex; and OM: outermost moraine complex. R values: Schmidt hammer rebound value with a 95% confidence interval ($\pm t \cdot \alpha\bar{x}$); WR: weathering rind thickness; OS: oxidation stain percentage; MP: mineral projection height; and PD: pit depth.

Table 8 The complex-mean values with a 90 % confidence interval ($\pm t \cdot \sigma\bar{X}$) of the RD data by geology (Shiraiwa and Watanabe, 1991).

Complex	Geology	R values by Schmidt Hammer	Weathering rind (mm)	Oxidation stain (%)	Mineral projection (mm)	Pit depth (mm)	Hurst Color Index (×1000)
		Mean values	Mean values	Mean values	Mean values	Mean values	Mean values
R[a]	Gneiss	48.9	0	–	–	–	–
	Granite	52.2±4.5	0	12.0	0.0	0.0	–
	Total	51.1±2.9	0.0±0.0	12.0	0.0	0.0	6.37±8.24
IM	Gneiss	44.9±4.0	0.3±0.8	16.7± 4.2	0.0±0.0	0.0± 0.0	–
	Granite	49.7±0.5	0.4±0.7	25.0± 4.2	0.9±0.6	0.8± 1.3	–
	Total	48.4±1.4	0.4±0.5	22.7± 6.4	0.6±0.5	0.5± 0.9	3.74±1.26
I	Gneiss	37.9±4.9	1.2±0.9	46.0±26.8	0.0±0.0	0.0± 0.0	–
	Granite	47.2±1.7	0.8±1.6	36.5±14.5	2.3±2.2	2.8± 5.6	–
	Total	44.9±3.0	0.9±1.0	39.7± 9.5	1.5±1.6	1.8± 3.4	3.01±0.66
O	Gneiss	35.8±1.5	2.9±1.2	72.3± 4.9	9.9±2.6	27.4± 7.7	–
	Granite	42.3±1.6	2.8±1.2	56.3± 8.0	7.4±1.7	16.4± 3.1	–
	Total	39.9±1.7	2.8±0.8	63.7± 6.0	8.4±1.5	20.9± 4.1	2.03±0.28
OM	Gneiss	32.7±5.9	4.0	76.0	14.0±0.0	53.0±19.5	–
	Granite	36.3±1.3	4.8±5.8	84.0	14.3±5.7	35.0±35.7	–
	Total	34.8±2.2	4.5±1.8	80.0±17.9	14.3±3.5	42.2±24.9	1.24±0.19

[a]R: debris covering the stagnant ice.

the debris covering the stagnant ice), 48.4±1.4 (IM), 44.9±3.0 (I), 39.9±1.7 (O), and 34.8±2.2 (OM) (Table 8; Shiraiwa and Watanabe, 1991). Statistically ($p<0.05$), it is possible to differentiate between each moraine complex at the granitic sites. However, no significant difference is apparent at the gneissic sites ($p<0.05$). The reason for this is at present not apparent, although it may partly be caused by small sampling numbers at the gneissic sites.

Despite the fine differentiation in the granitic sites, the rebound values for some moraines (locs. 13, 28, 44, and 45) do not overlap with the mean value of their own complexes, and are in fact similar to the values obtained for other complexes.

The distinct ridges at the Numothang Kalkha (locs. 36, 37, and 38) are correlated with the innermost or inner moraine complex by their rebound values, although they were not assigned to any complex in the field. The terminal moraines located on the south-west facing slope of Mt. Tserko (locs. 53 and 54) and at the foot of Mt. Gangchenpo (loc. 40) gave rebound values similar to those of the outermost moraine complexes.

V.5.2. Other RD tests related to the rock weathering

The site-mean thickness of weathering rind (WR) and the percentage of clasts with oxidation stain (OS) are shown in Table 7. The weathering rind thickness varies from 0.0 mm to 6.0 mm and the oxidation-stain percentage ranges from 0 % to 84 %. The mean values for moraine complexes with a 90 % confidence interval ($\pm t \cdot \sigma\bar{X}$) are shown in Table 8. The results appear to be consistent with increasing weathering rind thickness and oxidation-stain percentage with increasing relative age. Lithological differences do not seem to influence the results of either tests (Table 8). Significant differences between the

site- and complex-mean values are seen at locs. 4, 5, 25, 26, 34, 35, 39, 40, and 54 for the weathering rind data, and locs. 4, 24, 28, 39, and 45 for the oxidation stain data.

The site-maximum height of mineral projections (MP) and site-maximum pit depth (PD) are shown in Table 7. Both parameters show an interesting feature. That is, the values are smaller in the gneissic sites than in the granitic sites for the innermost and inner moraine complexes, while the inverse relation is observed within the outer and outermost moraine complexes (Table 8). This seems to be due to the difference in clast surface texture between the gneissic and granitic sites. Among the gneissic sites, augen-gneiss is dominant, and it shows variable surface characteristics from minerals projecting out several centimeters when the clast is deeply weathered, *i.e.*, in the outer and outermost moraine complexes, to a much smoother surface within the innermost and inner moraine complexes.

A large difference between the site values and the complex-mean values was recorded at locs. 24, 25, 26, 32, 39, 44, 45, and 51 for the mineral projection data, and locs. 24, 29, 30, and 51 for the pit depth data.

V.5.3. RD tests related to the soil sequence

Table 9 (Shiraiwa and Watanabe, 1991) shows the soil profile developed on the moraine crests and the Hurst Color Index (HCI). The soil profiles on the crests of each moraine complex are as follows:

Innermost moraine complex (IM): a localized occurrence of an O horizon overlying a slightly oxidized C horizon (Cox) characterizes this soil profile. A very thin A horizon is found at some locations (locs. 24, 39 and 43 in Table 9).

Inner moraine complex (I): the existence of a thick A horizon clearly separates the inner moraine complex from the innermost moraine complex. Occasionally, an illuvial horizon (Bw horizon) is developed on the moraine, *i.e.*, in front of the Langshisa Glacier (loc. 28).

Outer moraine complex (O): the existence of a B horizon (Bt and Bw horizon) clearly distinguishes this complex from the younger ones, although the thickness of the B horizon varies considerably within this complex. An eluvial horizon (E horizon) with platy structure is found at some locations (*i.e.*, loc. 16). Soils originating from allochthonous materials also characterize the outer moraine complex. These materials are considered to be eolian in origin as they are well sorted and fine-textured.

Outermost moraine complex (OM): the soil profiles are similar to those of the outer moraine complex. It is rather difficult to differentiate the outermost moraine complex and the outer moraine complex by the thickness of the B horizons.

The soil color index of Hurst (1977) varies from 8213 (loc. 48) to 959 (loc. 52, Table 9). The mean values of each complex are shown in Table 8. Although the sampling number is small, their mean values with 90 % confidence intervals suggest that the outer and outermost moraine complexes can be differentiated from innermost and inner moraine complexes. It is also useful for distinguishing the outermost moraine complex from the outer moraine

Table 9-1 Field description of the soils on the moraines and Hurst Color Index (HCI) (Shiraiwa and Watanabe, 1991).

Loc. no.	Moraine comp.	Horizon	Basal depth (cm)	Moist color	HCI (×1000)
2	IM	O	3	10YR 2/2	
		Cox	13+	2.5YR 5/3	2.69
3	I	A	4	10YR 2/1	
		Bw	13	10YR 3.5/3	
		Cox	35+	2.5Y 5/3	2.62
4	O	A	5	10YR 2/3	
		Bt	13	7.5YR 3/4	
		Cox	26+	10YR 4/4	1.37
5	O	A	6	10YR 2/2	
		Bw	13	7.5YR 3/2	
		Cox	27+	2.5Y 3/2	2.38
6	OM	A	9	10YR 2/3	
		AB	15	10YR 3/2	
		Bt	36+	7.5YR 3/3	1.31
7	O	O	3	10YR 1.7/1	
		A	10	10YR 1.7/1	
		Bw	16	2.5Y 4/3	
		Cox	34+	2.5Y 4/2	3.03
8	I	O	1.5	10YR 2/1	
		A	12	10YR 2/2	
		Bw	16	10YR 4/4	
		Cox	29+	2.5Y 5/3	2.70
9	IM	O	7	10YR 2/1	
		Cox	17+	2.5Y 5/1	6.58
10	O	A	7	10YR 2/2	
		Bt	21	7.5YR 3/3	
		Bw	35+	7.5YR 3/4	1.33
11	IM	–	–	–	–
12	O	A	16	–	
		Bt	24	–	
		Cox	37+	–	–
13	O	A	6	10YR 2/2	
		Bt	27	7.5YR 4/4	
		2Bt	38	10YR 4/6	
		2Cox	55+	10YR 3/3	1.31
14	OM	A	8	10YR 2/3	
		Bt	33	7.5YR 4/6	
		2Cox	73+	10YR 4/3	1.47
15	OM	A	6	–	
		E	13	–	
		Bt	28	–	
		2Cox	43+	–	–
16a	O	A	12	10YR 1.7/1	
		2Ab	14	–	
		2E	26	7.5YR 4/1.5	
		2Bt	55+	7.5YR 3/4	–
16b	O	A	11	10YR 1.7/1	
		E	31	7.5YR 4/1.5	
		2Ab	36	–	
		2Bt	58+	7.5YR 3/4	–
20	IM	Cox	19	2.5Y 4/1.5	
		Cu	41+	2.5Y 5/1	–
21	IM	Cox	21+	2.5Y 4/2	–
22	OM	A	12	10YR 2/2	
		Bt	26	7.5YR 2/3	
		2Bt	49	7.5YR 4/6	
		2Cox	64+	2.5Y 4/3	1.39

complex (Tables 8 and 9).

V.5.4. RD data for the older till

Figure 43-B shows the weathering condition of the clasts in the till which were collected from the outcrops along the rivers. The weathering of clasts exposed at the outcrops is strongly influenced by hydrological conditions, however, Figure 43-B clearly shows two groups which have undergone a different degree of weathering; the unweathered till (the *Upper till*) and the weathered till (the *Lower till*), although it is difficult to distinguish between samples 4, 5, and 12 from the unweathered till.

The outermost moraine complex is the oldest one that can be recognized by its morphology: it is composed of fresh materials which can be correlated with the *Upper till*. The altitudinal continuity between the lateral moraine of the Lirung Glacier (loc. 6 in Figure 41) and the *Upper till* of the Shindum Surface also supports the idea that the outermost moraine complex is correlated with the *Upper till*.

Table 9-2 (cont'd). Field description of the soils on the moraines and Hurst Color Index (HCI) (Shiraiwa and Watanabe, 1991).

Loc. no.	Moraine comp.	Horizon	Basal depth	Moist color	HCI (X1000)
23	O	A	4	10YR 2/2	
		Cox	9	10YR 3/2	
		2Ab	17	10YR 2/2	
		2Btb	23	7.5YR 4/3	
		2Bwb	51	10YR 3/4	
		2Cox	69+	10YR 4/4	1.39
24	IM	A	2	10YR 2/2	
		Cox	24+	10YR 4/3	1.94
25	O	A	5	10YR 2/2	
		Bt	23	7.5YR 3/4	
		2Cox	48+	10YR 5/3	2.00
26	O	A	6	10YR 2/2	
		Bt	15	10YR 4/4	
		Bw	33	10YR 4/5	
		2Cox	69+	10YR 4/3	1.60
27	IM	O	1	–	
		Cox	39+	2.5Y 5/2	–
28	O	A	5	10YR 2/2	
		Bw	10	10YR 3/4	
		Cox	51	10YR 3/3.5	
		Cu	61+	2.5Y 4/2	1.87
29	O	A	10	10YR 2/1	
		Bt	20	10YR 4/4	
		Cox	29	2.5Y 4/3	
		2Cox	55+	2.5Y 4/2	2.79
30	O	O	4	10YR 2/1	
		Cox	14	10YR 5/2	
		2Bt	26	10YR 3/4	
		2Cox	57	10YR 5/2	
		3Cox	62+	10YR 5/3	2.32
31	I	AO	3	10YR 2/2	
		Bw	21	10YR 3/3	
		Cox	47+	2.5Y 4/2	2.76
32	IM	–	–	–	–
33	I	A	1	10YR 2/1	
		Cox	25+	2.5Y 5/2	4.09
34	I	A	2	10YR 2/2	
		Cox	28+	2.5Y 5/2	4.04
35	O	A	6	10YR 2/2	
		Bt	16	10YR 3/3	
		2Bw	43	7.5YR 3/3	
		2Cox	58+	2.5Y 4/4	1.47
36	?	A	5	10YR 2/2	
		Bt	15	10YR 3/3	
		Bw	42	7.5YR 3/3	
		Cox	50+	2.5Y 4/4	1.47
37	?	A	5	10YR 2/2.5	
		Bt	24	7.5YR 3/4	
		2Bt	50	7.5YR 3/4	
		2Cox	73+	10YR 4/2	1.59
38	?	A	4	10YR 2/2	
		Bt	13	7.5YR 3/4	
		2Bt	26	7.5YR 3/3	
		2Cox	43+	7.5YR 3/3	1.07
39	IM	A	1	10YR 2/2	
		Cox	18+	2.5Y 5/2	4.07
40	OM	A	10	10YR 2/2	
		Bt	28	7.5YR 4/5	
		2Bt	37	7.5YR 4/4	
		2Cox	49+	7.5YR 3/4	1.09
43	IM	AO	2	10YR 2/1	
		A	3	10YR 2/2.5	
		Cox	20+	2.5Y 5.5/2	4.43
44	I	A	8	10YR 2/2	
		Cox	39+	2.5Y 5/3	2.60
45	I	A	6	10YR 2/2.5	
		Cox	19+	10YR 5/3	2.33
46	R	Cox	30+	2.5Y 5/3	2.74
47	R	Cu	12+	2.5Y 5.5/2	4.52
48	R	Cu	25+	2.5Y 5/1	8.21
49	I	A	10	10YR 2/2	
		Cox	13+	2.5Y 5/3	2.56
50	OM	A	7	10YR 2/3	
		E	13	7.5YR 4/2.5	
		Bt	16	7.5YR 3/4	
		Bw	41	7.5YR 3/4	
		Cox	61+	7.5YR 3/4	1.05
52	O	A	10	10YR 2/2	
		Bt	29	7.5YR 3/4	
		Cox	33+	7.5YR 4/6	0.96
53	OM	A	16	10YR 2/2	
		Bt	10	10YR 3/4	
		Cox	21+	10YR 3/2.5	0.97
54	OM	A	8	7.5YR 2/2	
		Bt	18	10YR 3/4	
		Cox	51+	10YR 3/2	1.94

V.6. *Reconstruction of glacial chronology*

The RD data obtained by seven RD methods (RV, WR, OS, MP, PD, soil profile development, and HCI) generally support the initial classification of the moraines by their geographical positions. However, in 50 % of the cases, one or more of the RD methods did not support this initial classification. In such instances, the moraines are re-classified according to the result which occurs most frequently among the seven RD methods. Modifications are as follows: loc. 24 from the innermost to the inner, and locs. 44 and 45 from

Table 10 The list of ^{14}C data obtained from the Langtang Valley (Shiraiwa and Watanabe, 1991). Locations of a-e are shown in Figure 43-A.

Location	Material	^{14}C date (yr BP)	Lab. No.	Significance
e. Lirung Gl., IM moraine	Superposed organic layer	40±130	NUTA-740	Maximum date for the innermost moraine of the Yala II Stage
Langshisa, valley train	Buried A-horizon	550± 70	GaK-14029	Minimum date for the valley train of the Lirung Stage
Tangdemo, slope deposit	Buried A-horizon	2800±110	GaK-10996	Relatively warm phase around indicated date
a. Mundro, till	Buried A-horizon	2850±140	NUTA-739	Minimum date for the Upper Till of the Langtang Stage
d. Lharung Chu, till	Superposed A-horizon	2980±110	GaK-14028	Maximum date for the moraines of the Lirung Stage
c. Mundro, till	Buried A-horizon	3650±320	GaK-10997	Maximum date for the Upper Till of the Langtang Stage
b. Mundro, till	Wood, not in situ	3860±110	GaK-14027	Possible indication of warm phase around indicated date. After that, the wood was incorporated in the Upper Till

the outer to the inner. Four sites are classified solely on the basis of their RD results as follows: loc. 37 as the outer, locs. 40, 53, and 54 as the outermost.

V.6.1. ^{14}C dating

Table 10 (Shiraiwa and Watanabe, 1991) summarizes the ^{14}C dates obtained in the Langtang Valley. Since no dates have been obtained from the *Lower till*, the following discussion focuses on the *Upper till* and the outermost to innermost moraine complexes.

The *Upper till* of column C3 in Figure 43-A is underlain by a humic silt layer dated at 3650±320 yr. BP (GaK-10997) some 60 cm below the till base. This is overlain by a stratified layer, within which is a buried organic layer dated at 2850±140 yr. BP (NUTA-739) 180 cm above the top of the till. An allochthonous wood fragment obtained from the *Upper till* was dated at 3860±110 yr. BP (GaK-14027). The *Upper till*, therefore, was deposited between 3650 yr. BP and 2850 yr. BP, probably before 3000 yr. BP, considering the continual phase of soil formation around 2980 to 2800 yr. BP as mentioned below. This is also supported by the ^{14}C dating (3310±80 yr. BP) for a chacoal layer which overlies the *Upper till* (Watanabe, 1992).

The stratified layer, 4.5 m thick above the *Upper till* is believed to have been deposited by damming of the southern Langtang Lirung Glacier (Heuberger *et al.*, 1984), because only a lacustrine environment can explain the formation of such a layer. The irregularity of the surface on which the Langtang village is situated indicates that the surface has been eroded by a tributary glacier, advancing from the Pääbe Chu, which dammed the main river before and/or after 2850 yr. BP. Evidence for damming is also indicated by a huge lateral moraine formed by the southern Langtang Lirung Glacier (locs. 17 and 18 in Figure 41) which is assigned to the outer moraine complex by the RD data.

Today, in the Langtang Valley, slopes are vegetated below about 4800 m. Thus, the

development of soil horizons at about 4300 m in the Langtang Valley, which gives a ^{14}C date of approximately just after 3000 yr. BP indicates a climate similar to that existing today.

Soil formation was interrupted by an accumulation of till as observed along the Lharung Chu (column C7 in Figure 43-A). This till is considered to be correlated with the outer moraine complex. The date of a humic layer (2980±110 yr. BP; Gak-14028) indicates the maximum date of the onset of the outer moraine complex. On the other hand, the valley train related to the outer moraine complex in front of the Langshisa Glacier is underlain by a buried A horizon dated as 550±70 yr. BP (GaK-14029). The outer moraine complex, therefore, was formed between 2980 yr. BP and 550 yr. BP, during which three or four advances occurred.

No dates have been obtained from the inner moraine complex. However, it is sure that this complex was formed after 550 yr. BP, since the valley train in the Langshisa Kalkha, which is correlated with the inner moraine complex, is not covered with any buried soil corresponding to the soil dated as 550 yr. BP. The inner moraine complex seems to represent an early advance in the Little Ice Age.

The youngest innermost moraine complex overlies a thin organic layer dated as 40±130 yr. BP (NUTA-740; e of column C12 in Figure 43-A). This complex, therefore, corresponds to the advance at the beginning of the present century (probably around A.D. 1910).

V.6.2. Summary of the glacial chronology

Although the glacial advances forming both the outer and outermost moraine complexes have been regarded as Late-glacial by many researchers (Heuberger *et al.*, 1984; Ono, 1986; Zheng, 1988), the results of RD and ^{14}C datings reveal that they occurred during Neoglaciation between 2980 and 550 yr. BP, and 3650 (3310) and 2850 yr. BP. I call these advances *Lirung* and *Langtang stages*, respectively.

Table 11 (Shiraiwa and Watanabe, 1991) shows the glacial chronology of the Langtang Valley, in which I have introduced four other stages corresponding to the construction of

Table 11 A tentative glacial chronology of the Langtang Valley (Shiraiwa and Watanabe, 1991). Abbreviation is the same as in Table 7.

Stage	Landform	^{14}C date (yr BP)	RV	WR (mm)	OS (%)	MP (mm)	PD (mm)	HCI x1000	Soil profile	% of weathered clasts[a] UW:J:D
Lama	U-shaped trough	–	–	–	–	–	–	–	–	–
Gora Tabela	Lower Till surface	–	–	–	–	–	–	–	–	54:37:9
Langtang	Upper Till surface or OM moraine complex	3650–3000	34.8	4.5	80.0	14.3	42.2	1.24	A/B/C	93:6:1
Lirung	O moraine complex	2800–550	39.9	2.8	63.7	8.4	20.9	2.03	A/(E)/B/C	–
Yala I	I moraine complex	<550	44.9	0.9	39.7	1.5	1.8	3.01	A/(Bw)/C	–
Yala II	IM moraine complex	A.D. 1910?	48.4	0.4	22.7	0.6	0.5	3.74	O/C	–

[a]UW: unweathered clasts; J: jointed clasts; D: disintegrated clasts.

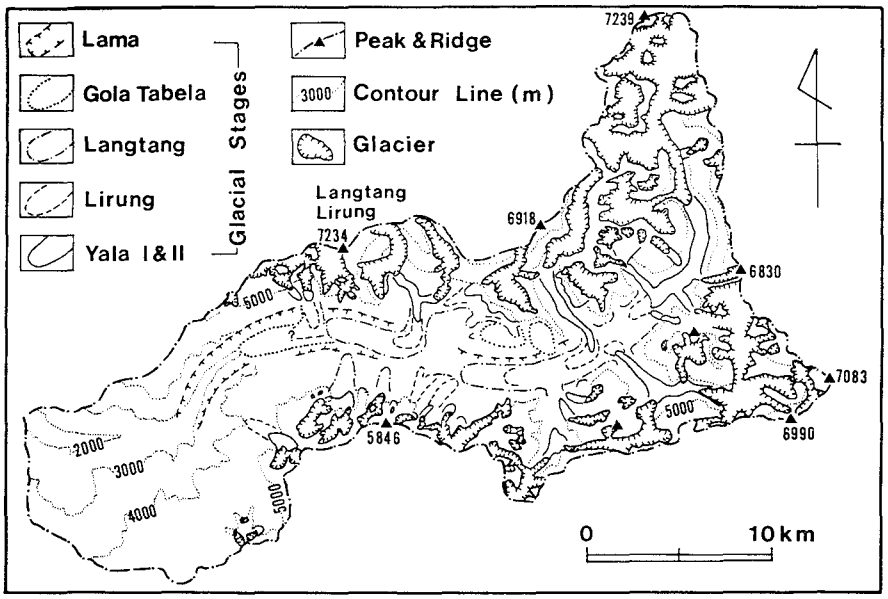

Figure 44 The spatial distribution of the glaciers during the late Quaternary (Shiraiwa and Watanabe, 1991).

moraine complexes and the *Lower till* member. Figure 44 (Shiraiwa and Watanabe, 1991) illustrates the spatial extent of the glaciers in each stage.

Lama Stage: the most extensive glaciation in the valley. Neither till nor moraine have been identified but a U-shaped trough is recognized. The terminus of the glacier seems to have extended down to the great bend of the Langtang Khola at an altitude of approximately 2600 m. No chronological data have been obtained.

Gora Tabela Stage: the advance indicated by a dissected terminal moraine at an altitude of 3200 m. The *Lower till* accumulated during this stage, originally forming the Chomki Surface. A glaciofluvial deposit overlain by the *Lower till* suggests that an interstadial existed between the *Lama* and the *Gora Tabela stages*. Severely weathered clasts of the *Lower till* (Figure 43-B) indicate that the *Gora Tabela Stage* is much older than the *Langtang Stage*.

Langtang Stage: the most spatially extensive Holocene advance. The Lirung Glacier extended almost to the Langtang village. The Shindum Surface was formed by this glaciation, and was smoothed afterwards by fluvial action. The lowest terminus of the Langtang Glacier in this stage is located at the Markujung Kalkha (3900 m). The small terminal moraines at the Mendang and Chadang kalkhas clearly show the recessional phase of this stage. The main valley was filled with the glaciofluvial deposits in the recessional phase, forming the Kyangchen Surface. The age of this stage, estimated by the ^{14}C dates of the

Upper till along the Numthang Chu, is between 3650 and 2850 yr. BP, and probably between 3310 and 2850 yr. BP.

Lirung Stage: three to four advances between 2980 yr. BP and 550 yr. BP are implied by the presence of the outer moraine complex. The lateral moraines below the Langtang village (locs. 17 and 18 in Figure 41) were formed in this stage by a tributary glacier (southern Langtang Lirung Glacier of Heuberger *et al.*, 1984).

Yala I Stage: this advance is implied by the presence of the inner moraine complex. The glacial extent of this stage was much smaller than those of the *Lirung Stage*, but was almost the same as that of the *Yala II Stage*, except for the flat-topped glaciers such as the Yala Glacier. No numerical dating data have been obtained from the inner moraine complex. However, the *Yala I Stage* may correspond to the Little Ice Age, because of the lack of a buried A horizon, which covers the valley train of the *Lirung Stage* and is dated at 550 yr. BP.

Yala II Stage: the latest glaciation in the valley. A ^{14}C date indicates that the latest maximum advance of the Lirung Glacier occurred probably around A.D. 1910, although Ono (1986) gave a date of A.D. 1815 for the latest advance of the Yala Glacier in the Little Ice Age.

VI. Reconstruction of the late Quaternary paleoclimate in the Langtang Valley

VI.I. *Introduction*

Although the reconstruction of the late Quaternary paleoclimate has been attempted in many parts of the world, only few studies have been done in the Himalaya-Tibetan sector of central Asia, because of a lack of sufficient data on past glacial fluctuations. Since this area greatly influences global atmospheric circulations, as stated in Chapter I, a paleoclimatic reconstruction of this area is needed in order to better understand the global climate of the past.

Paleoclimatic reconstruction by means of glacial fluctuation has been exclusively discussed by comparing present and past equilibrium line altitudes (ELA) of glaciers. The ELA is a boundary between an accumulation area where net balance $b_n > 0$ and an ablation area where $b_n < 0$ (Paterson, 1981). The boundary can be strictly defined by measuring the mass balance of a glacier. Past ELA, on the other hand, can only be estimated by geomorphological evidence, such as the altitude of remnant cirque floors, the altitude of the glaciation threshold, the maximum altitude of lateral moraines, the median altitude of reconstructed glaciers, and the areal relationship between accumulation and ablation zones of reconstructed glaciers (Meierding, 1982).

However, ELA data themselves cannot reconstruct any single climatic parameter, because ELA is determined by a combination of several climatic parameters; its areal distribution suggests only the past climatic circulation pattern (*e.g.*, Porter, 1977; Ono, 1991).

In this chapter, I present a steady-state glacier mass balance model by which the

paleoclimatic parameters in the Langtang Valley can be reconstructed quantitatively. The model is based on a couple of meteorological parameters to determine a terminal altitude of a glacier. Therefore, a reconstruction of a combination of past meteorological parameters becomes possible, once the terminal altitude of the past glacier is obtained. The reconstructed meteorological parameters, combinations of summer air temperature, summer precipitation and winter balance, are then compared with previously obtained geological data, and the most suitable combination is discussed.

VI.2. *Previous work*

The reconstruction of past ELA in the Himalaya has been attempted on the basis of glacial landforms by several researchers. After the classical work by Wissmann (1959) which covers all of central Asia, the past ELA was estimated in Khumbu (Müller, 1980; Williams, 1983; Kuhle, 1986b, 1987), in Dhaulagiri and Annapurna (Kuhle, 1982), in the Langtang Valley (Heuberger *et al.*, 1984; Ono, 1986), and in Kangchenjunga (Kuhle, 1990) in the Nepal Himalaya.

Reconstructed past ELA depressions in each proposed stage differ considerably among researchers because of regional differences and possible errors related to misinterpretations of glacial landforms on which the ELA depressions depend. The estimated maximum ELA depression for the late Quaternary ranges from 1660 m in Kangchenjunga (Kuhle, 1990) to 210 m in the northern part of Dudh Kosi (Müller, 1980). The estimated amount of ELA depression during the Holocene varies from 500–600 m in Dhaulagiri-Annapurna and Khumbu (Kuhle, 1982, 1987) to 160 m in the Langtang Valley (Ono, 1986).

Although the past ELA has been estimated by several authors, few have interpreted the reconstructed ELAs climatically in the Nepal Himalaya. This is because that ELA is not a linear function of air temperature: its altitudinal change has different meanings in relation to a precipitation condition (Ageta, 1983b; Shi, *et al.*, 1992). Therefore, it is necessary to develop a model to reconstruct past climatic conditions from the glacial fluctuation data.

VI.3. *A steady-state glacier mass balance model*

In simulating glacial fluctuations, various models have been proposed. They involve a wide range of models, from a simple one based on a steady-state glacier mass balance to a three dimesional mass-energy coupled and time-dependent one. In the Himalaya, a lack of detailed glaciological as well as meteorological and topographical data prevents us from adopting any complicated models. A simple model is therefore employed in this study.

A steady state condition of mass balance in any glacier is expressed as,

$$\int_{he}^{ho} S(h)\{B_s(h)+B_w(h)\}\mathrm{d}h+\int_{ht}^{he} S(h)\{B_s(h)+B_w(h)\}\mathrm{d}h=0 \qquad (1)$$

where h_o, h_e and h_t are altitudes (m) of the highest point, equilibrium line and terminus of a

glacier; S, the area of ground surface ($km^2 \cdot 50\ m^{-1}$); B_s and B_w, the mass balance (mm water equivalent) at certain altitudes of the glacier during summer and winter. The seasonal mass balance can be obtained by the summation of accumulation and ablation in each period;

$$B_s = C_s + A_s \quad (2)$$

$$B_w = C_w + A_w \quad (3)$$

where C_s and C_w are the accumulation (mm water equivalent) during summer and winter, while A_s and A_w are the ablation (mm water equivalent) during summer and winter.

Mass balance was divided into summer and winter components because winter balance currently contributes up to 47 % of the annual net balance of small glaciers in the Langtang Valley (Chapter III-6; Figure 22). The summer season is defined as the months from June to September, while the other months are included in winter. The summer season is characterized by the Indian monsoon circulation, while winter is dominated by a westerly circulation.

In the present modelling, I ignored the insulating effect of debris cover of glaciers on surface ablation. Although Yasunari (1987) emphasized the importance of this effect, the present debris cover on the glaciers in the Langtang Valley seems to be a result of rather rapid melting of valley glaciers after the Holocene maximum advance. Therefore, the neglecting the effect of debris cover on glacier surface ablation is a reasonable assumption for the period of maximum glacier extension.

Altitudinal distribution of the ground surface S is considered for the modeling. The hypsometric curve of S (Figure 45) was made by measuring areas every 50 m in altitude on the official 1 : 50,000 map of Nepal. Figure 45 indicates a relatively large area exists between 5500 m and 4500 m which significantly influences the glaciation in the Langtang Valley as already suggested by Fushimi (1978) and Kuhle (1988a) in the Khumbu region.

I assume that the altitude and the form of the valley have been the same since the Last Glacial time. The assumption seems to be reasonable because the uplift of the Great Himalaya during the last several hundred thousand years is considered to be negligible (Nakata *et al.*, 1984). The uplift rate of at most $0.6-0.9\ mm \cdot yr^{-1}$ which was estimated from geomorphological evidence concerning the Nepal Himalaya (Iwata, 1987) also supports this idea. The glaciation in this valley was mainly dominated by that of the Langtang Glacier; therefore, h_0 was set at the present altitude of 7200 m. The lowest altitude of the valley is approximately 1400 m; therefore, both values, h_e and h_t, fall between 7200 m and 1400 m.

Both C_s and A_s were computed according to a model proposed by Ageta (1983a). The model describes the relationship between accumulation and ablation of a small glacier and climatic factors. It was proposed to simulate the glacier mass balance in the Shorong region, about 100 km east of the Langtang Valley. Ozawa (1991), however, confirmed that this model is also applicable to the glaciers in the Langtang Valley.

In the model, the summer balance B_s is obtained by,

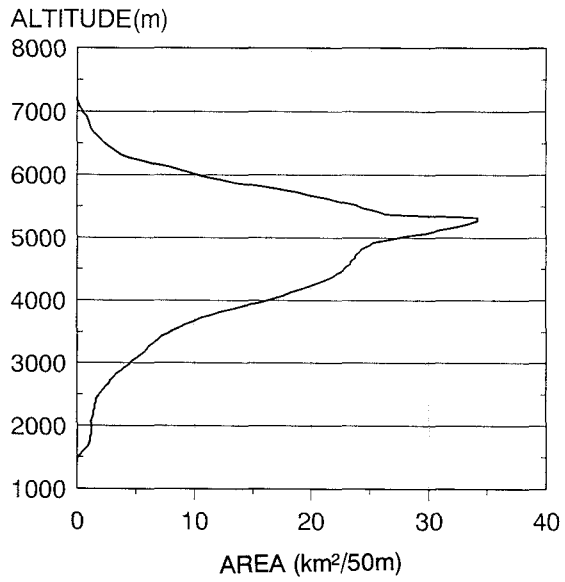

Figure 45 Hypsometric curve of the ground surface in the Langtang Valley.

$$B_s = C_s + A_s \tag{4}$$

C_s is obtained by,

$$C_s = P_s(0.80 - 0.23T_s), \tag{5}$$
when $T_s < -0.8$ then $C_s = P_s$
$T_s > 3.4$ then $C_s = 0$,

where P_s is the total summer precipitation (mm) and T_s is the mean summer air temperature (°C). Summer ablation A_s is expressed as,

$$A_s = -(T_s + 3.2)^{3.2}, \tag{6}$$
when $T_s \leq -3.2$, then $A_s = 0$.

This study regards an altitudinal lapse rate of T_s as -6 °C·km^{-1}, following the results obtained in the valley by Takahashi *et al.* (1987a). In addition, the altitudinal amplification factor of P_s is determined as 25 %·km^{-1} (Ozawa, 1991) after observations by Seko (1987). This value was determined by the altitudinal difference of precipitation amount between Kyangchen (3920 m) and Glacier Camp (5090 m) during the summer season of 1985.

Winter balance B_w is the summation of C_w and A_w. However, since these values are not modeled yet as a function of climatic parameters, B_w itself is tentatively input to the model for the first approximation.

Ohta *et al.* (1990) estimated an altitudinal change of seasonally deposited snow in April at the lower altitudes of the Langtang Valley, and presented a formula expressing the

altitudinal dependence of seasonally deposited snow in April. The water equivalent amount of deposited snow H_w (mm) at an altitude h (m) is expressed as follows;

$$H_w = 0.225 \times h - 778.5. \tag{7}$$

The amount of H_w decreases as a season proceeds, and finally it remains positive only on the accumulation area of a glacier to supply B_w. For this reason, the equation cannot be applied directly to the model. The gradient of h is, however, reported to be constant in a mountainous region during ablation season (Yamada, 1982). Equation (7) can therefore be modified to a general form as follows,

$$H_w = 0.225 \times h - t. \tag{8}$$

From equation (8),

$$t = 0.225 \times h - H_w. \tag{9}$$

Now, t is obtained by inputting the value H_w ($=B_w$) and the altitude h. In the simulation model, B_w at 5350 m is input on the basis of the snow core study conducted in the accumulation area (5350 m) of the Yala Glacier (Figure 22). In this way, B_w at 5350 m for the past glaciation was tentatively assumed.

The computation of both h_e and h_t was carried out using a step of 50 m in altitude.

VI.4. *Evaluation of the model*

First, I evaluated the model by comparing an observed h_e with a simulated h_e in the Yala Glacier. The h_e of the Yala Glacier in 1990 and 1991 was estimated by the studies of deposited snow profiles (Figures 17 and 18); h_e corresponds to the lowest limit of the annually-deposited firn layer, *i.e.*, firn line. The firn line was between 5098 and 5170 m high in 1990, between 5310 and 5350 m high in 1991. Although an internal accumulation by superimposed ice formation (Ozawa, 1991) lowers the actual ELA of this glacier, altitudinal differences between the firn line and ELA is considered to be small.

The model predicts a h_e value for the Yala Glacier as 5050 m in 1990 and 5350 m in 1991, by inputting the value of the observed T_s at 5090 m (2.6 °C in 1990; 3.8 °C in 1991), P_s at 5090 m (826 mm in 1990; 336 mm in 1991; Figure 13), and B_w at 5350 m (230 mm in 1989/90; 105 mm in 1990/91; Figure 22) at the Yala Glacier. The value is slightly under-estimated, compared with the observed h_e in 1990, while h_e in 1991 is well reconstructed. The error in 1990 is less than 100 m; therefore, the model is applicable to estimate h_e.

The second step of the evaluation is to simulate both h_e and terminal altitude h_t of the Langtang Glacier. In this evaluation, meteorological data around the Langtang Glacier are very limited and thus pose a problem. Data are only available from the ablation area of the glacier. The data for the evaluation are taken from the Kyungka Ri (KY) and Langtang Glacier (LA) stations (Figure 8). The following observed values were input to the model: 3.1

°C for T_s (Figure 11) and 556 mm for P_s (Figure 13) at 5090 m in 1990, and 3.4 °C and 512 mm for 1991 (Figure 13). B_w at 5350 m was tentatively given as 230 mm in 1989/90 and 105 mm in 1990/91; the values are the same as those in the middle reaches of the valley in the same years.

The ELA of the Langtang Glacier has never been observed before, however it can be located at 5500 m or slightly higher, on the basis of the highest altitude of supra-glacial moraines. Chinese literature also gives a value of 5560 m (Academia Sinica, 1986), probably depending on the same method. In this simulation, therefore, a value of 5560 m is used for h_e for the Langtang Glacier. The active terminus, on the other hand, exists at an altitude of approximately 4800 m above which well-organized surface patterns such as an ogive structure can be found, although the ice body extends down to an altitude of approximately 4480 m where a series of Little Ice Age moraines is formed. The terminal part of the glacier is considered to be fossil, since it has no structural patterns indicating glacial flow.

The model simulated the values of h_e, 5150 and 5300 m, and h_t, 4450 m and 4650 m for 1990 and 1991, respectively. The model simulations, therefore, under-estimate the actual values considerably. Input of the data obtained at the lower part of the glacier seems to be the reason for under-estimation. The accumulation area of the Langtang Glacier is situated further north adjacent to the Tibetan Plateau where a drier climatic condition is suggested. Such a situation decreases the precipitation and increases the air temperature during summer, as a result, the ELA rises considerably. In the following discussion, an ELA of 5560 m is used for the present Langtang Glacier.

VI.5. *Simulation of past climatic conditions*

VI.5.1. Simulation of past glacial terminus altitude

Paleoclimatic reconstruction was examined especially for the *Gora Tabela* and *Langtang stages*, the Last Glacial Maximum (LGM) and the Holocene maximum glaciations, respectively. The terminal altitudes of the glaciers in both stages are 3200 m and 3900 m, as shown in Chapter V. Table 12 shows possible solutions for both h_e and h_t, by changing T_s at 5090 m from 6 to −3 °C, P_s at 5090 m to be 200, 400 and 800 mm, and B_w at 5350 m from 0 to 600 mm by 100 mm steps. Hatched areas give several combinations which reconstruct the terminal altitudes of the *Gora Tabela* and *Langtang stages*. Assuming that P_s and B_w have been constant, the same as present (P_s=400 mm; B_w=200 mm), the *Gora Tabela Stage* glaciation can be reconstructed with a summer air temperature of approximately −1.5 °C at 5090 m, while the *Langtang Stage* can be made with a value of about 0.5 °C of T_s at 5090 m. The ELAs both in the *Gora Tabela* and *Langtang Stages* result in altitudes of 4550 m and 4850 m which are converted to ELA depressions of approximately 1000 m and 700 m elevation.

When, P_s was reduced to 200 mm, maintaining B_w to be 200 mm both in the *Gora Tabela* and *Langtang Stages*, T_s should be maintained at −2.5 and 0 °C at 5090 m high for the *Gora Tabela* and *Langtang stages*. The resulting ELAs are 4500 and 4800, which mean the ELA

Table 12 Possible solutions for both h_e and h_t by changing T_s at 5090 m from 6 to −3 °C, P_s at 5090 m to be 200, 400 and 800 mm, and B_w at 5350 m from 0 to 600 mm by 100 mm steps. Hatched areas give several combinations which reconstruct the terminal altitudes of the *Gora Tabela* (thick) and *Langtang* (thin) stages.

Ts(C), Ps, Bw(mm)	Ts at 5090 m	6			5			4			3			2		
Bw at 5350 m	Ps at 5090 m	200	400	800	200	400	800	200	400	800	200	400	800	200	400	800
Bw = 0	he (m)	5800	5750	5700	5650	5600	5550	5500	5450	5400	5400	5300	5250	5250	5150	5100
	ht (m)	5450	5400	5300	5300	5200	5100	5150	5000	4800	4950	4750	4550	4700	4550	4300
Bw=100	he	5700	5650	5650	5550	5550	5500	5450	5400	5350	5300	5250	5200	5150	5100	5050
	ht	5350	5300	5200	5200	5100	5000	5000	4900	4700	4750	4650	4450	4550	4400	4150
Bw=200	he	5650	5600	5600	5500	5450	5450	5350	5300	5300	5200	5200	5150	5100	5050	5000
	ht	5250	5200	5150	5100	5000	4900	4850	4750	4600	4600	4500	4350	4400	4250	4050
Bw=300	he	5550	5550	5550	5400	5400	5400	5300	5250	5250	5150	5100	5100	5000	5000	4950
	ht	5200	5150	5050	4950	4900	4800	4700	4650	4500	4500	4400	4250	4250	4150	3950
Bw=400	he	5500	5500	5500	5350	5350	5350	5200	5200	5200	5100	5050	5050	4950	4900	4900
	ht	5100	5050	4950	4850	4800	4700	4600	4550	4400	4350	4300	4150	4100	4000	3800
Bw=500	he	5450	5450	5450	5300	5300	5300	5150	5150	5150	5000	5000	5000	4850	4850	4850
	ht	5000	4950	4900	4750	4700	4600	4500	4450	4350	4250	4200	4050	4000	3900	3700
Bw=600	he	5400	5400	5400	5250	5250	5250	5100	5100	5100	4950	4950	4950	4800	4800	4800
	ht	4900	4850	4800	4650	4600	4550	4400	4350	4250	4150	4100	3950	3850	3750	3600
Ts(C), Ps, Bw(mm)	Ts at 5090 m	1			0			-1			-2			-3		
Bw at 5350 m	Ps at 5090 m	200	400	800	200	400	800	200	400	800	200	400	800	200	400	800
Bw = 0	he (m)	5150	5050	4950	5000	4900	4800	4900	4750	4650	4800	4650	4500	4700	4500	4350
	ht (m)	4550	4300	4000	4350	4100	3650	4150	3850	3250	3950	3550	2800	3750	3200	2100
Bw=100	he	5050	4950	4900	4900	4800	4750	4800	4700	4600	4650	4550	4450	4550	4400	4300
	ht	4350	4150	3850	4150	3900	3500	3900	3600	3050	3650	3250	2500	3350	2850	1750
Bw=200	he	4950	4900	4850	4800	4750	4700	4700	4600	4550	4550	4450	4400	4450	4350	4250
	ht	4150	4000	3700	3950	3700	3300	3650	3350	2850	3350	2950	2100	3000	2500	<1500
Bw=300	he	4850	4850	4800	4750	4700	4650	4600	4550	4500	4450	4400	4350	4350	4250	4200
	ht	4000	3850	3550	3750	3500	3100	3400	3150	2550	3050	2650	1800	2650	2050	<1500
Bw=400	he	4800	4800	4750	4650	4650	4600	4500	4500	4450	4400	4350	4300	4250	4200	4150
	ht	3850	3700	3400	3550	3300	2950	3150	2900	2250	2750	2300	<1500	2200	1650	<1500
Bw=500	he	4750	4700	4700	4600	4550	4550	4450	4450	4400	4300	4300	4250	4150	4150	4100
	ht	3700	3550	3250	3350	3150	2700	2950	2650	1950	2400	1950	<1500	1800	<1500	<1500
Bw=600	he	4650	4650	4650	4500	4500	4500	4400	4400	4350	4250	4250	4200	4100	4100	4050
	ht	3550	3400	3100	3150	2950	2500	2700	2300	1650	2050	1600	<1500	<1500	<1500	<1500

depressions are 1050 and 750 m. In this case, if B_w is increased to 400 mm, T_s of −1.0 and 1.0 °C at 5090 m are sufficient for the two glaciations, and the ELA depressions are 1000 and 750 m.

VI.5.2. Effect of P_s and B_w on the glacial extension

At first, altitudinal changes of h_e and h_t are examined in relation to the changes of T_s, by assuming P_s and B_w to be constant. Taking B_w as 0 mm (Figure 46-A), for instance, both h_e and h_t descend accordingly as T_s decreases. The lowering rate of h_e is steeper when P_s is larger (=800 mm) than when P_s is smaller (=200 mm). This indicates that a decrease in summer air temperature affects the lowering of ELA more effectively in a humid condition than in an arid one. The result is consistent with observations in the Himalaya and the Tibetan Plateau where a decrease in air temperature cannot lower the ELA effectively in an arid environment (Ageta, 1983b; Shi, *et al.*, 1992).

The lowering of h_t, however, does not linearly change with decreases in T_s. The colder T_s is, and also the larger P_s is, the exponentially larger the gradient becomes. This is because the descent of h_e around an altitude of 5000 m causes exponential increase in the accumulation area (Figure 45), and a large amount of P_s requires an extensive ablation area,

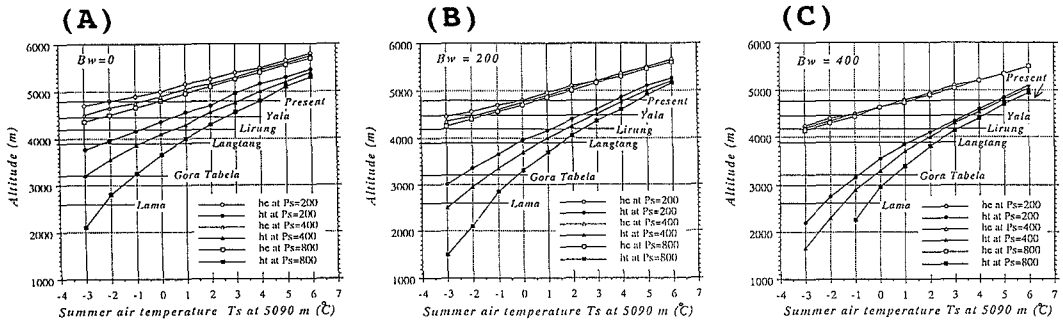

Figure 46 Simulation of the altitudinal change of both h_e and h_t in relation to the changes of T_s. B_w is assumed to be zero(A), 200(B) and 400 mm (C). The present condition is plotted by the known altitude of h_e, while the *Lama, Gora Tabela, Langtang, Lirung*, and *Yala stages* are plotted by geomorphologically obtained h_t.

and consequently this results in a significant lowering of h_t.

Next, I demonstrate the effect of B_w, by changing B_w to 200 and 400 mm (Figure 46-B, C). The increase of B_w resulted in an approaching of h_e with different P_s, and in further lowering of h_t. The approaching of h_e indicates that h_e does not depend on the precipitation, if precipitation is sufficiently supplied to the glacier. This implies that an increase in B_w becomes the most important contributor to the glacier development, when the summer precipitation is small. On the other hand, h_t descends largely as B_w increases, in conjunction with the amount of P_s, because this is necessary for ablating the large amount of mass input resulting from the increase in precipitation.

VI.5.3. Simulation of the present climatic condition of the Langtang Glacier

It is necessary to clarify the present climatic condition of the Langtang Glacier for a comparison between the present and past climatic conditions. It is, however, difficult to determine due to the lack of direct meteorological observations in the uppermost part of the Langtang Valley where the accumulation area of the glacier is situated. The climatic condition of the glacier is, therefore, deduced from the model.

Since the ELA of 5560 m in the Langtang Glacier is estimated by myself and from the Chinese literature, this value is used. The average P_s at 5090 m and that of B_w at 5350 m are assumed to be 400 and 200 mm, respectively, which indicates a slightly drier condition than the observed values. When I put these values in Table 13, it gives 5.5 °C as the value of T_s at 5090 m, and 5100 m for h_t. T_s at ELA of the present Langtang Glacier is, therefore, calculated as 2.7 °C using an air temperature lapse rate of 6 °C·km^{-1}. Although the value of T_s is considerably high compared to the observed values in the valley, and the simulated value of h_t is slightly higher than the actual terminus at 4800 m, these values are adopted to represent the present climatic condition of the Langtang Glacier.

Table 13. Simulation of present climatic condition of the Langtang Glacier. Input of known ELA (5560 m), P_s (400 mm) and B_w (200 mm) gives the T_s between 5 and 6 °C (=−5.5 °C), and h_t between 5000 and 5200 m (=5100 m).

Ts(C), Ps, Bw(mm)	Ts at 5090 m	6			5			4			3			2		
Bw at 5350 m	Ps at 5090 m	200	400	800	200	400	800	200	400	800	200	400	800	200	400	800
Bw = 0	he (m)	5800	5750	5700	5650	5600	5550	5500	5450	5400	5400	5300	5250	5250	5150	5100
	ht (m)	5450	5400	5300	5300	5200	5100	5150	5000	4800	4950	4750	4550	4700	4550	4300
Bw=100	he	5700	5650	5650	5550	5550	5500	5450	5400	5350	5300	5250	5200	5150	5100	5050
	ht	5350	5300	5200	5200	5100	5000	5000	4900	4700	4750	4650	4450	4550	4400	4150
Bw=200	he	5650	5600	5600	5500	5450	5450	5350	5300	5300	5200	5200	5150	5100	5050	5000
	ht	5250	5200	5150	5100	5000	4900	4850	4750	4600	4600	4500	4350	4400	4250	4050
Bw=300	he	5550	5550	5550	5400	5400	5400	5300	5250	5250	5150	5100	5100	5000	5000	4950
	ht	5200	5150	5050	4950	4900	4800	4700	4650	4500	4500	4400	4250	4250	4150	3950
Bw=400	he	5500	5500	5500	5350	5350	5350	5200	5200	5200	5100	5050	5050	4950	4900	4900
	ht	5100	5050	4950	4850	4800	4700	4600	4550	4400	4350	4300	4150	4100	4000	3800
Bw=500	he	5450	5450	5450	5300	5300	5300	5150	5150	5150	5000	5000	5000	4850	4850	4850
	ht	5000	4950	4900	4750	4700	4600	4500	4450	4350	4250	4200	4050	4000	3900	3700
Bw=600	he	5400	5400	5400	5250	5250	5250	5100	5100	5100	4950	4950	4950	4800	4800	4800
	ht	4900	4850	4800	4650	4600	4550	4400	4350	4250	4150	4100	3950	3850	3750	3600
Ts(C), Ps, Bw(mm)	Ts at 5090 m	1			0			-1			-2			-3		
Bw at 5350 m	Ps at 5090 m	200	400	800	200	400	800	200	400	800	200	400	800	200	400	800
Bw = 0	he (m)	5150	5050	4950	5000	4900	4800	4900	4750	4650	4800	4650	4500	4700	4500	4350
	ht (m)	4550	4300	4000	4350	4100	3650	4150	3850	3250	3950	3550	2800	3750	3200	2100
Bw=100	he	5050	4950	4900	4900	4800	4750	4800	4700	4600	4650	4550	4450	4550	4400	4300
	ht	4350	4150	3850	4150	3900	3500	3900	3600	3050	3650	3250	2500	3350	2850	1750
Bw=200	he	4950	4900	4850	4800	4750	4700	4700	4600	4550	4550	4450	4400	4450	4350	4250
	ht	4150	4000	3700	3950	3700	3300	3650	3350	2850	3350	2950	2100	3000	2500	<1500
Bw=300	he	4850	4850	4800	4750	4700	4650	4600	4550	4500	4450	4400	4350	4350	4250	4200
	ht	4000	3850	3550	3750	3500	3100	3400	3150	2550	3050	2650	1800	2650	2050	<1500
Bw=400	he	4800	4800	4750	4650	4650	4600	4500	4500	4450	4400	4350	4300	4250	4200	4150
	ht	3850	3700	3400	3550	3300	2950	3150	2900	2250	2750	2300	<1500	2200	1650	<1500
Bw=500	he	4750	4700	4700	4600	4550	4550	4450	4450	4400	4300	4300	4250	4150	4150	4100
	ht	3700	3550	3250	3350	3150	2700	2950	2650	1950	2400	1950	<1500	1800	<1500	<1500
Bw=600	he	4650	4650	4650	4500	4500	4500	4400	4400	4350	4250	4250	4200	4100	4100	4050
	ht	3550	3400	3100	3150	2950	2500	2700	2300	1650	2050	1600	<1500	<1500	<1500	<1500

VI.6. *Comparison between simulated climatic conditions and paleoclimatic data by geological evidences*

In the previous section, several combinations of past climatic conditions were suggested, especially for the *Gora Tabela Stage* of the LGM (Last Glacial Maximum) and the *Langtang Stage* just before 3000 yr. BP. It is difficult to reconstruct a single climatic parameter from the reconstructed combinations without fixing the other two. In this section, several geological data are introduced to deduce possible paleoclimatic conditions for these two stages.

The air temperature of the LGM, to which the *Gora Tabela Stage* is correlated, is reviewed by Li (1988) who concludes that lowering of annual mean air temperature at Qinghai-Xizang Plateau was at least 5−6 °C, on the basis of periglacial environmental changes (Figure 47; modified from Li, 1988).

In addition, Bhattacharyya (1989) reconstructed the paleoenvironment in the Ladak Himalaya, western part of the Himalayan Range, by a palynological method. According to his study, the climate of the LGM was dominated by cold and dry (cryoxerotic) conditions, shortly interrupted by a cold and humid (cryohygrotic) episode dated at 21290 to 18375 yr.BP (Figure 47, A). The dry condition is considered to be caused by a weakened summer monsoon, which is suggested by a deep-sea sediment analysis in the Arabian Sea where up-

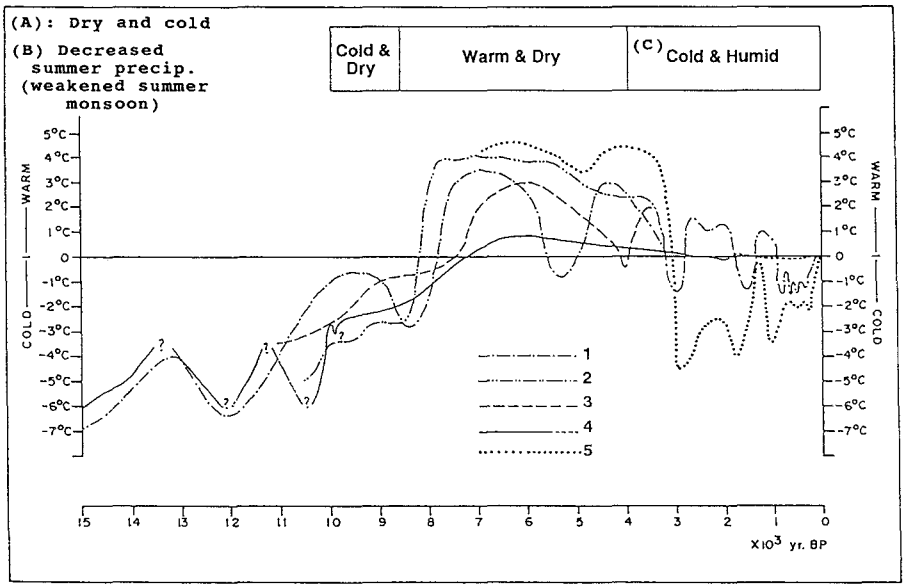

Figure 47 Fluctuation of mean annual temperature, humidity and precipitation in East Asia since the last 15000 years: 1–4: Li, 1988: 1: North China Plain, 2: southern part of Liaoning Province, 3: Shanghai and northern Zhenjiang Province, 4: Japan, and 5: Qinghai-Xizang Plateau (Wang and Fan, 1987). Humidity condition (A) is taken from the palynological data in Kashimir (Bhattacharyya, 1989), (B): from deep sea sediment data in the Arabian Sea (Niitsuma, 1990), and (C) from the palynological study in West Nepal (Yasuda and Tabata, 1987).

welling by a south-western summer monsoon was considerably reduced during the LGM (Figure 47, B: Niitsuma, 1990).

If the climate of the LGM (the *Gora Tabela Stage*) is characterized by lowering of air temperature of about 6 °C, and by a significant decrease in the summer precipitation, the combination of T_s, P_s and B_w for the *Gora Tabela Stage* is likely to be as follows: a reduced air temperature by about 6 °C from the present T_s (about −0.5 °C), considerably reduced summer precipitation P_s (200 mm; half of the present value), and as a result, increased winter balance B_w (400 mm; double of the present) (Table 14). The resulting increase in the winter balance is consistent with the theoretical consideration that the Ice Age glaciation was maintained by weakened summer monsoon circulations accompanying intensified western disturbances (Yasunari and Fujii, 1983).

The *Langtang Stage*, 3650 (3310) to 2850 yr. BP, is correlated to the Neoglaciation (Porter and Denton, 1967). Glaciers advanced significantly during this stage in southeastern Tibet (Academia Sinica, 1986; Wang and Fan, 1987; Iwata and Jiao, 1992) and on the southern slope of Kunlun Shan (Zheng, 1987). This can be explained by air temperature data from Tibet

Table 14 Reconstruction of paleoclimatic conditions, by introducing geological evidence to the model. Thick-hatched area indicates the condition during the *Gora Tabela Stage*, while thin-hatched does that during the *Langtang Stage*.

Ts(C), Ps, Bw(mm)	Ts at 5090 m	6			5			4			3			2		
Bw at 5350 m	Ps at 5090 m	200	400	800	200	400	800	200	400	800	200	400	800	200	400	800
Bw = 0	he (m)	5800	5750	5700	5650	5600	5550	5500	5450	5400	5400	5300	5250	5250	5150	5100
	ht (m)	5450	5400	5300	5300	5200	5100	5150	5000	4800	4950	4750	4550	4700	4550	4300
Bw=100	he	5700	5650	5650	5550	5550	5500	5450	5400	5350	5300	5250	5200	5150	5100	5050
	ht	5350	5300	5200	5200	5100	5000	5000	4900	4700	4750	4650	4450	4550	4400	4150
Bw=200	he	5650	5600	5600	5500	5450	5450	5350	5300	5300	5200	5200	5150	5100	5050	5000
	ht	5250	5200	5150	5100	5000	4900	4850	4750	4600	4600	4500	4350	4400	4250	4050
Bw=300	he	5550	5550	5550	5400	5400	5400	5300	5250	5250	5150	5100	5100	5000	5000	4950
	ht	5200	5150	5050	4950	4900	4800	4700	4650	4500	4500	4400	4250	4250	4150	3950
Bw=400	he	5500	5500	5500	5350	5350	5350	5200	5200	5200	5100	5050	5050	4950	4900	4900
	ht	5100	5050	4950	4850	4800	4700	4600	4550	4400	4350	4300	4150	4100	4000	3800
Bw=500	he	5450	5450	5450	5300	5300	5300	5150	5150	5150	5000	5000	5000	4850	4850	4850
	ht	5000	4950	4900	4750	4700	4600	4500	4450	4350	4250	4200	4050	4000	3900	3700
Bw=600	he	5400	5400	5400	5250	5250	5250	5100	5100	5100	4950	4950	4950	4800	4800	4800
	ht	4900	4850	4800	4650	4600	4550	4400	4350	4250	4150	4100	3950	3850	3750	3600
Ts(C), Ps, Bw(mm)	Ts at 5090 m	1			0			-1			-2			-3		
Bw at 5350 m	Ps at 5090 m	200	400	800	200	400	800	200	400	800	200	400	800	200	400	800
Bw = 0	he (m)	5150	5050	4950	5000	4900	4800	4900	4750	4650	4800	4650	4500	4700	4500	4350
	ht (m)	4550	4300	4000	4350	4100	3650	4150	3850	3250	3950	3550	2800	3750	3200	2100
Bw=100	he	5050	4950	4900	4900	4800	4750	4800	4700	4600	4650	4550	4450	4550	4400	4300
	ht	4350	4150	3850	4150	3900	3500	3900	3600	3050	3650	3250	2500	3350	2850	1750
Bw=200	he	4950	4900	4850	4800	4750	4700	4700	4600	4550	4550	4450	4400	4450	4350	4250
	ht	4150	4000	3700	3950	3700	3300	3650	3350	2850	3350	2950	2100	3000	2500	<1500
Bw=300	he	4850	4850	4800	4750	4700	4650	4600	4550	4500	4450	4400	4350	4350	4250	4200
	ht	4000	3850	3550	3750	3500	3100	3400	3150	2550	3050	2650	1800	2650	2050	<1500
Bw=400	he	4800	4800	4750	4650	4650	4600	4500	4500	4450	4400	4350	4300	4250	4200	4150
	ht	3850	3700	3400	3550	3300	2950	3150	2900	2250	2750	2300	<1500	2200	1650	<1500
Bw=500	he	4750	4700	4700	4600	4550	4550	4450	4450	4400	4300	4300	4250	4150	4150	4100
	ht	3700	3550	3250	3350	3150	2700	2950	2650	1950	2400	1950	<1500	1800	<1500	<1500
Bw=600	he	4650	4650	4650	4500	4500	4500	4400	4400	4350	4250	4250	4200	4100	4100	4050
	ht	3550	3400	3100	3150	2950	2500	2700	2300	1650	2050	1600	<1500	<1500	<1500	<1500

where fossil periglacial features indicate a rapid lowering of air temperature by 4.0 °C around 3000 yr. BP (Wang and Fan, 1987; Figure 47).

The precipitation condition at this stage is reported in the Nepal Himalaya by a palynological study (Yasuda and Tabata, 1987; Figure 47, C), which showed that the climate just after 4000 yr. BP was considered to be relatively cold and humid, probably experiencing a slight increase in winter precipitation.

If I adopt the data that the air temperature was 4 °C lower than the present, and that the B_w slightly increased (300 mm) during the Langtang Stage, the terminal altitude of 3900 m is reconstructed by keeping P_s to be 400 mm the same as the present (Table 14).

VII. Conclusions

This study aims to reconstruct the past glacial extent and the climatic conditions of the Langtang Valley, Nepal Himalaya. For this purpose, (1) I attempted the glacier inventory works in the Langtang Valley to clarify the present glacier distribution; (2) On the basis of the 5 years meteorological and glaciological observations, I clarified the present glacier -climate relationship in the valley: detailed analysis of snow profiles on the glacier revealed

that the contribution of winter snowfall by westerly disturbance is much more important for the present glacier mass balance than previously estimated; (3) the study on the permafrost environments also supports the importance of snow cover in winter in the valley; (4) By using these results, I proposed a steady-state glacier mass balance model and applied it to the glaciers in the valley at the Last Glacial and Holocene maximum, the extent of which was clarified geomorphologically through my field works; (5) Then finally, I estimated the summer air temperature, summer precipitation, and winter balance in the Langtang Valley, during the Last Glacial and Holocene glacial maximum. The contents of each chapter are summarized as follows;

Chapter I describes the significance of the reconstruction of the glacial fluctuations and past cryogenic environments of the Himalaya. Especially, the need for a quantitative reconstruction of the paleoclimate of the Himalaya by means of a steady-state glacier mass balance model is emphasized.

Chapter II explains the geomorphological and climatological setting of the Nepal Himalaya in which the Langtang Valley is located. The Himalaya are characterized by mountains with significant relief, and the most extensive glaciers in Asia. The Himalaya significantly influences global climate by its extremely high elevation.

The climate in the Himalaya is mainly divided into two systems: the monsoon circulation in summer and the westerly in winter. The former supplies most of the annual precipitation to the Nepal Himalaya, while the latter gives less precipitation toward the east.

The longitudinal change and distribution of glaciers is strongly influenced by the amount of precipitation: the glaciers develop larger in the western and eastern ends of the Himalaya where annual precipitation is more than that in the central part of the Himalaya (Nepal Himalaya). Because of this climatic system, the glaciers in the central part of the Himalaya (Nepal Himalaya) have been believed to be maintained mostly by monsoonal precipitation.

Chapter III presents the results of the glacier inventory work, and of the meteorological and glaciological studies on the several glaciers in the Langtang Valley. Glaciers of the Langtang Valley cover an area of 137.5 km^2. The glaciers are divided into two types: the *clean-type* and *debris-covered type*. The recent terminal fluctuation of the Yala Glacier (*clean-type*) suggests that the glacier is in a quasi-steady state, and the surface change of the Lirung Glacier (*debris-covered type*) indicates that the glacier is in a steady-state.

Mass input on the glaciers in the valley varies spatially: the upper reaches are much drier and warmer than in the middle during the monsoon season. This resulted in a significant northward rise of ELA, from 5120 m at the southern end to 5560 m at the northern end.

The most important result of the snow survey is the findings of the non-negligible contribution of non-monsoonal precipitation to the glacier mass balance in the Langtang Valley. Detailed observation of snow profiles on the Yala Glacier revealed that the monsoonal snow deposits on the glacier are distinguished from the non-monsoonal ones by the snow types characteristics and the existence of a thin dirt layer. The idea is subsequently

applied to the snow cores recovered on the Yala Glacier which indicates that the contribution of non-monsoonal precipitation to the annual mass balance amounted to approximately 30 % on average during the last nine years. This is the first quantitative data that show the importance of non-monsoonal precipitation to the accumulation of glaciers in the Nepal Himalaya.

Chapter IV deals with the present cryogenic condition of the Langtang Valley. Measurements of the ground temperature indicate that the forefields of the glaciers in the valley lack an alpine permafrost, regardless of sufficient coldness. This is because the large amount of winter snow, as stated in the previous chapter, covers the forefields enough to prevent the ground from deep-freezing in winter.

The distribution of periglacial landforms is also influenced by the glaciers. There exist three periglacial belts in the Langtang Valley. The highest *non-vegetated periglacial belt* is limited in altitude, and carries less developed sorted polygons. The belt becomes higher northward, reflecting the northward rise of ELA and herbaceous vegetation. The *upper vegetated periglacial belt* is characterized by various periglacial features such as vegetated polygons, vegetated solifluction lobes, turf-banked terraces, and talus slopes. The belt clearly rises northward. The *lower vegetated periglacial belt* carries less various periglacial landforms: the talus slopes and the earth hummocks are naturally formed features.

Rock breakdown by frost-shattering currently occurs in the altitudinal belt between 4100 and 4700 m. The measurements of rock surface temperature show that the number of freeze-thaw cycles is significantly large, compared to other parts of the world. The estimated altitudinal peak of the freeze-thaw cycles appears at altitudes of 5600 m on the south-facing slopes, and 6200 m on the north-facing ones.

Chapter V clarifies the fluctuation of glaciers in the Langtang Valley since the late Quaternary. There exists six glacial stages, the *Lama* of the oldest (the penultimate) or the early stage of the Last Glacial glaciation, the *Gora Tabela* of the LGM, the *Langtang* dated between 3650 (3310) and 2850 yr.BP, the *Lirung* dated between 2980 and 550 yr.BP, and the *Yala I* and *II* stages of the Little Ice Age in origin. The glacier extent decreases from the older to the younger. The most significant result is the discovery of the *Langtang Stage* which is the most extensive glaciation during the Holocene. This stage has previously been correlated to the LGM or Late Glacial advances by many researchers; however, this study questioned this correlation, and indicates further study is required for the Holocene glacial advance in the Nepal Himalaya.

Chapter VI is devoted to the reconstruction of the paleoclimate in the Langtang Valley, by introducing a steady-state glacier mass balance model which considers both the summer and winter balances of a glacier. The model needs the climatic parameters such as the summer mean air temperature (T_s), the summer total precipitation (P_s), the winter balance (B_w), and topographical parameters of the ground surface area (S). After evaluating the model by reconstructing the present glaciation using the observed meteorological data in the

valley, I simulated the changes of both the terminal altitudes and the ELAs of glaciers in the valley, by changing the climatic parameters: T_s, P_s and B_w. The simulated result indicates that the lowering of air temperature decreases the ELA more in a humid climate than in an arid one. The increase of B_w can lower the ELA and terminus considerably in case that summer precipitation is small.

Finally, the amount of summer precipitation and the winter balance of both the *Gora Tabela* and *Langtang stages* is reconstructed by referring to the previously obtained paleoclimatic data for both stages. During the LGM, an air temperature decrease of approximately 6 °C is reported in east Asia. In addition, a deep sea sediment record in the Arabian Sea indicates that the summer monsoon was considerably weakened during the LGM. Using these data, the model predicts the reduced summer total precipitation (200 mm) as half as that of present, and increased winter balance (400 mm) as double of the present under the assumption that the LGM air temperature decrease was 6 °C. As for the *Langtang Stage*, an air temperature decrease of about 4 °C at approximately 3000 yr. BP has been reported in the Qinghai-Xizang Plateau, just north of the Langtang Valley. In addition, a palynological study in west Nepal has revealed a slight increase in winter precipitation in this period. When an air temperature decrease of 4 °C and a slight increase in the winter balance (300 mm) is adopted for the *Langtang Stage*, the model predicts the same amount of summer precipitation (400 mm) as that of today.

The simulated results suggest that the glacier extent of the *Gora Tabela Stage* is mainly supported by non-monsoonal precipitation, the amount of which has a crucial influence on the glacier development when the amount of summer precipitation is small. This can explain the dilemma how the Himalayan glaciers developed during the LGM when the summer monsoon, that mainly supports the current Himalayan glaciers, was weakened.

Acknowledgments

First of all, I would like to express my most sincere gratitude to Professor Yugo Ono, Graduate School of Environmental Science, Hokkaido University, who has been my supervisor since the beginning of my study in the Langtang Valley in 1987. He provided me with numerous invaluable data and ideas on the glacial and periglacial features in the valley. He supported my field work in the Himalaya both financially and mentally, and revised my thesis at every stages of preparation.

I would like to thank Prof. Eizi Akitaya, Assoc. Prof. Renji Naruse, and Mr. Takuya Fukuzawa, the Institute of Low Temperature Science, Hokkaido University. They instructed me on the study of snow and its metamorphism by which Chapter III of this thesis greatly advanced. Dr. Renji Naruse kindly revised part of Chapter VI in an icebreaker "Shirase" heading toward the Antarctica.

Gratitude also goes to Dr. Tomomi Yamada, the Institute of Low Temperature Science,

Hokkaido University, for giving me a chance to participate in GEN 1987 which enabled me to continue my work in the Langtang Valley. He gave me other chances to take part in GEN 1989, 1991 and 1992, all of which were successfully finished owing to his constant guidance and encouragements.

I am also indebted to Profs. Masami Fukuda and Katsuhiro Kikuchi, Hokkaido University, for their help in editing the manuscript and in preparing my presentation of this thesis.

Sincere thanks are extended to Prof. Yutaka Ageta, Nagoya University, for his continuous support in conducting my research in the Himalaya, and his critical advice on many parts of my work.

Discussions with Drs. Teiji Watanabe, Hokkaido University, and Ken'ichi Ueno, the University of Tsukuba, both in the Langtang Valley and in the laboratory, provided me with many basic ideas concerning both the periglacial and meteorological phenomena in the valley. Dr. T. Watanabe, in particular, helped me in editing the final version of this thesis.

I thank Drs. Hisashi Ozawa, ETH of Switzerland, Norikazu Matsuoka, the University of Tsukuba, Shiro Kohshima, Tokyo Institute of Technology, and Messrs. Hajime Iida, Yoshida Science Museum, Tsutomu Kadota and Katsumoto Seko, Nagoya University, for invaluable data on the glacial and periglacial phenomena in the Himalaya.

Thanks are also due to Ms. Tomoko Nakayama, Messrs. Tsukasa Kawahara and Shoji Hashimoto, Hokkaido University, for their generous assistance during the field work.

I also thank Miss Nobuki Watanabe, Messrs. Shuji Yamada and Koh'ichiro Harada, Hokkaido University for helping me in preparing several figures in this thesis.

The field work was greatly facilitated by the staff members of the Department of Hydrology and Meteorology, His Majesty's Government of Nepal. My special thanks are due to Dr. Sharad P. Adhikary, the director of the department, Messrs. Adarsha P. Pokhrel, Kiran Shankar, Om R. Bajracharya, and Birbal Rana, for their constant help and hospitality in Nepal.

My sincere appreciation should also be expressed to my Nepalese friends; Mr. J. P. Lama Sherpa and his staff members, and villagers in the Langtang Valley, who assisted me greatly during my total seventeen months stay in the valley.

Several instruments used in this study were provided by Mr. Minoru Yoshida, Hakusan Kohgyo Co., Tokyo, and Mr. Takashi Sato, KONA System Co., Sapporo, whom I deeply acknowledge.

References

Academia Sinica. 1986 *Glaciers of Xizang (Tibet).* The Series of the Scientific Expedition to the Qinghai-Xizang Plateau. Science Press, Beijing, 328pp. (in Chinese).

Ageta, Y. 1983a Characteristics of mass balance of the summer-accumulation type glacier in the Nepal Himalaya (I) —Mass balance of Glacier AX010 in east Nepal. *Seppyo,* **45**, 2, 81—90 (in Japanese with English abstract).

Ageta, Y. 1983b Characteristics of mass balance of the summer-accumulation type glacier in the Nepal Himalaya (II) —Mass balance models of small glaciers in Nepal. *Seppyo,* **45**, 2, 91-105 (in Japanese with English abstract).

Ageta, Y. *person. commu.* Personal communication on base points for the survey of the Yala Glacier. Nagoya University, Japan.

Ageta, Y., Iida, H. and Watanabe, O. 1984 Glaciological studies on Yala Glacier in Langtang Himal. In Higuchi, K.(ed.) "*Glacial Studies in Langtang Valley, report of the glacier boring project 1981—1982 in the Nepal Himalaya*", Data Center for Glacier Research, Japanese Society of Snow and Ice, 41—47.

Akitaya, E. 1974 Studies on depth hoar. *Contributions from the Institute of Low Temperature Science,* Ser. **A**, **26**, 1—67.

Ballantyne, C.K. and Matthews, J.A. 1982 The development of sorted circles on recently deglaciated terrain, Jotunheimen, Norway. *Arctic and Alpine Research,* **14**, 341—354.

Bhattacharyya, A. 1989 Vegetation and climate during the last 30,000 years in India. *Palaeogeography, Palaeoclimatology, Palaeoecology*, **73**, 25—38.

Birkeland, P.W. 1973 Use of relative age-dating methods in a stratigraphic study of rock glacier deposits, Mt. Sopris, Colorado. *Arctic and Alpine Research,* **5**, 401—416.

Birkeland, P.W. 1984a *Soils and Geomorphology*. New York: Oxford University Press. 372pp.

Birkeland, P.W. 1984b Holocene soil chronofunctions, Southern Alps, New Zealand. *Geoderma,* **34**, 115—134.

Brown, R.J.E. and Péwé, T.L. 1973 Distribution of permafrost in North America and its relationship to the environment: a review, 1963—1973. *Proceedings of the Second International Conference on Permafrost*, Yakutsk, USSR, North American Contribution, Washington D.C.: Nat. Acad. Sci., 71—100.

Burbank, D.W. and Fort, M. 1985 Bedrock control on glacial limits: examples from the Ladakh and Zanskar Ranges, north-western Himalaya, India. *Journal of Glaciology*, **31**, 143—149.

Colman, S.M. and Pierce, K.L. 1981 Weathering rinds on andesitic and basaltic stones as a Quaternary age indicator, western United States. *U.S. Geological Survey Professional Paper*, **1210**, 1—56.

Day, M.J. and Goudie, A.S. 1977 Field assessment of rock hardness using the Schmidt test hammer. *British Geomorphological Group, Technical Bulletin*, **18**, 19—29.

Department of Irrigation, Hydrology and Meteorology of Nepal. 1984 "Climatological Records of Nepal 1981—1982". Kathmandu, Nepal.

Department of Irrigation, Hydrology and Meteorology of Nepal. 1986 "Climatological Records of Nepal 1983—1984". Kathmandu, Nepal.

Department of Irrigation, Hydrology and Meteorology of Nepal. 1988 "Climatological Records of Nepal 1985—1986". Kathmandu, Nepal.

Dhar, O.N. and Mandal, B.N. 1986 A pocket of heavy rainfall in the Nepal Himalayas —a brief appraisal, In S.C. Joshi (ed.) *Nepal Himalaya: Geo-Ecological Perspectives*, Nainital, UP, India, Himalayan Research Group, 75—81.

Dronia, A. 1978 Gesteinstemperaturmessungen im Himalaya mit einem Infrarot-Thermometer. *Zeitschrift für Geomorphologie* N.F., **22**, 101−114.

Flohn, H. 1968 Contribution to a meteorology of the Tibetan highlands. *Atmospheric science paper*, **130**, Colorado State University, 121pp.

Fort, M. 1976 Quaternary deposits of the middle Kali Gandaki Valley. *Himalayan Geology*, **6**, 499−507.

Fort, M. 1979 *Études sur le Quaternaire de l'Himalaya: la haute vallée de la Buri Gandaki, Népal*. Editions du CNRS, Paris, 232pp.

Fort, M. 1980 Les formations quaternaires lacustves de la Basse Thakkhola (Himalaya du Népal): intérêt paléogéographique, néotectonique, et chronologique. *C.R. Acad. Sco. Pris*, t. **290** (21 janvier 1980), Sêrie D, 171−174.

Fort, M. 1986 Glacial extension and catastrophic dynamics along the Annapurna Front, Nepal Himalaya. In M. Kuhle (ed.) *Internationales Symposium über Tibet und Hochasien* vom 8−11 Oktober 1985 im Geographischen Institut der Universität Göttingen, 105−125.

Franceschetti, B. 1968 Observazioni sulla morfologia glaciae della media valle del Langtang (Nepal Centrale). *Memorie della Societã Geologica Italiana*, VII (Fascìcolo 3), 345−360.

Francou, B. 1989 Temperatures de parois rocheuses mesurees en hiver dans l'Himalaya du Khumbu vers 6000 m. *Inter-Nord*, **19**.

Fujii, Y. 1976 Periglacial phenomena in Hidden Valley, Mukut Himal. *Seppyo*, **38**, Special issue, 120−124.

Fujii, Y. 1977 "*Glacier*". In J. Kawakita (ed.) "*Himalaya*", Asahi Shinbun Co., Tokyo, 136−144 (in Japanese).

Fujii, Y. 1980 Studies on the permafrost in Khumbu Himal and Mukut Himal, in Nepal Himalayas. *Seppyo*, **42**, 2, 81−92 (in Japanese with English abstract).

Fujii, Y. and Higuchi, K. 1976 Ground temperature and its relation to permafrost occurrences in the Khumbu Region and Hidden Valley. *Seppyo*, **38**, Special issue, 125−128.

Fukuzawa, T. and Akitaya, E. 1991 Observations of quick formation of a depth hoar layer. *Low Temperature Science*, Ser. **A, 50**, 1−7 (in Japanese with English summary).

Fusejima, Y. and Yagi, K. 1992 An active fault cutting glacial landforms in the Gurja Himal, western Nepal. —Chronological study of the glacial landforms. *Annual meeting of the Association of Japanese Geographers*, 40−41 (in Japanese).

Fushimi, H. 1977a Structural studies of glaciers in the Khumbu region. *Seppyo*, **39**, Special Issue, 30−39.

Fushimi, H. 1977b Glaciations in the Khumbu Himal (1). *Seppyo*, **39**, Special Issue, 60−67.

Fushimi, H. 1978 Glaciations in the Khumbu Himal (2). *Seppyo*, **40**, Special Issue, 71−77.

Fushimi, H. 1980 Glaciers in the Interior Asia: on their regionality and history (Nairiku Ajiano hyogagun: hyogagensho no chiikisei to rekisisei ni tuite). *The Earth Monthly (Gekkan Chikyu)*, **3**, 201−210 (in Japanese).

Fushimi, H. and Ohata, T. 1980 Fluctuation of glaciers from 1970 to 1978 in the Khumbu Himal, East Nepal. *Seppyo*, **41**, Special Issue, 71−81.

Fushimi, H., Yoshida, M., Watanabe, O. and Upadhyay, B.P. 1980 Distributions and grain sizes of supraglacial debris in the Khumbu Glacier, Khumbu region, east Nepal. *Seppyo*, **41**, Special Issue, 18−25.

Gulati, T.D. 1972 Role of snow and ice hydrology in India. *The Role of Snow and Ice in Hydrology*. IAHS Publication, UNESCO-WMO-IAHS, **117**, 610−623.

Haeberli, W. 1983 Permafrost-glacier relationships in the Swiss Alps —today and in the past. *Proceedings of the Forth International Conference on Permafrost*, National Academy Press, Washington, 1396−1401.

Hahn, D.G. and Shukla, J. 1976 An apparent relationship between Eurasian snow cover and

Indian monsoon rainfall. *Journal of Atmospheric Science*, **33**, 2461−2462.
Harris, S.A. 1981 Distribution of active glaciers and rock glaciers compared to the distribution of permafrost landforms, based on the freezing and thawing indices. *Canadian Journal of Earth Sciences*, **18**, 376−381.
Heuberger, H. 1956 Beobachtungen über die heutige und eiszeitliche Vergletscherung in Ost-Nepal. *Zeitschirft für Gletscherkunde und Glazialgeologie*, **3**, 349−363.
Heuberger, H., Masch, L., Preuss, E., and Schrocker, A. 1984 Quaternary landslides and rock fusion in central Nepal and in the Tyrolean Alps. *Mountain Research and Development*, **4**, 345−362.
Heuberger, H. and Weingartner, H. 1985 Die ausdehnung der leztzeitlichen vergletscherung an der Mount-Everest-Südflanke. *Mitteilgn. Österr. Geograph. Gesellsch.*, **127**, 71−80.
Hewitt, K. 1968 The freeze-thaw environment of Karakoram (Himalaya). *Canadian Geographer*, **12**, 85−98.
Higashi, A. 1954 Soil freezing in Hokkaido. *Report of the Institute of Agricultural Physics*, **34**, 145−157 (in Japanese).
Higuchi, K. 1984 Outline of the Glaciological Expedition of Nepal: Boring Project 1981 and 1982. In Higuchi, K. (ed.) "*Glacial Studies in Langtang Valley, report of the glacier boring project 1981−1982 in the Nepal Himalaya.*", Data Center for Glacier Research, Japanese Society of Snow and Ice, 99−105.
Higuchi, K., Fushimi, H., Ohata, T., Iwata, S., Yokoyama, K., Higuchi, H., Nagoshi, A. and Iozawa, T. 1978 Preliminary report on glacier inventory in the Dudh Kosi Region. *Seppyo*, **40**, Special Issue, 78−83.
Higuchi, K., Fushimi, H., Ohata, T., Takenaka, S., Iwata, S., Yokoyama, K., Higuchi, H., Nagoshi, A. and Iozawa, T. 1980 Glacier inventory in the Dudh Kosi region, East Nepal. Proceedings of Riederalp Workshop, IAHS-AISH Publication, 126, 95−100.
Höllerman, P.W. 1967 Zur Verbreitung rezenter periglazialer Kleinformen in den Pyrenaen und Ostalpen. *Göttinger. Geogr. Abh.*, **40**, 198pp.
Holmes, J.A. and Street-Perrott, F.A. 1989 The Quaternary glacial history of Kashmir, north-west Himalaya: a revision of de Terra and Paterson's sequence. *Zeitschrift für Geomorphologie,* N.F., Suppl. Bd. **76**, 195−212.
Hurst, V.J. 1977 Visual estimation of iron in saprolite. *Geological Society of America, Bulletin*, 88, 174−176.
Iida, H., Watanabe, O. and Takikawa, M. 1984a First results from Himalayan Glacier Boring Project in 1981−1982: Part II. Studies on internal structure and transformation process from snow to ice of Yala Glacier, Langtang Himal, Nepal. In Higuchi, K.(ed.) "*Glacial Studies in Langtang Valley, report of the glacier boring project 1981−1982 in the Nepal Himalaya*", Data Center for Glacier Research, Japanese Society of Snow and Ice, 25−33.
Iida, H., Watanabe, O., Mulmi, D.D. and Thapa, K.B. 1984b Glacier distribution in the Langtang River Region, Nepal. In Higuchi, K.(ed.) "*Glacial Studies in Langtang Valley, report of the glacier boring project 1981−1982 in the Nepal Himalaya*", Data Center for Glacier Research, Japanese Society of Snow and Ice, 117−120.
Iida, H., Endo, Y., Kohshima, S., Motoyama, H. and Watanabe, O. 1987 Characteristics of snowcover and formation process of dirt layer in the accumulation area of Yala Glacier, Langtang Himal, Nepal. *Bulletin of Glacier Research*, **5**, 55−62.
Inoue, J. and Yoshida, M. 1980 Ablation and heat exchange over the Khumbu Glacier. *Seppyo*, **41**, Special Issue, 26−33.
Ives, J.D. and Messerli, B. 1989 *The Himalayan Dilemma: Reconciling development and conservation.* The United Nations University, Routledge, London and New York, 295pp.
Iwata, S. 1976a Late Pleistocene and Holocene moraines in the Sagarmatha (Everest) region,

Khumbu Himal. *Seppyo*, **38**, Special Issue, 105−114.
Iwata, S. 1976b Some periglacial morphology in the Sagarmatha (Everest) Region, Khumbu Himal. *Seppyo*, **38**, Special Issue, 115−119.
Iwata, S. 1978 Soil creep measurements in Khumbu. *Seppyo*, **40**, Special Issue, 60−63.
Iwata, S. 1984 Geomorphology of the Thakkola-Muktinath region, Central Nepal, and its late Quaternary history. *Geographical Reports of the Tokyo Metropolitan University*, **19**, 25−42.
Iwata, S. 1987 Mode and rate of uplift of the central Nepal Himalaya. *Zeitschrift für Geomorphologie*, N.F., Suppl. Bd. **63**, 37−49.
Iwata, S., Fujii, Y., and Higuchi, K. 1976 Patterned ground of the Nepal Himalayas. *Journal of Geography (Chigaku Zasshi)*, **85**, 3, 21−39 (in Japanese with English abstract).
Iwata, S., Yamanaka, H., and Yoshida, M. 1982 Glacial landforms and river terraces in the Thakkhola region, Central Nepal. *Journal of Nepal Geological Society*, **2**, Special Issue, 81−94.
Iwata, S. and Jiao, K. 1992 Late Holocene fluctuations of the Zepu Glacier, the eastern Nyainqentanglha Mountains, Qinzang (Tibet) Plateau. *Journal of Glaciology and Cryopedology.*
Kalvoda, J. 1978 Genesis of the Mount Everest (Sagarmatha). *Rozpr. Cs. Akad. Ved*, **88**, 1−62.
Kalvoda, J. 1979 The Quaternary history of the Barun glacier, Nepal Himalayas. *Vestnik Ustredniho ustavu geologickeho*, **54**, 1, 11−23.
Koaze, T. 1981 Geomorphology of glacial valleys of Khumbu Region, eastern Nepal —a preliminary study. Meiji University *'Jinbun-Kagaku Kenkyujyo Kiyo'*, 1−18.
Kohshima, S. 1984 Living micro-plants in the dirt layer dust of Yala Glacier, Nepal Himalaya. In K. Higuchi (ed.), *"Glacial Studies in Langtang Valley, report of the glacier boring project 1981−1982 in the Nepal Himalaya"*, Data Center for Glacier Research, Japanese Society of Snow and Ice, 91−98.
Kohshima, S. 1987 Formation of dirt layers and surface dust by micro-plant growth in Yala (Dakpatsen) Glacier, Nepal Himalayas. *Bulletin of Glacier Research*, **5**, 63−68.
Kuhle, M. 1982 Der Dhaulagiri- und Annapurna-Himalaya. Ein Beitrag zur Geomorphologie extremer Hochgebirge. *Zeitschrift für Geomorphologie*, Suppl. Bd. **41**, 1−229.
Kuhle, M. 1986a The upper limit of glaciation in the Himalayas. *GeoJournal*, **13**, 331−346.
Kuhle, M. 1986b Former glacial stades in the Mountain areas surrounding Tibet —in the Himalayas. In S.C. Joshi (ed.) *Nepal Himalaya: Geo-Ecological Perspectives*, Nainital, UP, India, Himalayan Research Group, 437−473.
Kuhle, M. 1987 Subtropical mountain-and highland glaciation as Ice Age triggers and the waning of the glacial periods in the Pleistocene. *GeoJournal*, **14**, 4, 393−421.
Kuhle, M. 1988a Topography as a fundamental element of glacial systems —a new approach to ELA calculation and typological classification of paleo- and recent glaciations. *GeoJournal*, **17**, 4, 545−568.
Kuhle, M. 1988b On the geoecology of Southern Tibet: measurements of climatic parameters including surface-and soil-temperatures in debris, rock, snow, firn, and ice during the South Tibet-and Mt. Everest Expedition 1984. *GeoJournal*, **17**, 597−613.
Kuhle, M. 1990 New data on the Pleistocene glacial cover of the southern border of Tibet: the glaciation of the Kangchenzönga Massif (8585m E Himalaya). *GeoJournal*, **20**, 4, 415−421.
Li, T. 1988 A preliminary study on the climatic and environmental changes at the turn from Pleistocene to Holocene in east Asia. *GeoJournal*, **17**, 4, 649−657.
Manabe, S. and Terpstra, T.B. 1974 The effect of mountains on the general circulation of the atmosphere as identified by numerical experiments. *Journal of the Atmospheric Science*, **31**, 3−42.
Matsuoka, N. 1984 Frost shattering of bedrocks in the periglacial regions of the Nepal Himalaya. *Seppyo*, **46**, 19−25 (in Japanese with English abstract).

Matsuoka, N. 1990a The rate of bedrock weathering by frost action: field measurements and a predictive model. *Earth Surface Processes and Landforms*, **15**, 73–90.

Matsuoka, N. 1990b Mechanisms of rock breakdown by frost action: an experimental approach. *Cold Regions Science and Technology*, **17**, 253–270.

Matthews, J.A. and Shakesby R.A., 1984 The status of the Little Ice Age in the southern Norway: relative-age dating of Neoglacial moraines with Schmidt hammer and lichenometry. *Boreas*, **13**, 334–346.

McGreevy, J.P. and Whalley, W.B. 1982 The geomorphic significance of rock temperature variations in cold environments: a discussion. *Arctic and Alpine Research*, **14**, 157–162.

Meier, M.F. 1965 Glaciers and climate. In H.E. Wright and D.G. Frey (eds.) *The Quaternary of the United States*. Princeton University Press, Princeton, New Jersey, U.S.A.

Meierding, T. C. 1982 Late Pleistocene glacial equilibrium-line altitudes in the Colorado Front Range: a comparison of methods. *Quaternary Research*, **18**, 289–310.

Minz, Y. 1968 Very long-term global integration of the primitive equations of atmospheric motion: An experiment in climate simulation. *Meteor. Monog.*, 8, 30, 20–36.

Moribayashi, S. and Higuchi, K. 1977 Characteristics of glaciers in the Khumbu Region and their recent variations. *Seppyo*, **39**, Special Issue, 3–6.

Motoyama, H. and Yamada, T. 1989 Hydrological observations in Langtang Valley, Nepal Himalayas during 1987 monsoon-postmonsoon season. *Bulletin of Glacier Research*, **7**, 195–201.

Motoyama, H., Ohta, T., Endo, Y. and Iida, H. 1990 Air temperature and snow depth on Yala glacier of Langtang Valley, Nepal Himalayas. *Bulletin of Glacier Research*, 8, 55–60.

Müller, F. 1958/59 Eight months of glacier and soil research in the Everest region. In *The Mountain World* (Swiss Foundation for Alpine Research), 191–208, George Allen and Unwin Ltd. London.

Müller, F. 1970 A pilot study for an inventory of the glaciers in the Eastern Himalayas —Inventory of glaciers in the Mount Everest region—. "*Perennial ice and snow masses*", UNESCO-IASH, 47–59.

Müller, F. 1980 Present and late Pleistocene equilibrium line altitudes in the Mt. Everest region —an application of the glacier inventory. *Proceedings of the Riederalp Workshop*, IAHS-AISH Publication **126**, 75–94.

Müller, F., Caflisch, T. and Müller, G. 1977 Instructions for compilation and assemblage of data for a World Glacier Inventory. TTS/WGI, Dept. of Geography, ETH Zurich, 19pp.

Nagaoka, S. 1990 The glacial landforms in the Manang Valley, north of the Great Himalayas, central Nepal. *Geographical Reports of Tokyo Metropolitan University*, **25**, 109–123.

Nagaoka, S., Maemoku, H. and Tanaka Y. 1990 Late Quaternary moraines of the Ngojumba Glacier, Khumbu Himal, eastern Nepal. *Journal of Geography* (*Chigaku Zasshi*), **99**, 3, 62–70 (in Japanese with English abstract).

Nakata, T., Iwata, S., Yamanaka, H., Yagi, H. and Maemoku, H. 1984 Tectonic landforms of several active faults in the western Nepal Himalayas. *Journal of Nepal Geological Society*, **4**, Special Issue, 177–199.

Niitsuma, N. 1990 Desertification of "Green Sahara" and Monsoon. *The Earth Monthly (Gekkan Chikyu)*, **22**, 5, 255–262 (in Japanese).

Ohta, T., Motoyama, H. and Iida, H. 1990 Snow surveys on the north facing slope of Langtang Valley, Nepal Himalayas. *Bulletin of Glacier Research*, 8, 29–30.

Ono, Y. 1984 Annual moraine ridges and recent fluctuation of Yala (Dakpatsen) Glacier, Langtang Himal. In Higuchi, K.(ed.) "*Glacial Studies in Langtang Valley, report of the glacier boring project 1981–1982 in the Nepal Himalaya*", Data Center for Glacier Research, Japanese

Society of Snow and Ice, 73−83.

Ono, Y. 1985 Recent fluctuation of the Yala (Dakpatsen) Glacier, Langtang Himal, reconstructed from annual moraine ridges. *Zeitschrift für Gletscherkunde und Glazialgeologie*, **21**, 251−258.

Ono, Y. 1986 Glacial fluctuations in the Langtang Valley, Nepal Himalaya. *Göttinger Geographische Abhandlungen*, **81**, 31−38.

Ono, Y. 1991 Glacial and periglacial palaeoenvironments in the Japanese Islands. *The Quaternary Research*, **30**, 2, 203−211.

Ono, Y. and Sadakane, A. 1986 Natural background of the Yak transhumance in the Langtang Valley, Nepal Himalaya. *Geographical Reports of Tokyo Metropolitan University*, **21**, 95−109.

Osmaston, H. 1989 Problems of the Quaternary geomorphology of the Xixabangma region in South Tibet and Nepal. *Zeitschrift für Geomorphologie*, Suppl. Bd. **76**, 147−180.

Ozawa, H. 1991 Thermal regime of a glacier in relation to glacier ice formation. *Doctoral thesis of Hokkaido University*, 51pp.

Paterson, W.S.B. 1981 *The Physics of Glaciers*. 2nd edition, Pergamon Press, 380pp.

Porter, S. C. 1975 Quaternary glacial record in Swat Kohistan, West Pakistan. *Geological Society of America Bulletin*, **81**, 1421−1446.

Porter, S. C. 1975 Weathering rinds as a relative-age-criterion: Approach to subdivision of glacial deposits in the Cascade Range. *Geology*, **3**, 101−104.

Porter, S. C. 1977 Present and past glaciation threshold in the Cascade Range, Washington, U.S.A.: topographic and climatic controls, and paleoclimatic implications. *Journal of Glaciology*, **18**, 101−116.

Porter, S.C. and Denton, G.H. 1967 Chronology of neoglaciation in the North American Cordillera. *American Journal of Science*, **265**, 177−210.

Röthlisberger, F. 1986 *10000 Jahre Gletschergeschichte der Erde*. Arau, Verlag Sauerlander, 416pp.

Sanger, F.J. 1966 Degree-days and heat conduction in soils. In *Permafrost International Conference* (Lafayette, Ind., 11−15 Nov.,1963) *Proceedings*, Nat. Acad. Sci., 253−262.

Seko, K. 1987 Seasonal variation of altitudinal dependence of precipitation in Langtang Valley, Nepal Himalayas. *Bulletin of Glacier Research*, **5**, 41−47.

Seko, K. and Takahashi, S. 1991 Characteristics of winter precipitation and its effect on glaciers in the Nepal Himalaya. *Bulletin of Glacier Research*, **9**, 9−16.

Shi, Y. 1980 Some achievement on mountain glacier researches in China. *Seppyo*, **42**, 4, 215−228.

Shi, Y., Zheng, B. and Li, S. 1992 Last glaciation and maximum glaciation in the Qinghai-Xizang (Tibet) Plateau: a controversy to M. Kuhle's ice sheet hypothesis. *Zeitschrift für Geomorphologie* N.F., Suppl. Bd. **84**, 19−35.

Shiraiwa, T. 1992 Freeze-thaw activities and rock breakdown in the Langtang Valley, Nepal Himalaya. *Environmental Science, Hokkaido University*, **15**, 1, 1−12.

Shiraiwa, T. and Watanabe, T. 1991 Late Quaternary glacial fluctuations in the Langtang Valley,

Nepal Himalaya, reconstructed by relative dating methods. *Arctic and Alpine Research*, **23**, 4, 404–416.

Shiraiwa, T. and Yamada, T. 1991 Glacier Inventory of the Langtang Valley, Nepal Himalayas. *Low Temperature Science*, Ser. **A, 50**, Data Report, 47–72.

Shiraiwa, T., Ueno, K. and Yamada, T. 1992 Distribution of mass input on glaciers in the Langtang Valley, Nepal Himalayas. *Bulletin of Glacier Research*, 10, 21–30.

Sone, T. 1990 The permafrost environment of the Daisetsu mountains, central Hokkaido, northern Japan. *Environmental Science, Hokkaido University*, **13**, 2, 1–28.

Subramanian, V.P. and Upadhyay, B.P. 1982 A study of rainfall patterns in Nepal. *Proceedings of the seminar on "Hydrological investigations during the last 25 years in India"*, 43–50.

Takahara, H., Higuchi, K. and Mulmi, D.D. 1984 Heat balance study on Yala Glacier in Langtang Himal, Nepal. In K. Higuchi (ed.) "*Glacial Studies in Langtang Valley, report of the glacier boring project 1981–1982 in the Nepal Himalaya*", Data Center for Glacier Research, Japanese Society of Snow and Ice, 49–60.

Takahashi, S., Motoyama, H., Kawashima, K., Morinaga, Y., Seko, K., Iida, H., Kubota, H. and Turadahr, N.R. 1987a Meteorological features in Langtang Valley, Nepal Himalayas, 1985–1986. *Bulletin of Glacier Research*, **5**, 35–40.

Takahashi, S., Motoyama, H., Kawashima, K., Morinaga, Y., Seko, K., Iida, H., Kubota, H., and Turadahr, N.R. 1987b Summary of meteorological data at Kyangchen in Langtang Valley, Nepal Himalayas, 1985–1986. *Bulletin of Glacier Research*, **5**, 121–128.

Ueno, K. and Yamada, T. 1990 Diurnal variation of precipitation in Langtang Valley, Nepal Himalayas. *Bulletin of Glacier Research*, **8**, 93–101.

Ueno, K., Shiraiwa, T. and Yamada, T. in press Precipitation environment in the Langtang Valley, Nepal Himalayas. *Proceedings of the International Symposium on Snow and Glacier Hydrology*, Kathmandu, Nepal.

Usselmann, P. 1980 Cartographie gêomorphologique et evolution quaternaire d'une haute valle Himalayenne: Le Langtang. *Revue de gêomorphologie dynamique*, **29**, 1–7.

Vivian, R. 1971 Aux confins du Nêpal et du Tibet: le Langtang. *Revue de Gêogr. Alp.*, **59**, 4, 573–580.

Wang Fu-Bao and Fan C.Y. 1987 Climatic change in the Qinghai-Xizang (Tibetan) region of China during the Holocene. *Quaternary Research*, **28**, 50–60.

Watanabe, O., Endo, Y. and Ishida, T. 1967 Glaciers and glaciations in the Nepal Himalaya. I. Mainly on the results of field researches of two glaciers in the Nepal Himalaya. *Low Temperature Science*, Ser. **A. 25**, 197–213 (in Japanese with English summary).

Watanabe, O., Takenaka S., Iida, H., Kamiyama, K., Thapa, K.B. and Mulmi, D.D. 1984 First results from Himalayan Glacier Boring Project in 1981–1982: Part I. Stratigraphic analyses of full-depth cores from Yala Glacier, Langtang Himal, Nepal. In Higuchi, K.(ed.) "*Glacial Studies in Langtang Valley, report of the glacier boring project 1981–1982 in the Nepal Himalaya*", Data Center for Glacier Research, Japanese Society of Snow and Ice, 7–23.

Watanabe, O. and Higuchi, K. 1987 Glaciological studies in Asiatic Highland region during 1985–1986. *Bulletin of Glacier Research*, **5**, 1–10.

Watanabe, T. 1992 Human impact and landscape changes in the Nepal High Himalaya. *Doctoral dissertation, University of California, Davis*, 499pp.

Watanabe, T., Shiraiwa, T. and Ono, Y. 1989 Distribution of periglacial landforms in the Langtang Valley, Nepal Himalaya. *Bulletin of Glacier Research*, **7**, 209–220.

Whalley, W.B., McGreevy, J.P. and Ferguson, R.I. 1984 Rock temperature observations and chemical weathering in the Hunza region, Karakoram: preliminary data. In Miller, K.J. (ed.), *International Karakoram Project.* Vol. **2**, Cambridge, Cambridge University Press, 616–633.

Williams, V.S. 1983 Present and former equilibrium-line altitudes near Mount Everest, Nepal and Tibet. *Arctic and Alpine Research*, **15**, 2, 201–211.

Wissmann, H. 1959 Die heutige vergletscherung und shneegrenze in Hochasian mit hinweisen auf die vergletscherung der letzten eiszeit. *Abhandlungen der mathematisch-naturwissenschftlichen klasse, Akademie der Wissenschaften und der Literatur in Mainz in Kommission bei Franz Steiner verlag GMBH*, Wiesbaden, 1101–1407.

World Glacier Monitoring Service 1989 World Glacier Inventory —Status 1988—. IAHS/ICSI, GEMS/UNEP and UNESCO, Switzerland.

Yagi, H. and Minaki, M. 1991 Glacial landforms and their chronology in the vicinity of the Shiptong Pass, south of the Barun Khola, eastern Nepal. *The Science Reports of the Tohoku University, 7th Series (Geography)*, **41**, 2, 59–71.

Yamada, S. 1990 ELA and distribution of the most extensive glaciation in the Hiunchuli region, western Nepal. *Unpublished Diploma thesis, Mie University, Japan* (in Japanese).

Yamada, T. 1982 Studies on accumulation-ablation processes and distribution of snow in mountain regions, Hokkaido. *Contributions from the Institute of Low Temperature Science*, Hokkaido University, Ser. **A. 31**, 1–33.

Yamada, T. 1989 An outline of Glaciological Expedition of Nepal: Langtang Himal Project 1987–88. *Bulletin of Glacier Research*, **7**, 191–193.

Yamada, T. 1991 Outline of glaciological studies in the Nepal Himalayas, 1989. *Bulletin of Glacier Research*, **9**, 51–54.

Yamada, T., Motoyama, H. and Thapa, K.B. 1984 Role of glacier meltwater in discharge from the glaciated watersheds of Langtang Valley, Nepal Himalaya. In K. Higuchi (ed.), "*Glacial Studies in Langtang Valley, report of the glacier boring project 1981–1982 in the Nepal Himalaya*", Data Center for Glacier Research, Japanese Society of Snow and Ice, 61–71.

Yamada, T., Shiraiwa, T., Iida, H., Kadota, T., Watanabe, T., Rana, B., Ageta, Y. and Fushimi, H. 1992 Fluctuations of the glaciers from the 1970s to 1989 in the Khumbu, Shorong and Langtang regions, Nepal Himalayas. *Bulletin of Glacier Research*, **10**, 11–19.

Yasuda, Y. and Tabata, H. 1987 Climatic change in the Himalayan region —result of a palynological study in the Lake Rara. *The Earth Monthly (Gekkan Chikyu)*, **9**, 12, 691–695

(in Japanese).

Yasunari, T. 1987 Catastrophe in the variation of Himalayan glaciers. *Abstract paper in the annual meeting of Japanese Society of Snow and Ice*, **10** (in Japanese).

Yasunari, T. 1990 Impact of Indian monsoon on the coupled atmosphere/ocean system in the tropical Pacific. *Meteor. & Atmos. Phys.* **44**, 29–41.

Yasunari, T. and Fujii, Y. 1983 *Climate and Glaciers of the Himalayas*. Tokyo-do Syuppan, 254pp. (in Japanese).

Yokoyama, K. 1984 Ground photogrammetry of Yala Glacier, Langtang Himal, Nepal Himalaya. In Higuchi, K.(ed.) "*Glacial Studies in Langtang Valley, report of the glacier boring project 1981–82 in the Nepal Himalaya*", Data Center for Glacier Research, Japanese Society of Snow and Ice, 99–105.

Zheng, B. 1987 Preliminary studies of Quaternary glaciation and palaeogeography on the south slope of West Kunlun. *Bulletin of Glacier Research*, **5**, 93–102.

Zheng B. 1988 Quaternary glaciation of Mt. Qomolangma –Xixabangma region. *GeoJournal*, **17**, 525–543.

Zheng, B., Watanabe, O. and Mulmi, D.D. 1984 Glacier features and their variations in the Langtang Himal Region of Nepal. In Higuchi, K.(ed.) "*Glacial Studies in Langtang Valley, report of the glacier boring project 1981–1982 in the Nepal Himalaya*", Data Center for Glacier Research, Japanese Society of Snow and Ice, 99–105.